The Quark Gluon Plasma: results and prospects with the ALICE experiment

A. Rossi, INFN Padova

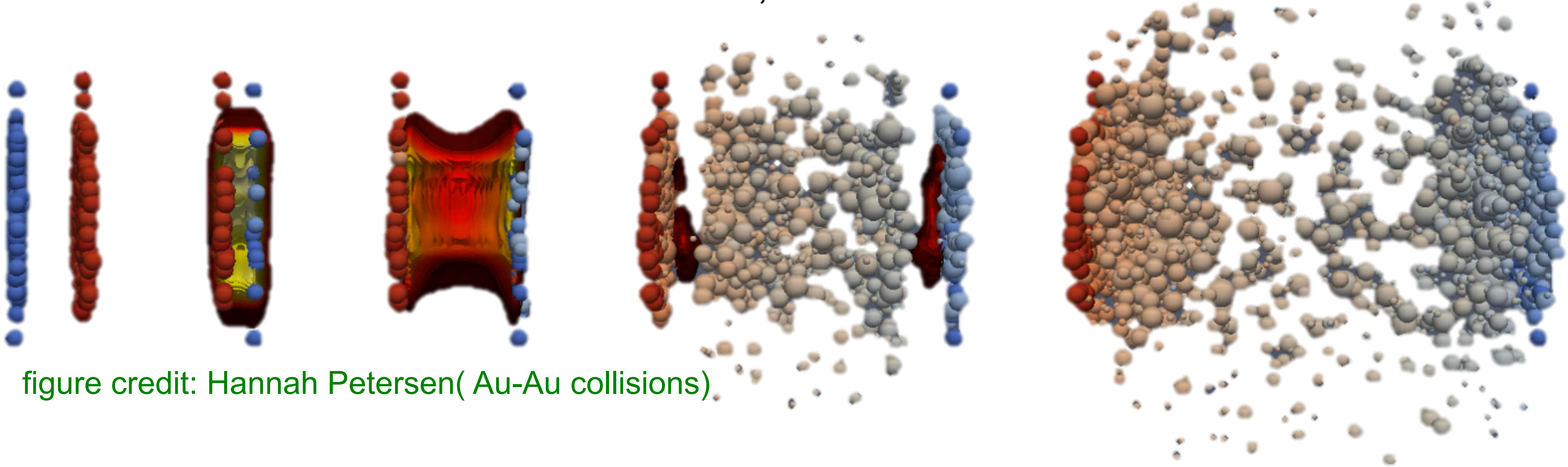

figure credit: Hannah Petersen(Au-Au collisions)

RICCI90 SYMPOSIUM

Legnaro, 5th July 2017

Phase diagram of strongly-interacting (QCD) matter

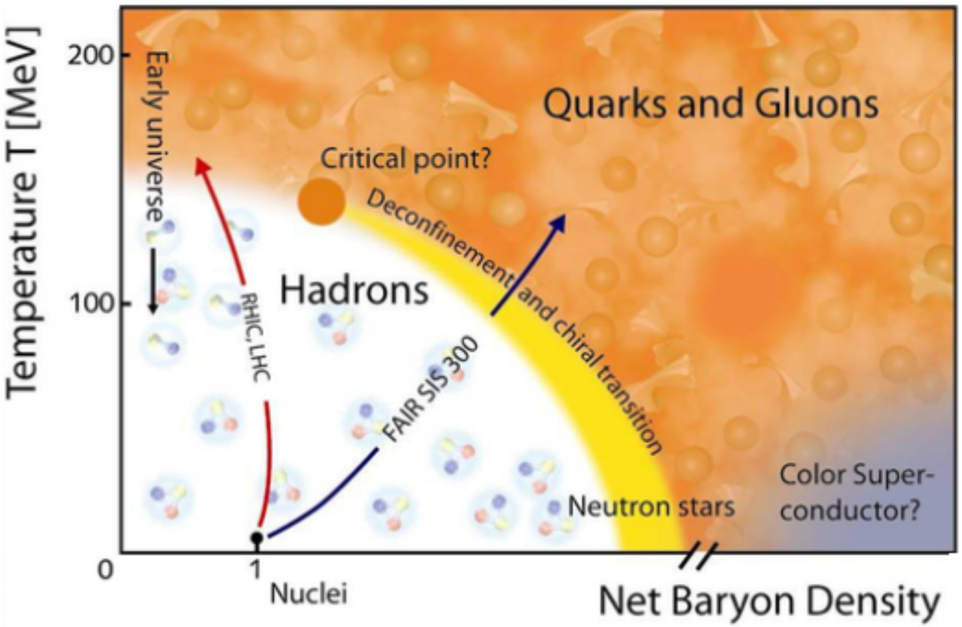

At high energy density ε (high temperature and/or high density) hadronic matter undergoes a phase transition to the *Quark-Gluon Plasma (QGP): a state in which colour confinement is removed*

Phase transition: confined state → deconfined state

Lattice QCD calculations:

Critical temperature at 0 baryon density~ 155 MeV

Critical energy density ε_c ~ 1 GeV/fm^3 ~ 6-7 $\varepsilon_{nucleus}$

QGP in laboratory: nucleus-nucleus collisions

- Can we form the QGP in laboratory? Need to compress/heat matter to very high energy densities.

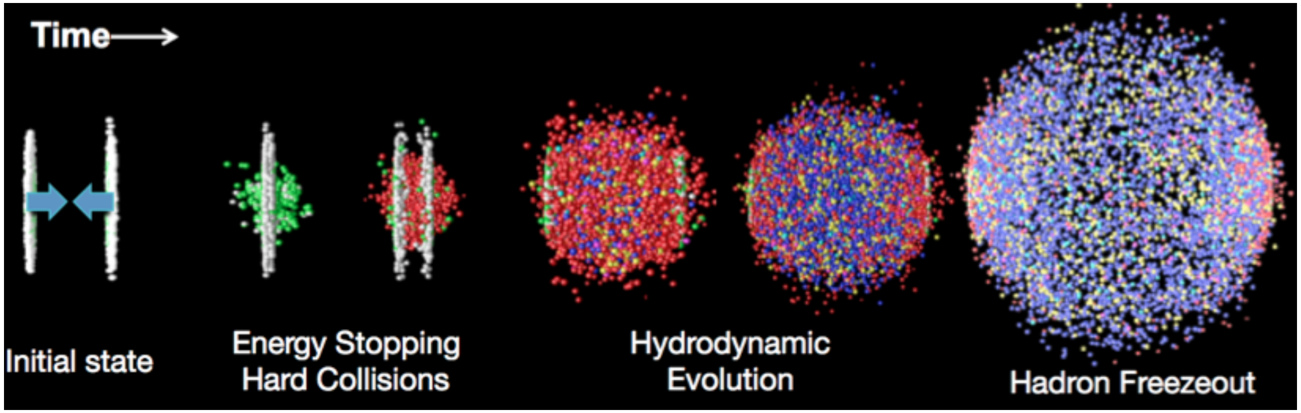

- By colliding two heavy nuclei at ultra-relativistic energies we recreate, for a short time span (about 10^{-23} s, or a few fm/c) the conditions for deconfinement
- As the system expands and cools down it undergoes a phase transition from QGP to hadron again, like at the beginning of the life of the Universe: we end up with confined matter again
- **Chemical freeze out**: time at which inelastic interactions cease →abundances of particle species (π,K,p,.. yields, not resonances) are fixed
- Kinetic freeze out: all interactions cease → free streaming of particles to detector

Ultra-relativistic heavy-ion accelerators

-- only main collision systems are indicated --

- **BNL-AGS**, early '90s, Au-Au up to $\sqrt{s_{NN}} = 5\ \text{GeV}$
- **CERN-SPS**, from 1994, Pb-Pb up to $\sqrt{s_{NN}} = 17\ \text{GeV}$
- **BNL-RHIC**, from 2000, Au-Au $\sqrt{s_{NN}} = 8 - 200\ \text{GeV}$
- **CERN-LHC**, from 2010, Pb-Pb $\sqrt{s_{NN}} = 2.76 - 5.5\ \text{TeV}$

Pb-ion facility at CERN

Approved 1990, started operating 1994

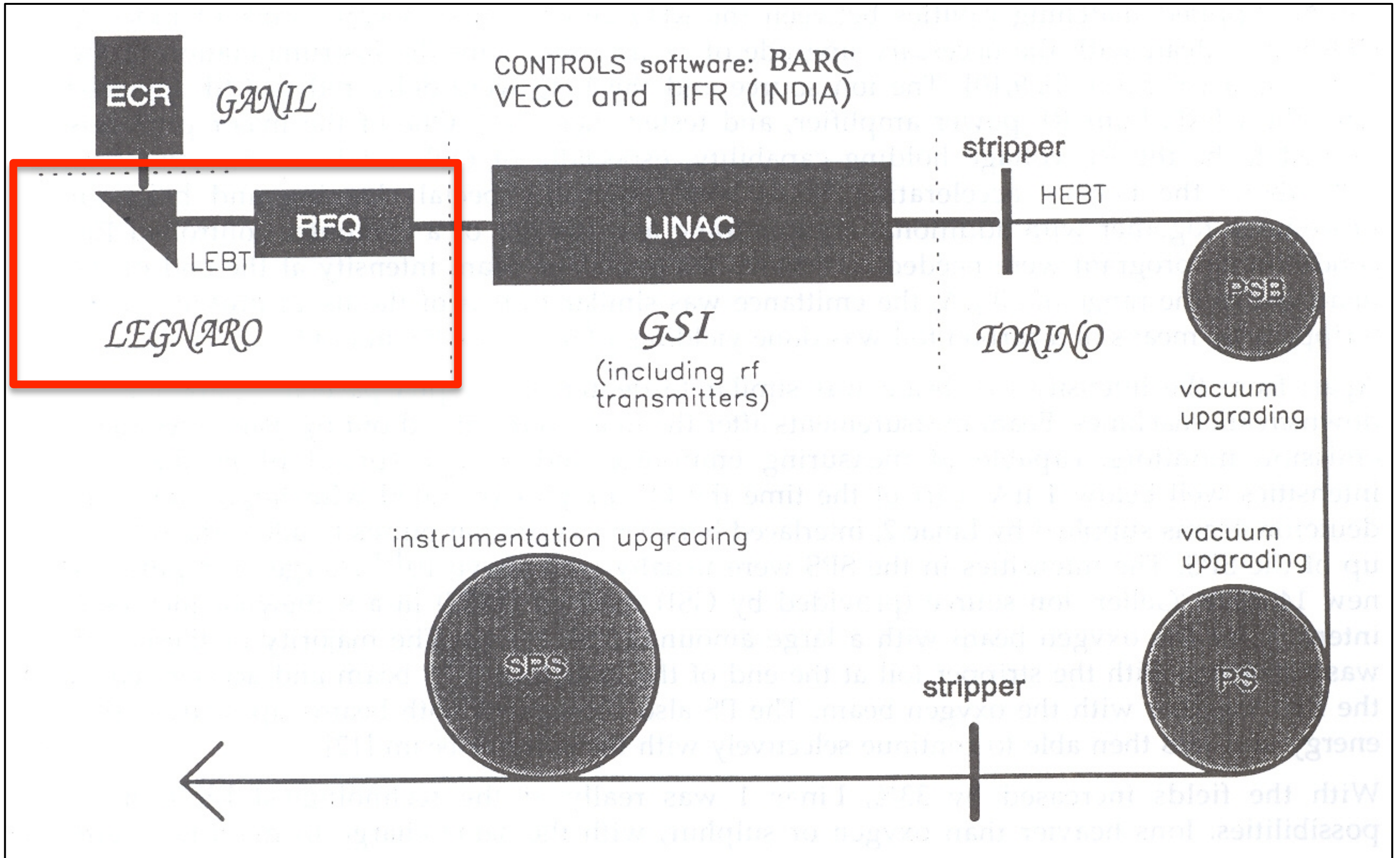

2 Fig. 1.1 Collaborations Involving Laboratories from France, Italy, Germany and India

First acceleration stage (LNL)

A Heavy Ion Linac for the CERN Accelerator Complex

G. Amendola*, N. Angert**, M.-P. Bourgarel***, B. Bru***, F. Cervellera#, G. Fortuna#, H. Haseroth*, C. Hill*, G. Hutter**, J. Klabunde**, H. Klein##, H. Kugler*, D. Liska###, A. Lombardi#, H. Lustig*, E. Marwitz**, A. Musso°, H. O'Hanlon*, G. Parisi#, A. Pisent#, U. Raich*, U. Ratzinger**, L. Riccati°, R. Ricci#, A. Schempp##, T. Sherwood*, P. Sortais***, E. Tanke*, P. Têtu*, A. van der Schueren*, M. Vretenar*, D. Warner*, M. Weiss*

*CERN (CH-1211 Geneva 23), **GSI (Gesellschaft für Schwerionenforschung, D-6100 Darmstadt), ***GANIL (F 14021 Caen), #INFN Legnaro (Laboratori Nazionali di Legnaro, I-35020 Legnaro), ##Univ. Frankfurt (Inst. für Angewandte Physik, D-6000 Frankfurt/Main 11), ###CERN Associate from LANL (Los Alamos National Lab., Los Alamos, NM 87545, USA), °University and INFN Torino (I-10125 Torino)

Abstract

The injector linac required by CERN for heavy ions, e.g. Pb^{28+}, is being made in collaboration with several

charge state ions, e.g. pulses of O^{6+} to O^{7+}, Ar^{10+} to Ar^{14+}, Pb^{25+} to Pb^{29+} could be obtained. The phenomenon is stable and reproducible and the afterglow peak, dependent on the adjustment of the source parameters, is about 2 or 3 times the

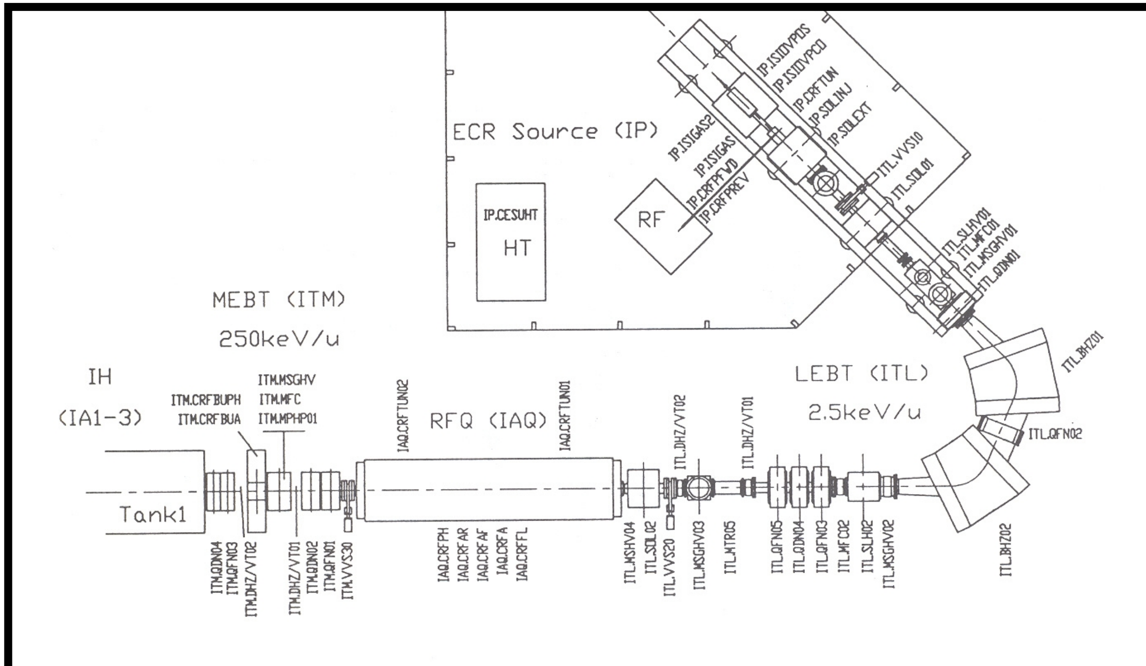

Fig. 2.6 Schematic Layout of LEBT, RFQ and MEBT Region

Still in use at the LHC!

Heavy-ion experiments at the LHC

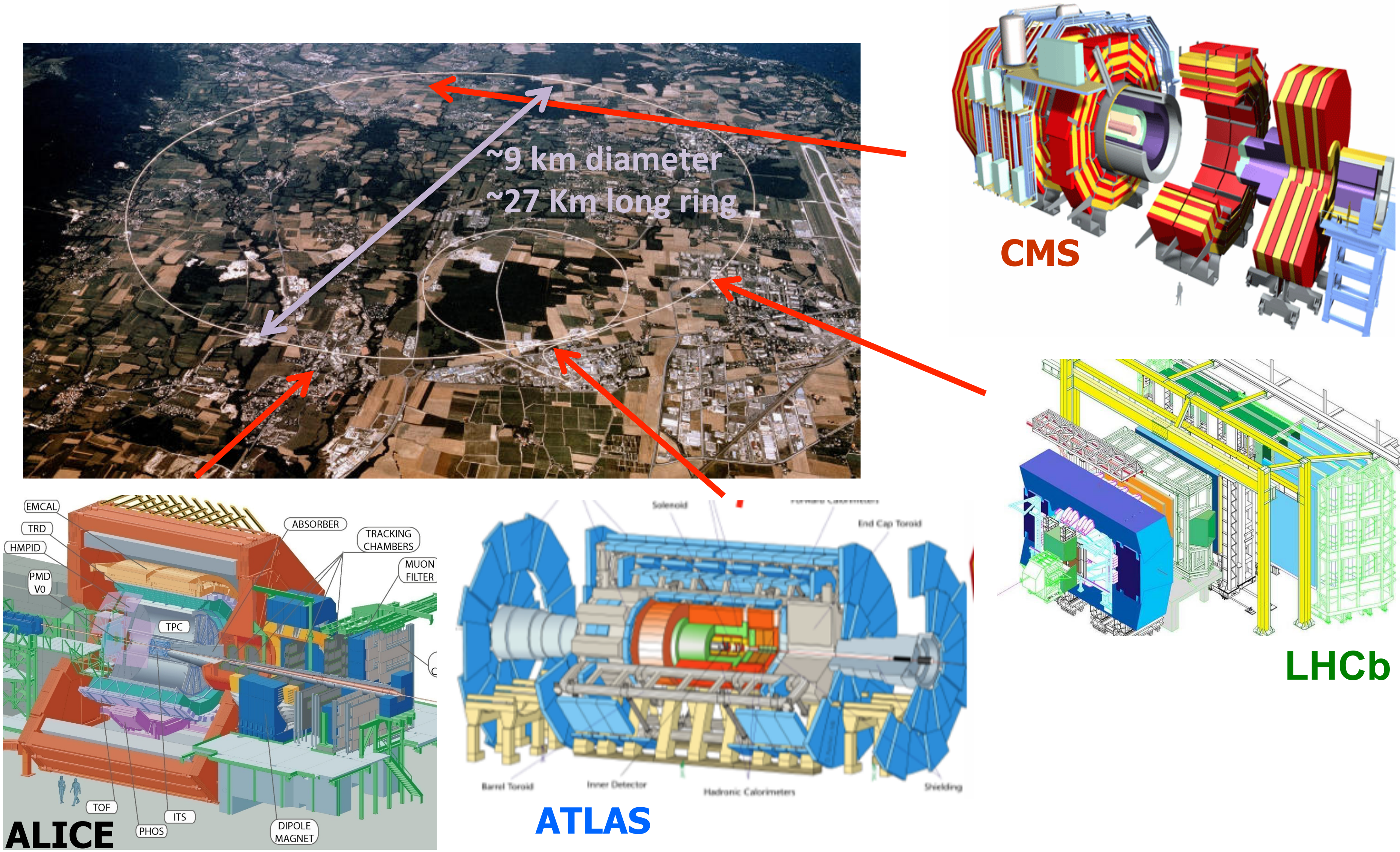

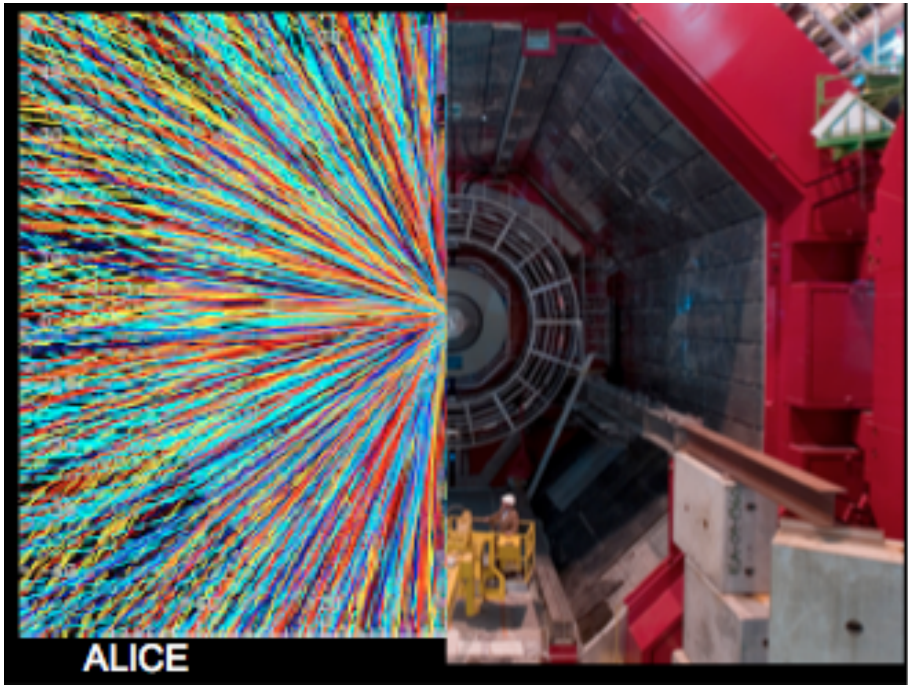
ALICE

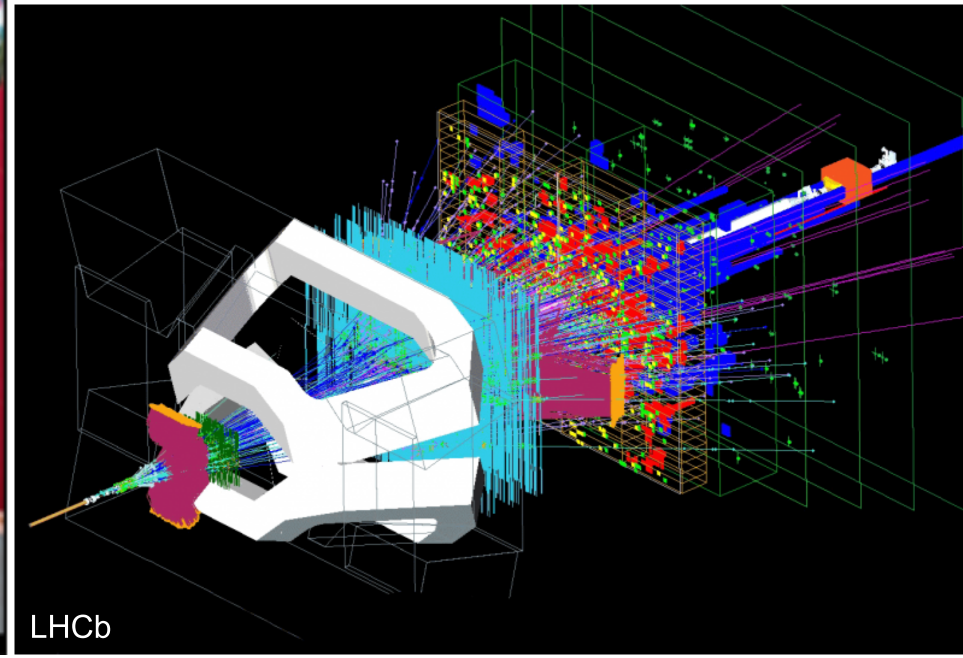
LHCb

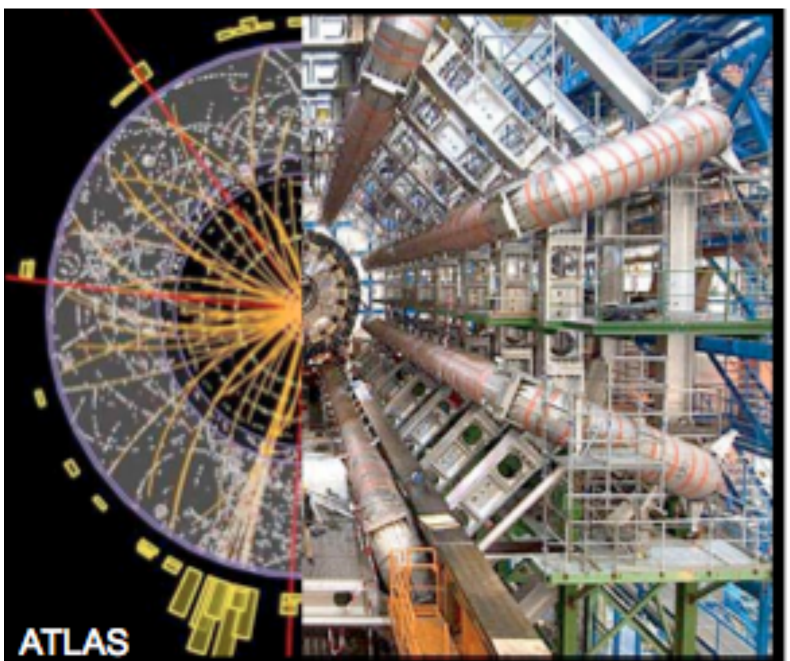
ATLAS

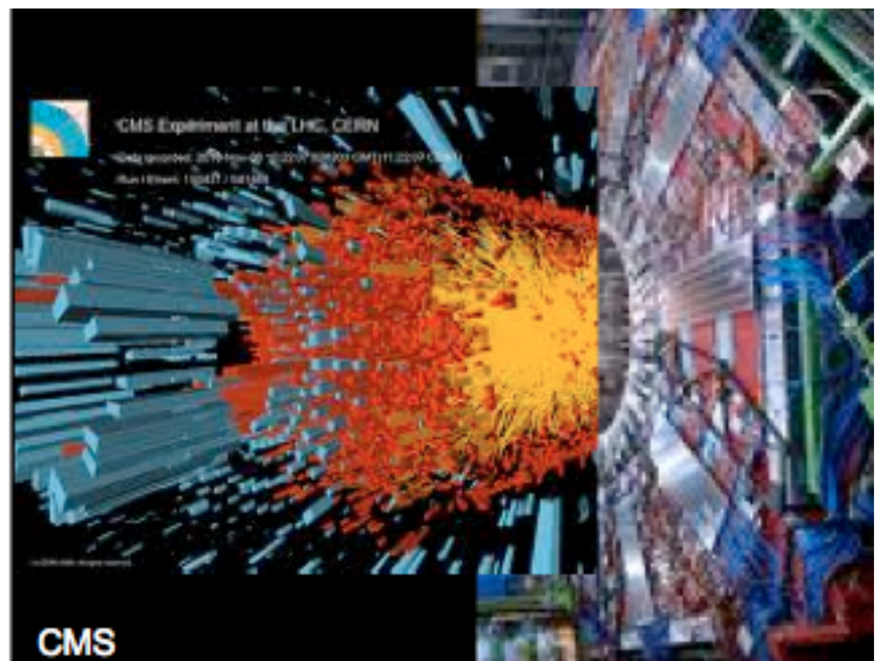
CMS Experiment at the LHC, CERN
CMS

The ALICE detector

Central barrel (|η|<0.9, B=0.5 T)

Track and vertex reconstruction (TPC, ITS)

Particle Identification

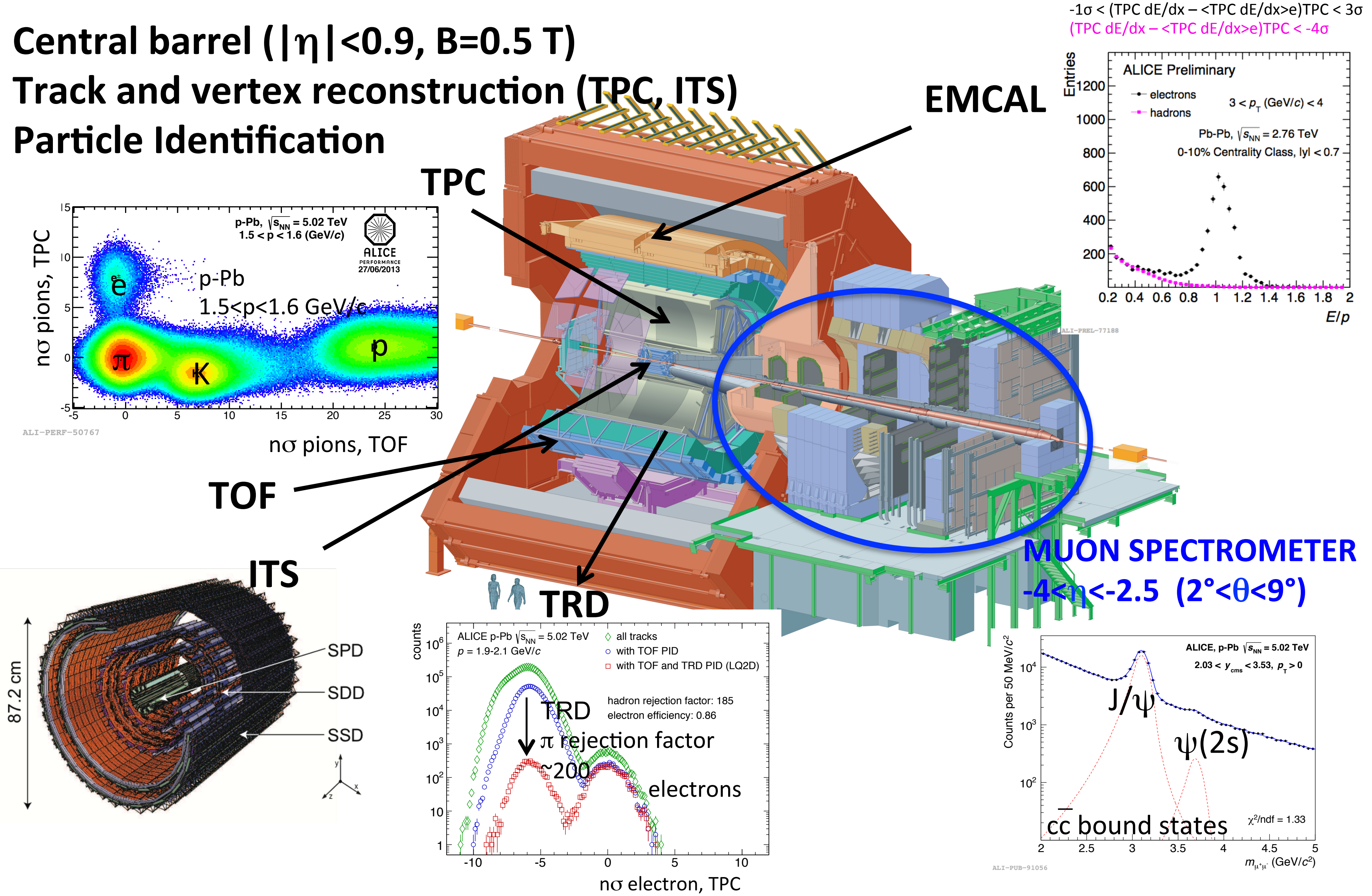

The Silicon Pixel Detector

Fundamental contributions from Legnaro and Padua

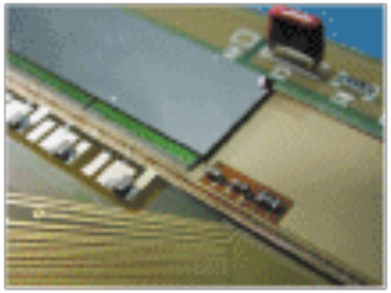

Photograph of a ladder mounted on a prototype bus

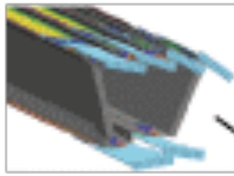

Design of the carbon fiber support of one sector

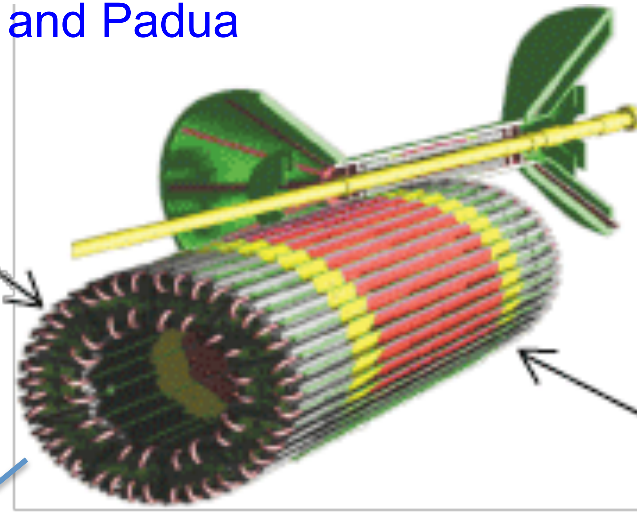

Schematic drawing of the two barrel layers

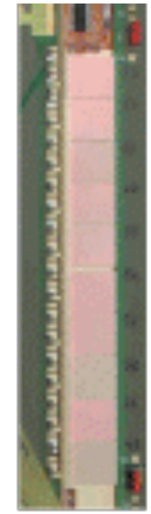

Pixel bus with 10 chips (half-stave configuration)

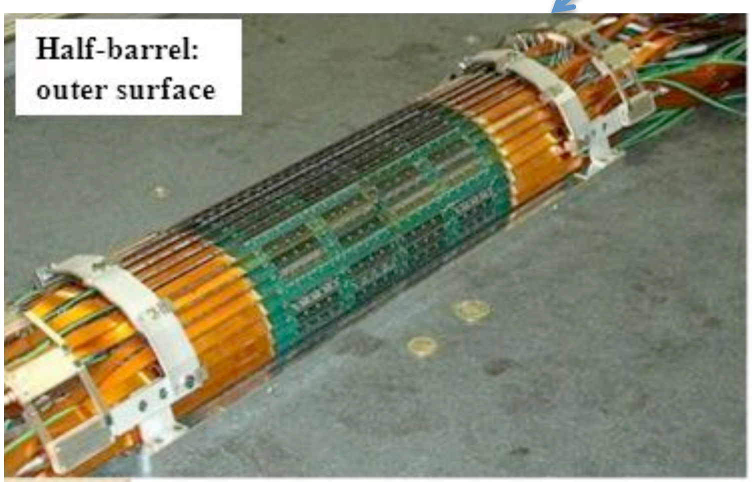

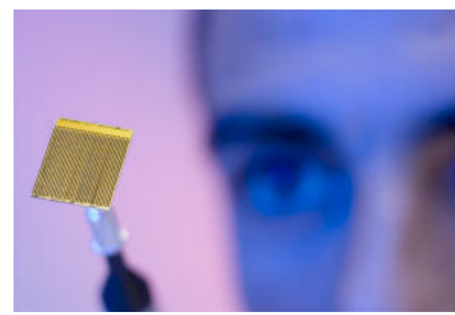

Photo of a chip (1.28x1.36mm^2): 8192 pixel cells (256x32) with size 50x425 μm^2

The Silicon Pixel Detector

Fundamental contributions from Legnaro and Padua

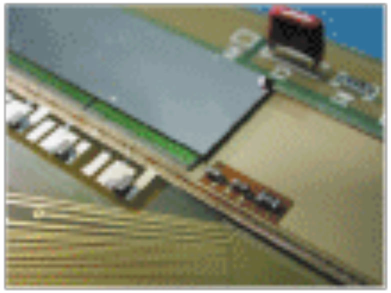

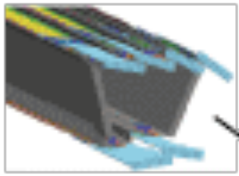

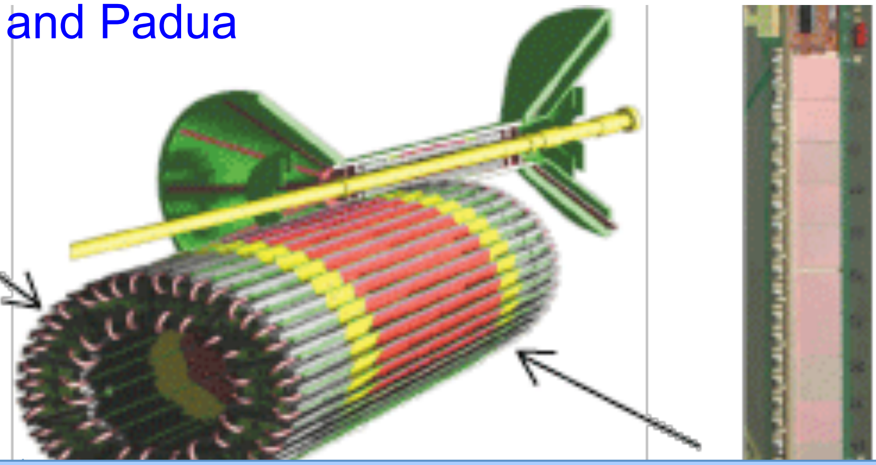

One of the most important ALICE sub-detectors
trigger, primary vertex reconstruction, event multiplicity, …

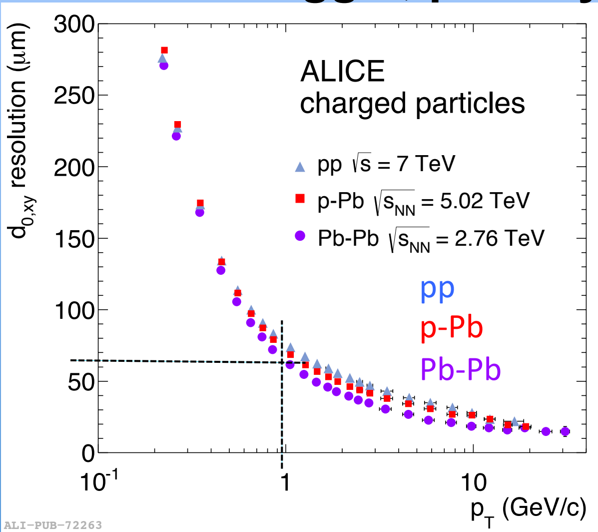

Int. J. Mod. Phys. A 29 (2014) 1430044

Resolution on track position at the primary vertex better than 70 micron for p_T>1 GeV/c

SPD crucial for charm and beauty measurements

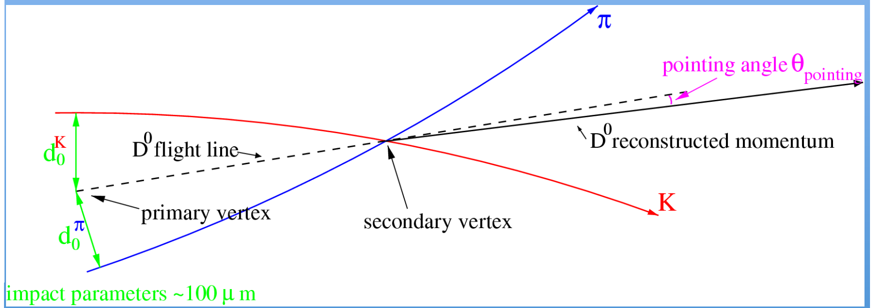

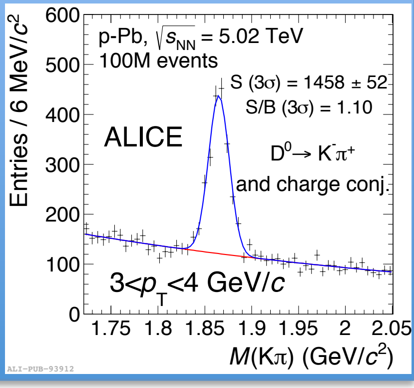

Few introductory concepts: centrality, R_{AA}

Nuclear modification factor (R_{AA}): compare particle production in Pb-Pb with that in pp scaled by a "geometrical" factor (from Glauber model) to account for the larger number of nucleon-nucleon collisions

$$R_{AA}(p_T) = \frac{dN_{AA}/dp_T}{\langle N_{coll} \rangle \times dN_{pp}/dp_T}$$

Pb-Pb

pp

Binary nucleon-nucleon collisions, encodes collision geometry

If $R_{AA}=1$ → no nuclear effects

If $R_{AA}\neq1$ → nuclear effects

Note: N_{coll} scaling expected to hold only for hard (rare) processes

$\langle N_{part}\rangle$,$\langle N_{coll}\rangle$ from "geometrical" Glauber model

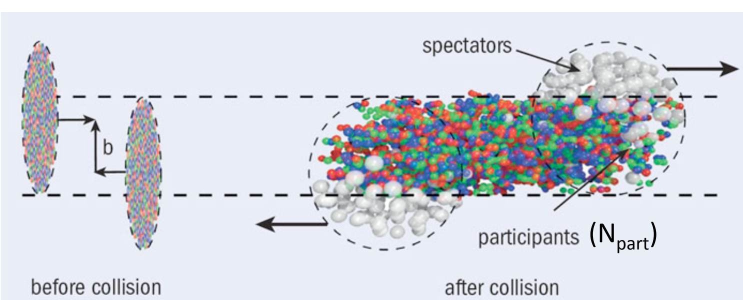

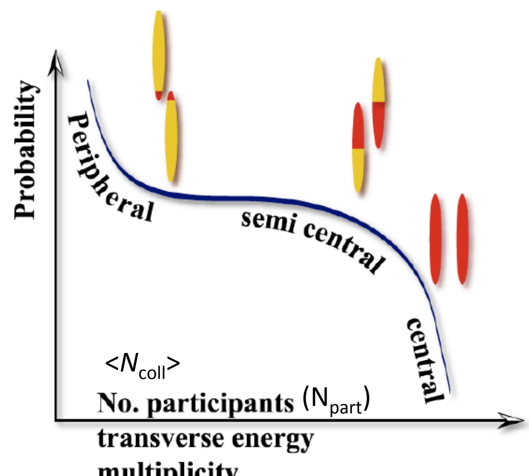

Quarkonia and QGP (re)discovery

Quarkonium in the QGP

Bound quark-antiquark states: "charmonia" χ_c , J/ψ, $\psi(2S)$,...
"bottomonia" Υ, $\Upsilon(2S)$, $\Upsilon(4S)$,..

Recall: quant-antiquark QCD potential

$$V(r) = -\frac{\alpha}{r} + kr$$

The QGP consists of deconfined colour charges → screening effect

$$V(r) = -\frac{\alpha}{r} e^{-r/\lambda_D}$$

λ_D: screening radius

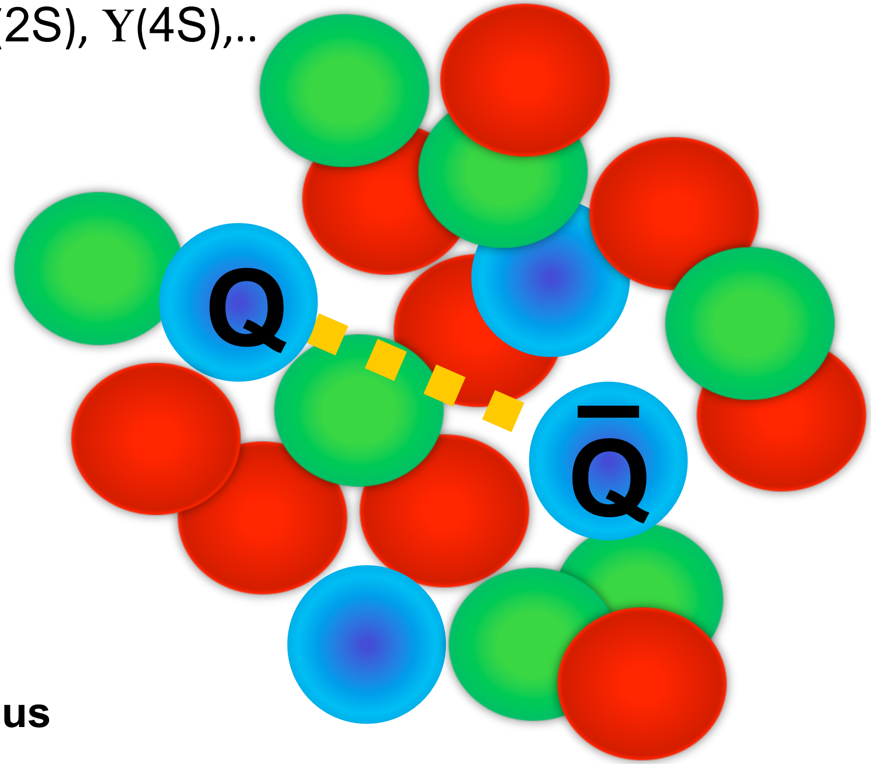

The binding of a $q\bar{q}$ pair is subject to the effects of colour Debye-like screening:

- the "confinement" contribution disappears
- the coulumbian term of the potential is screened by the high color density

Matsui, Satz, PLB178 (1986) 416

J/ψ suppression
-- QGP discovery smoking gun --

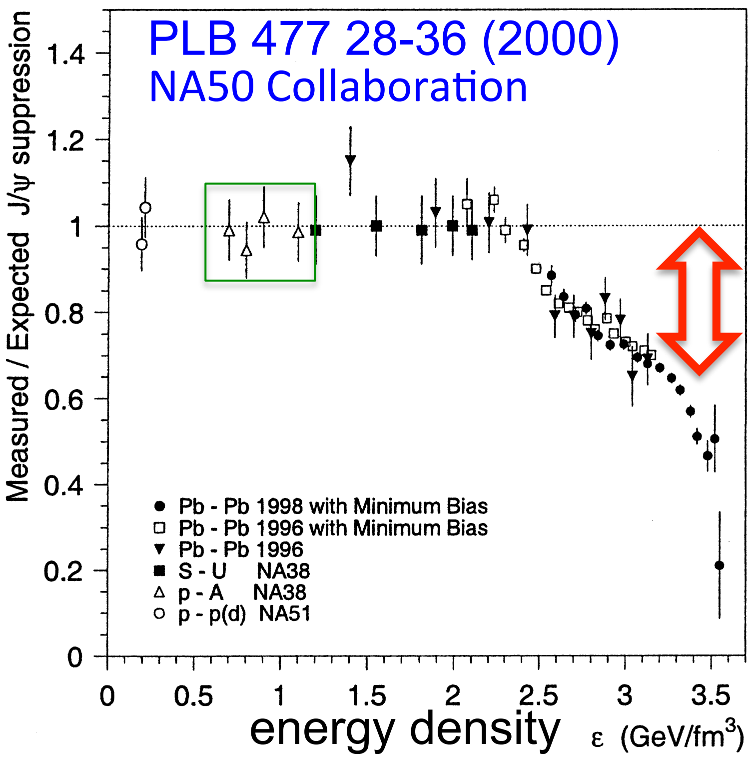

N.b. "expected suppression" = J/ψ absorption in "cold" nuclear matter (no QGP). Not discussed in the slides, but note: p-A needed as reference

Also previous indications:
NA51 Collaboration, PLB 438 35 (1998)
NA38 Collaboration, PLB 444 516 (1998); PLB 449 128 (1999)

J/ψ suppression
-- QGP discovery smoking gun --

N.B. different quantities plotted on both x and y axes

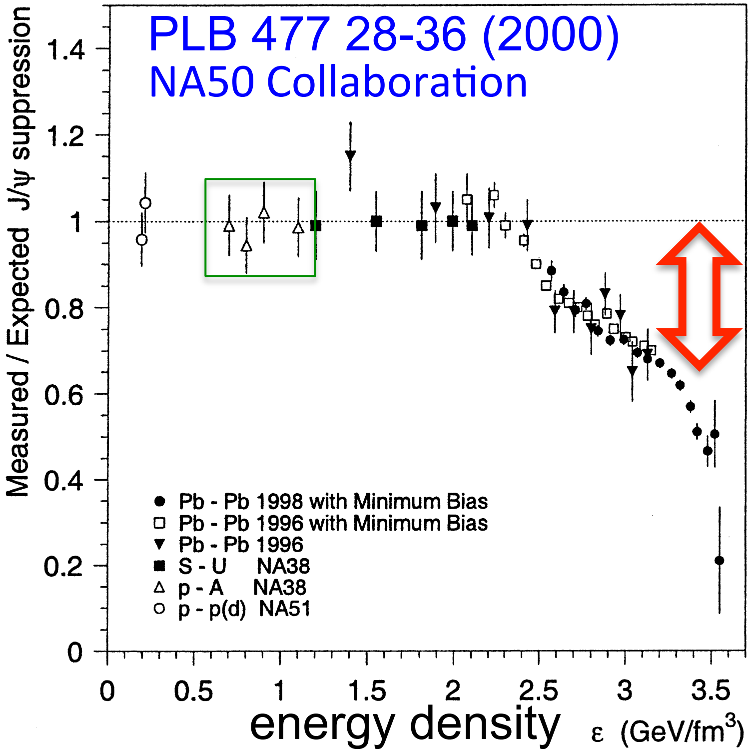

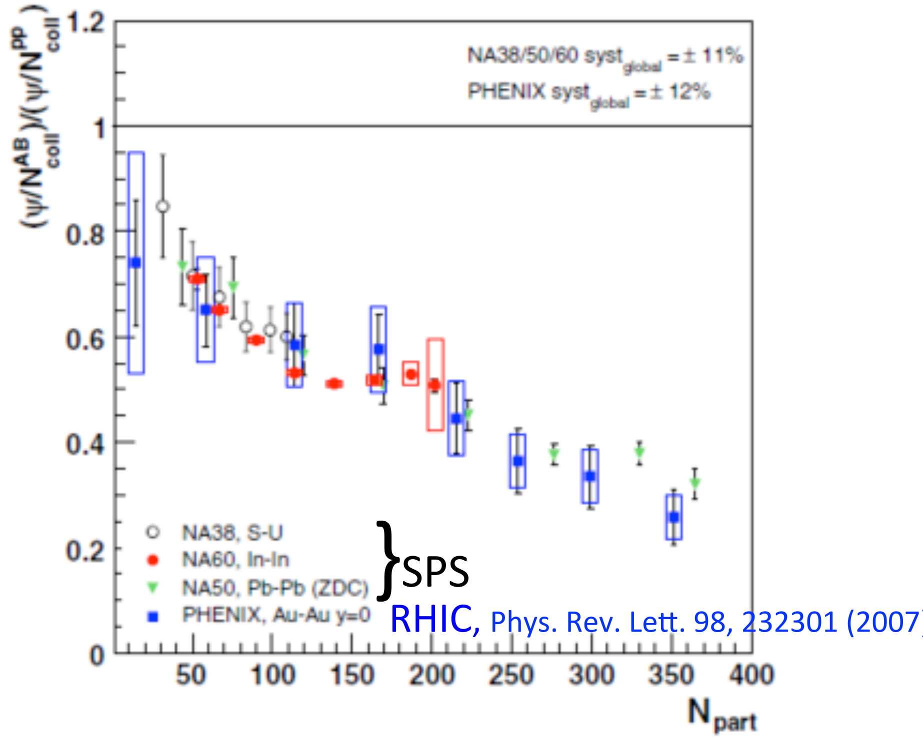

Also previous indications:
NA51 Collaboration, PLB 438 35 (1998)
NA38 Collaboration, PLB 444 516 (1998); PLB 449 128 (1999)

Adding RHIC data:
similar suppression than SPS,
despite the x12 larger collision energy (x2 ε)… unexpected!

Quarkonium suppression & regeneration

Hot QGP→ **quarkonia suppression** due to Debye-like screening of QCD $Q\bar{Q}$ potential ("melting" of bound $Q\bar{Q}$ states) → **signature of deconfinement**
(T. Matsui and H. Satz, PLB 178 (1986) 416)

Surprisingly **similar J/ψ suppression at SPS and RHIC (εx2) energies**

→ Could quarkonia states be **(re)generated via recombination (coalescence) of deconfined quarks**? (P. Braun-Munzinger, J. Stachel, PLB 490 (2000) 196)

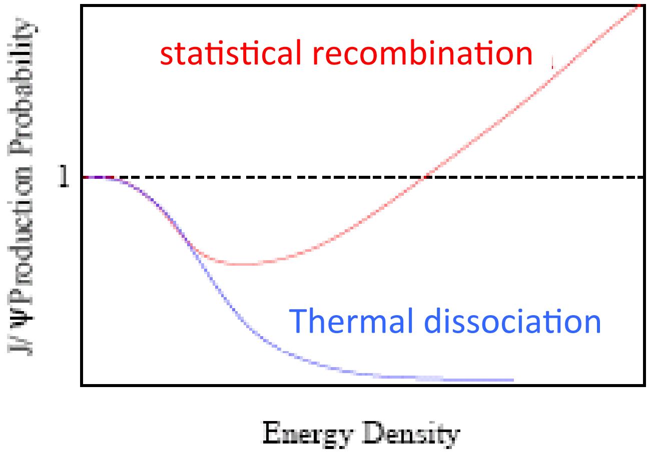

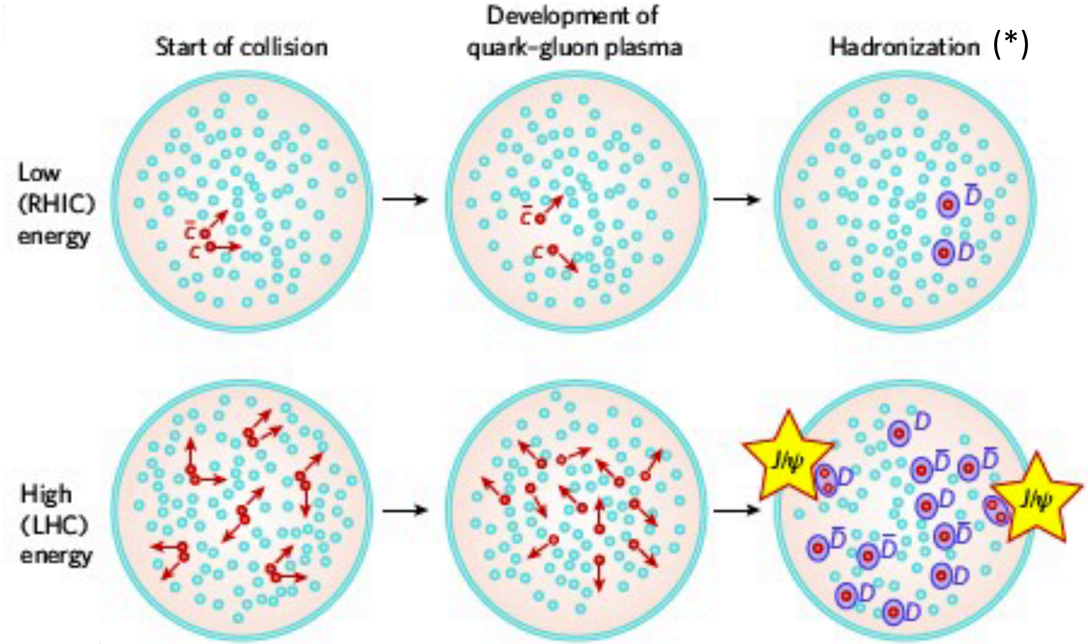

LHC vs. RHIC

Larger energy density →**stronger suppression**
Higher $c\bar{c}$ multiplicity →**larger recombination**

(*) Note that "in vacuum":
(ccbar →J/ψ) / (ccbar →DDbar) <<1 (~1-2%)

J/ψ suppression: LHC vs. RHIC

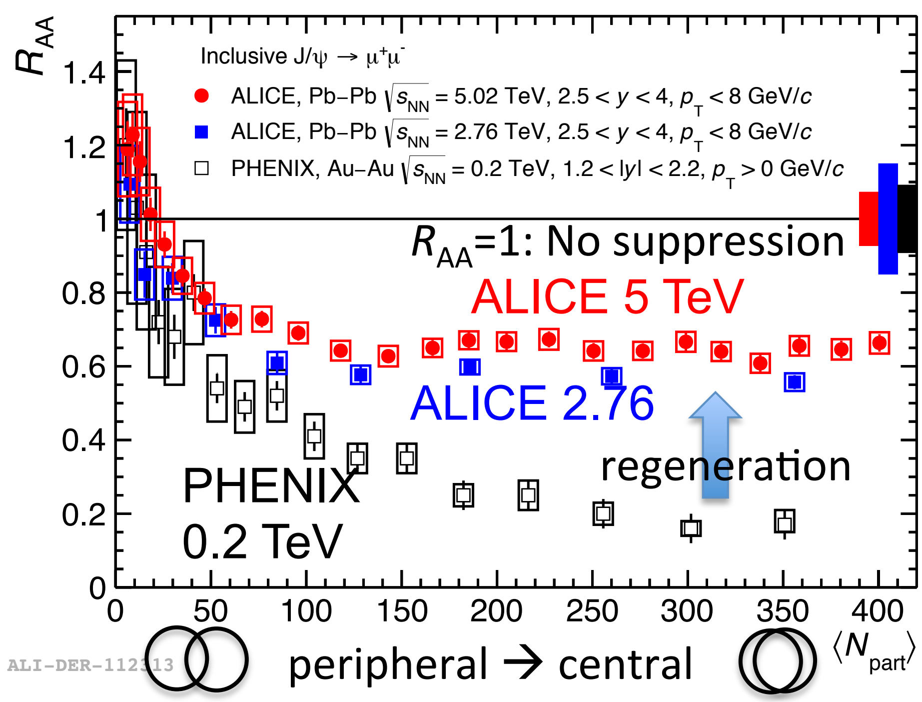

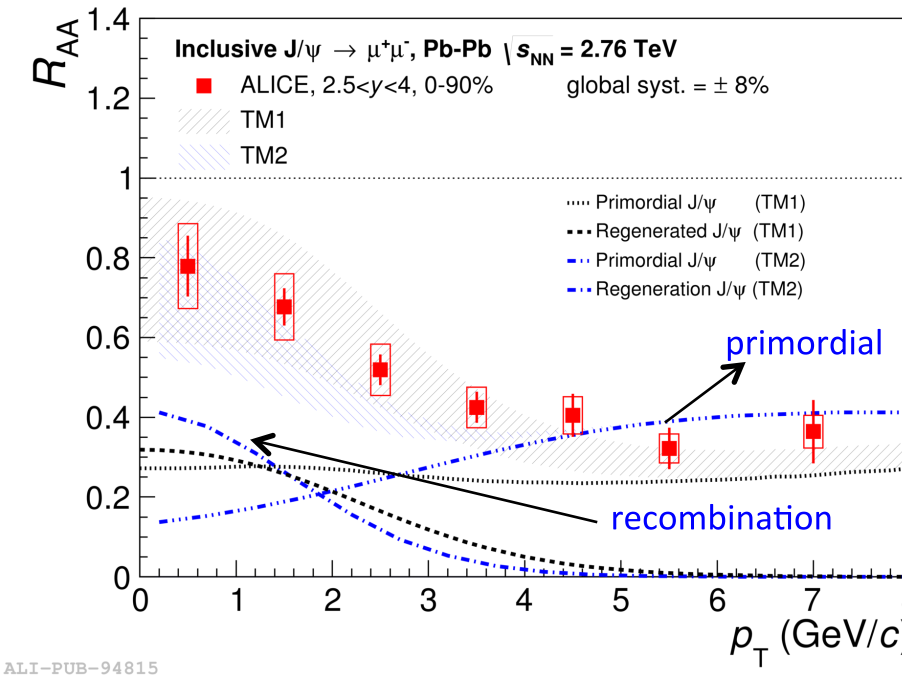

- J/ψ suppression stronger in central events than peripheral
- Smaller suppression at LHC than RHIC
- Analysis vs. transverse momentum: suppression stronger at higher momentum. In agreement with models expecting about 50% contribution of J/ψ from recombination at low p_T.

"Twice a signature of QGP"

Quarkonia: sequential suppression

Indication that ψ(2S) is more suppressed than J/ψ

ϒ (2S) ~4 times more suppressed than ϒ(1S)

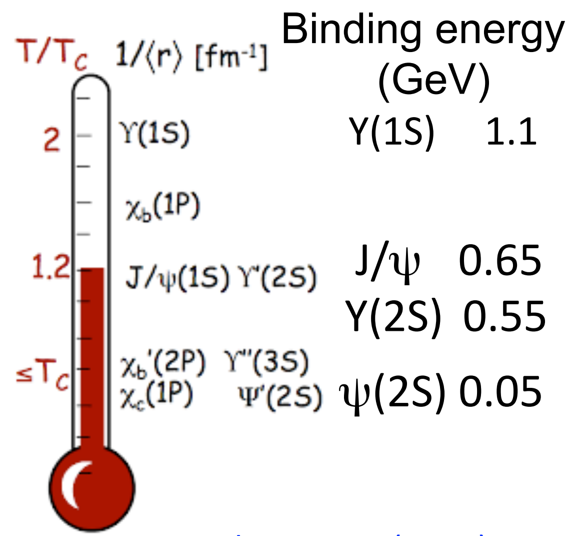

A. Mocsy, Eur.Phys.J. C61 (2009)

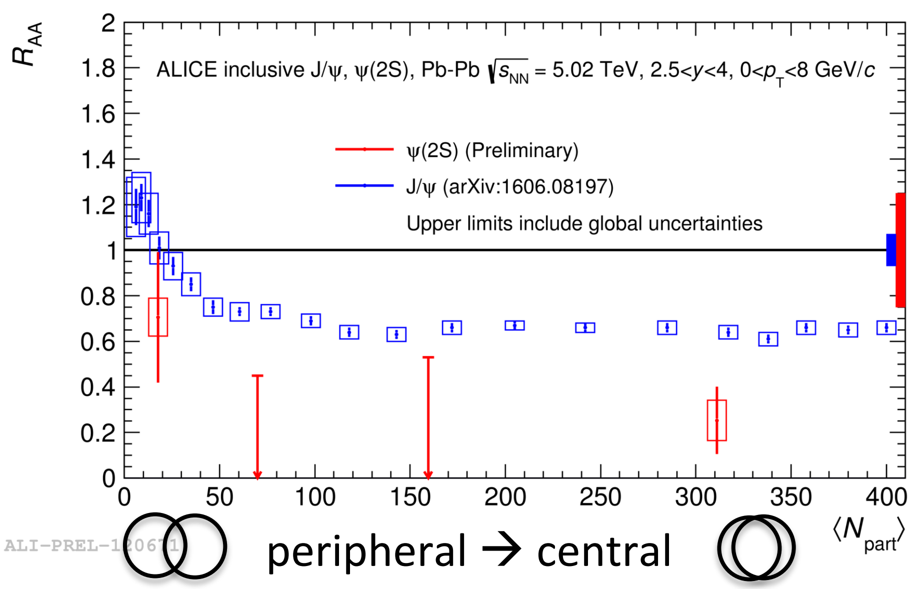

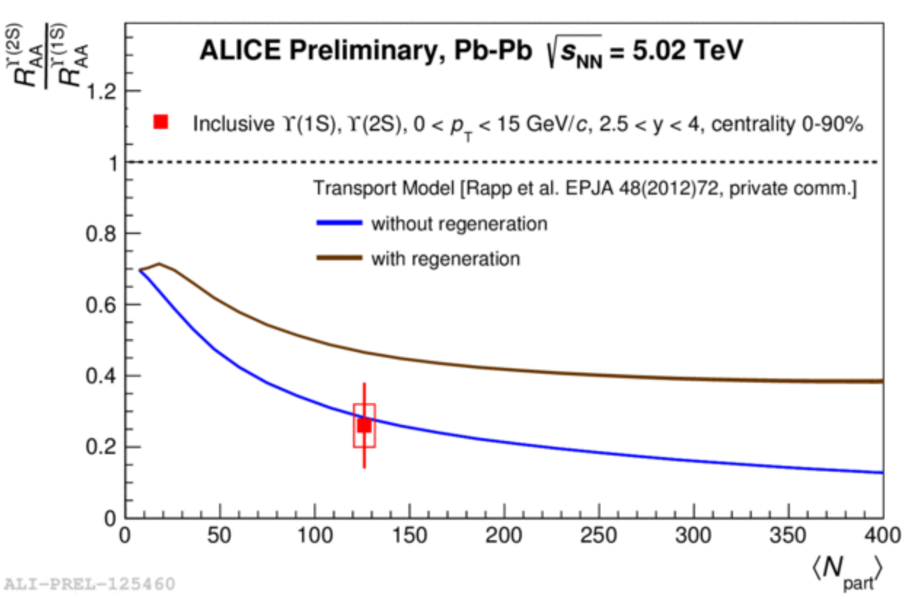

“Soft probes”
--few selected topics--

Particle ratios

Phys. Rev. C 93, 034913 (2016)

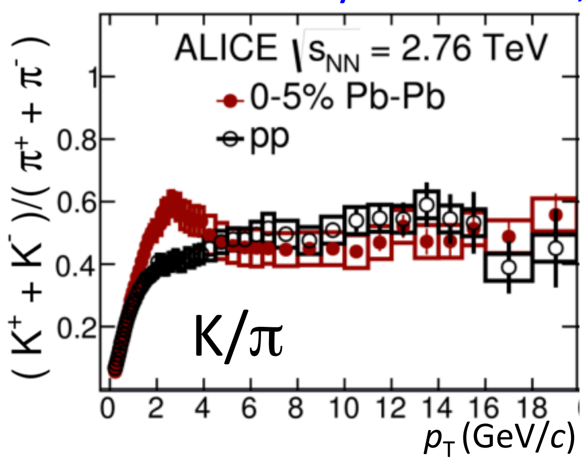

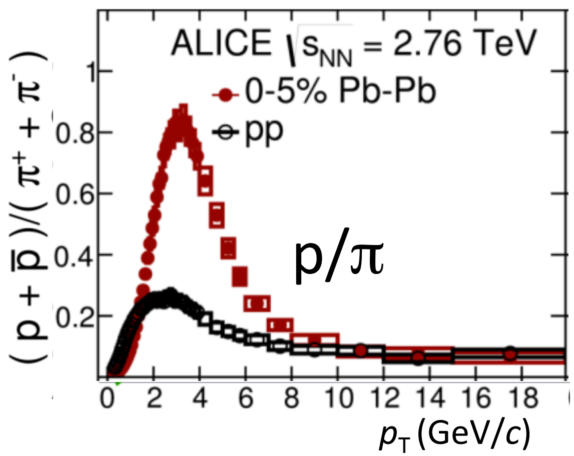

Phys. Rev. C 91 024609 (2015)

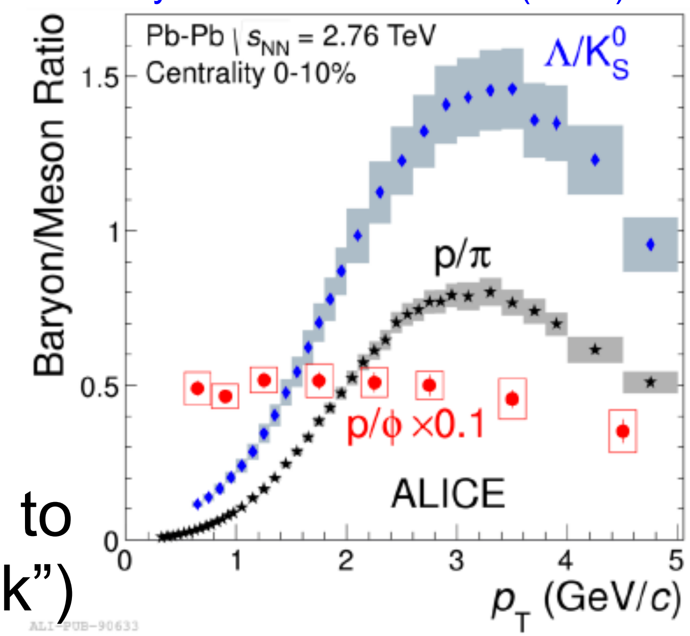

Strong modification of p/π vs. p_T from pp to central Pb-Pb collisions ("radial flow peak")

Indication of collective behaviour

- Pressure gradients leads to radial flow
- Same "velocity" boost gives larger momentum to heavier particles
- Alternative/concurrent explanation: hadronisation via quark coalescence → higher momentum for baryons (3 quarks) than mesons (2 quarks): challenged by φ/p ratio

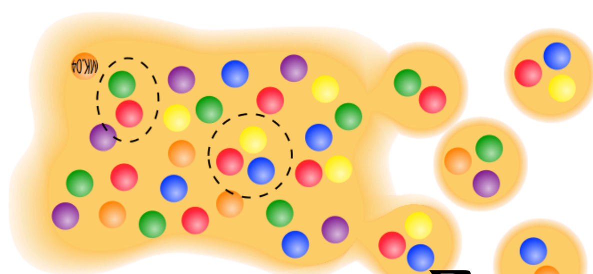

$p(qqq) > p(qq) \longleftarrow \vec{p} = \sum_{\text{quarks}} \vec{p}_i$

Anisotropic (Elliptic) flow

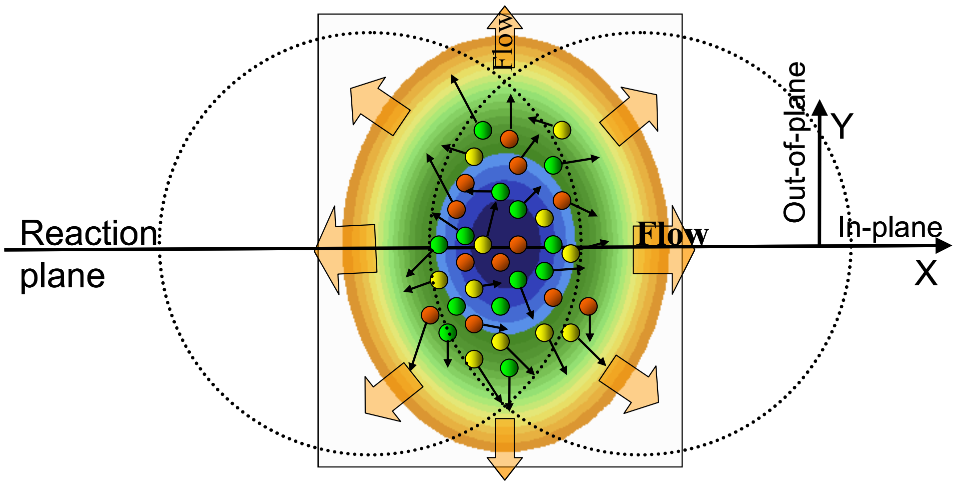

Non-central collisions: azimuthal anisotropy of nuclei overlap region

→ Asymmetric pressure gradients transfer the anisotropy to momentum space

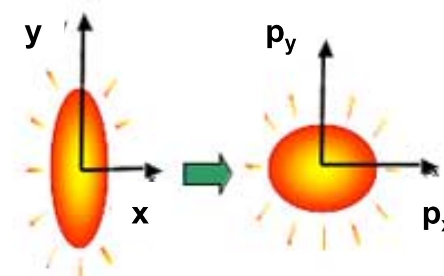

→ The transfer of this asymmetry to momentum space provides a measure of the strength of collective phenomena

Effects addressed by measuring the azimuthal distribution of the particles with respect to the "Reaction Plane" → Fourier analysis

$$N(\varphi) \propto 1 + 2\sum v_n \cos(n(\varphi - \psi_{RP})) = 1 + 2v_1 \cos(\varphi - \psi_{RP}) + 2v_2 \cos(2(\varphi - \psi_{RP})) + \ldots$$

v_2= Elliptic flow, main parameter

Anisotropic (Elliptic) flow

Points= data curves=model

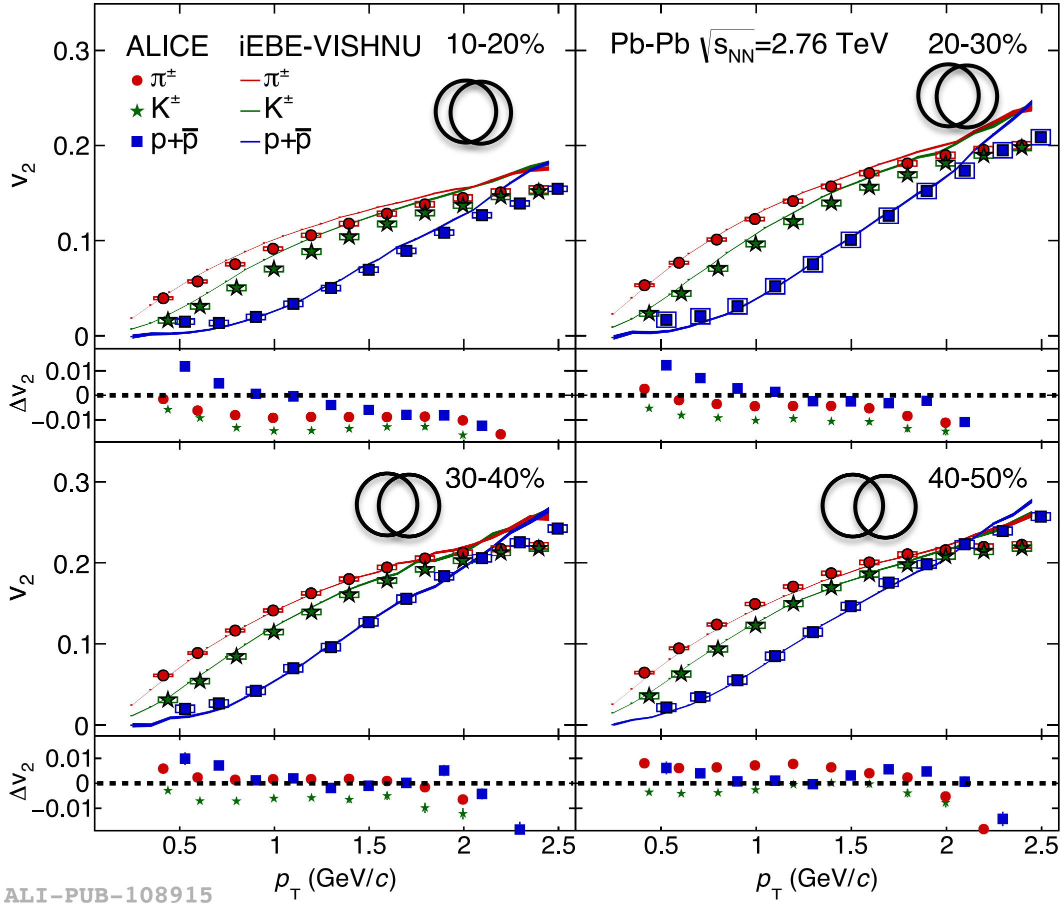

Elliptic flow (v_2) significantly>0

- Evidence of system collective motion
- "Early signal": develops in partonic phase
- Well described by hydrodinimical models
- Expected trends vs. particle mass

→ **Thermalized partonic system**

→ (via more detailed comparisons with models) **Data suggest very low viscosity (← small mean free path)**

System behaves as ~perfect liquid (the RHIC "paradigm")

JHEP 1609 (2016) 164

Constraining further viscosity: higher harmonics

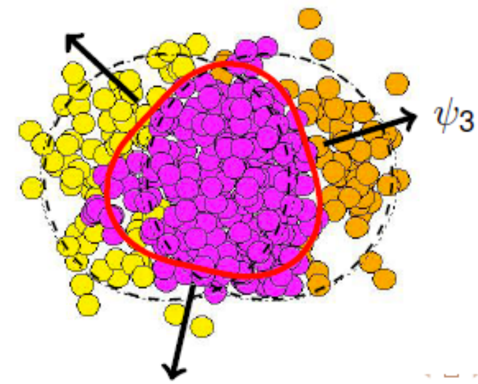

Initial geometry is not an ideal almond shape

- Fluctuations of initial energy/pressure distributions lead to "irregular" shapes (→ need more harmonics to describe them) that fluctuate event-by-event

Simulation of energy density evolution

(ideal and viscous hydro)

Schenke, Jeon, Gale, PRL 106:042301,2011

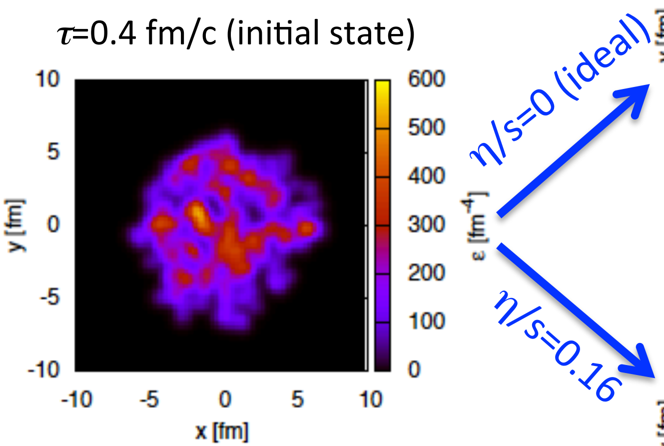

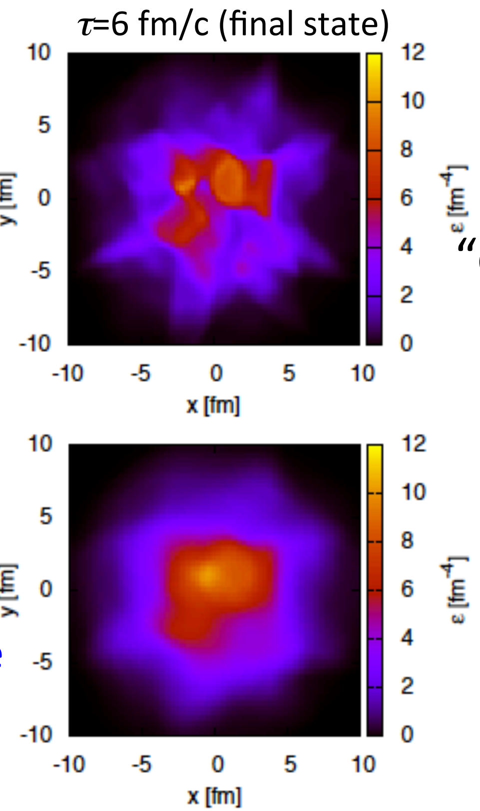

Fluctuations of initial state are damped by viscosity

Viscosity determines the "conversion efficiency" of the initial shape into final momentum azimuthal distribution

Higher harmonics add sensitivity to the value of shear viscosity

Constraining further viscosity: higher harmonics

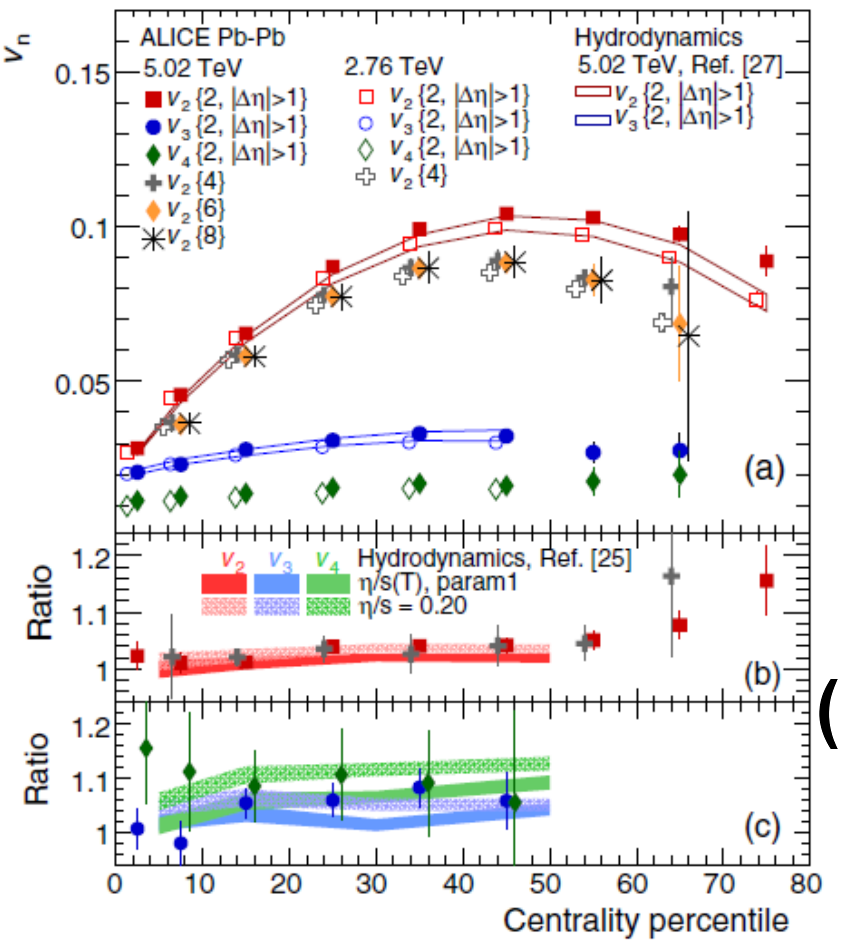

2.76 TeV (Run 1): PRL 107 (2011) 032301

5 TeV (Run 2): PRL116,132302 (2016)

Higher-harmonic coefficients significantly non-zero

QGP viscosity very low (lower than any atomic matter)

High-energy probes → microscopic processes (local interactions) in the medium

QGP tomography with high-energy partons

- Early production in hard-scattering processes with high Q^2
- Production cross sections calculable with pQCD
- Strongly interacting with the medium

⇨ **"Calibrated probes" of the medium**

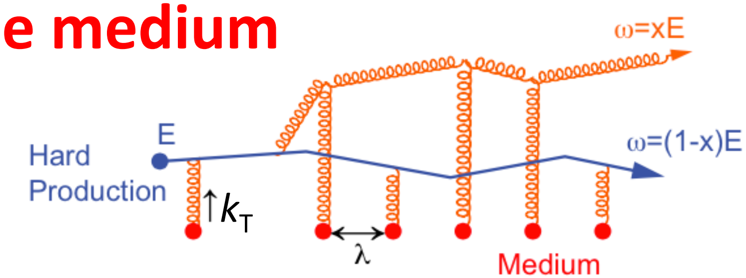

Study parton interaction with the medium

- **energy loss via radiative** ("gluon Bremsstrahlung")
  collisional processes

~ Study QCD "Bethe-Block" curve for partons in the QGP

⇩

Connection of "local" interactions with global medium properties
→ Microscopic description of the medium

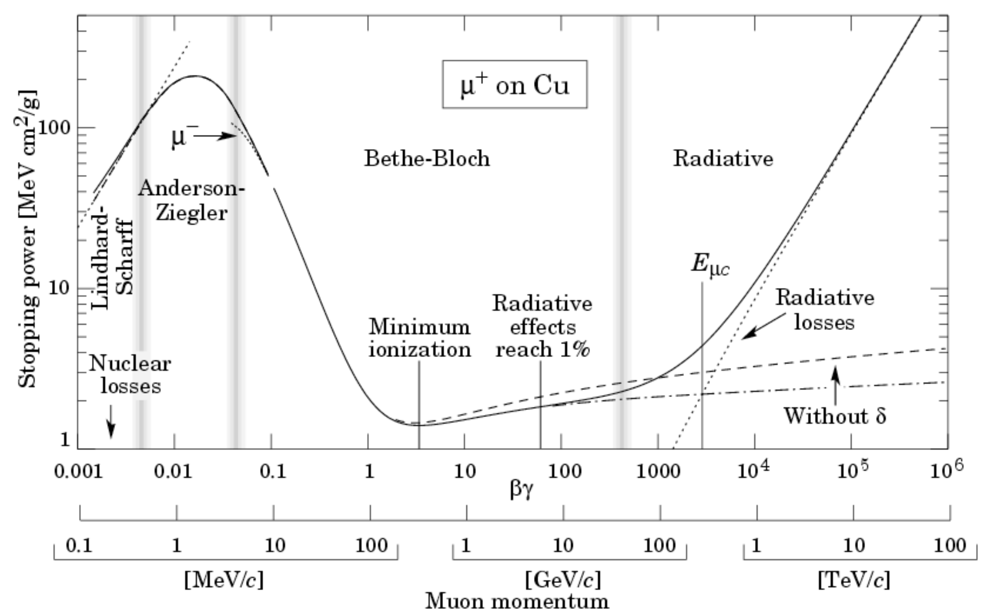

QGP tomography with high-energy partons

- Early production in hard-scattering processes with high Q^2
- Production cross sections calculable with pQCD
- Strongly interacting with the medium

⇨ **"Calibrated probes" of the medium**

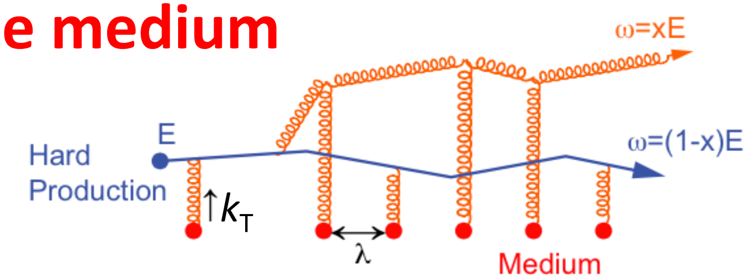

Study parton interaction with the medium

- **energy loss via radiative** ("gluon Bremsstrahlung")
  collisional processes

~ Study QCD "Bethe-Block" curve for partons in the QGP

⇩

Connection of "local" interactions with global medium properties
→ Microscopic description of the medium

e.g. in BDMPS-Z formalism*

$$\langle \Delta E \rangle^{\text{rad}} \propto \alpha_s C_R \hat{q} L^2$$

$$\hat{q} = \frac{\langle k_T^2 \rangle}{\lambda} = \langle k_T^2 \rangle \rho \sigma$$

Transport coefficient(s)

*Baier, Dokshitzer, Mueller, Peigné, Schiff, NPB 483 (1997) 29
Zakharov, JTEPL 63 (1996) 952.

QGP tomography with high-energy partons

ALICE, PRL 110 (2013) 082302

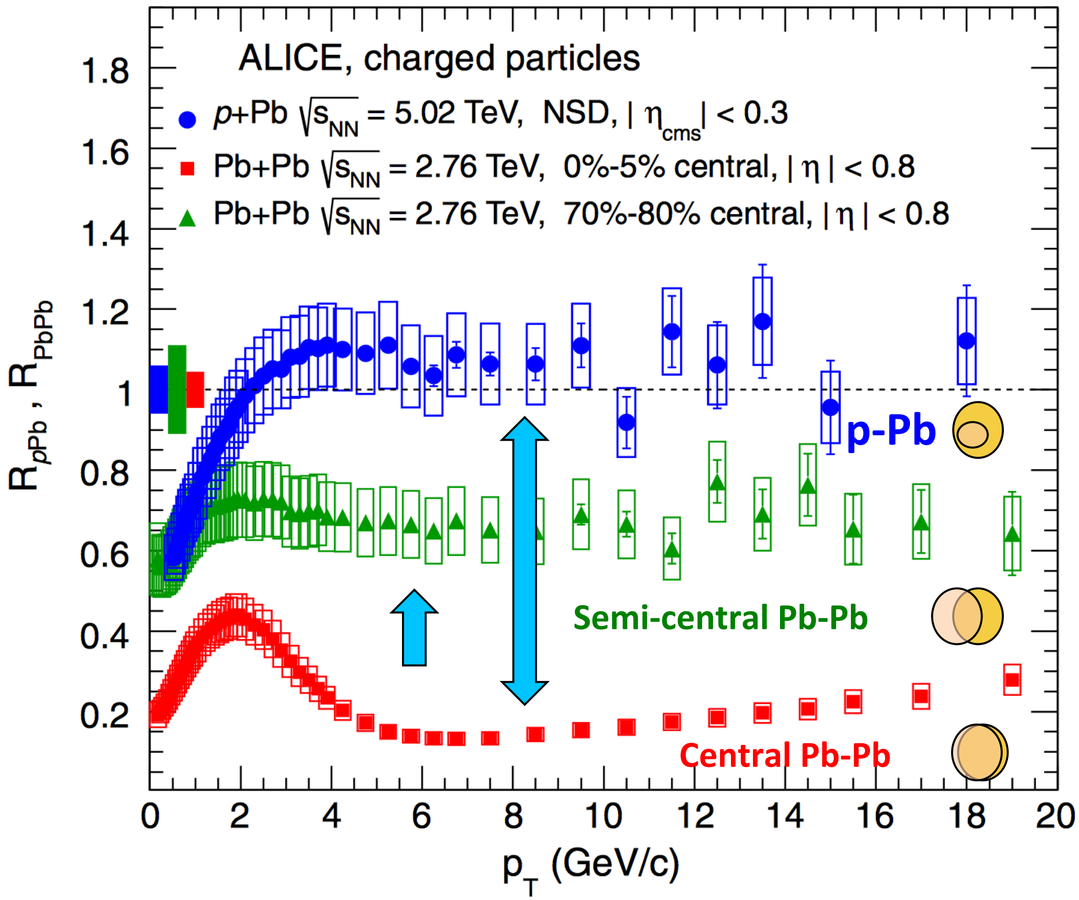

$$R_{AA}(p_T) = \frac{dN_{AA}/dp_T}{\langle N_{coll} \rangle \times dN_{pp}/dp_T}$$

Strong suppression of intermediate/ high p_T particles in central Pb-Pb collisions

Absent in p-Pb collisions (no QGP expected)

→ final-state effect

→ Evidence of in-medium partonic energy loss

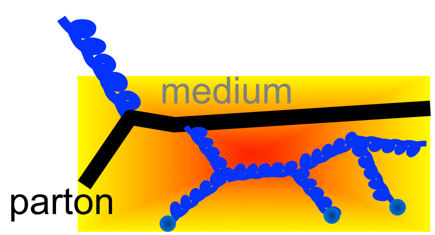

Jet quenching

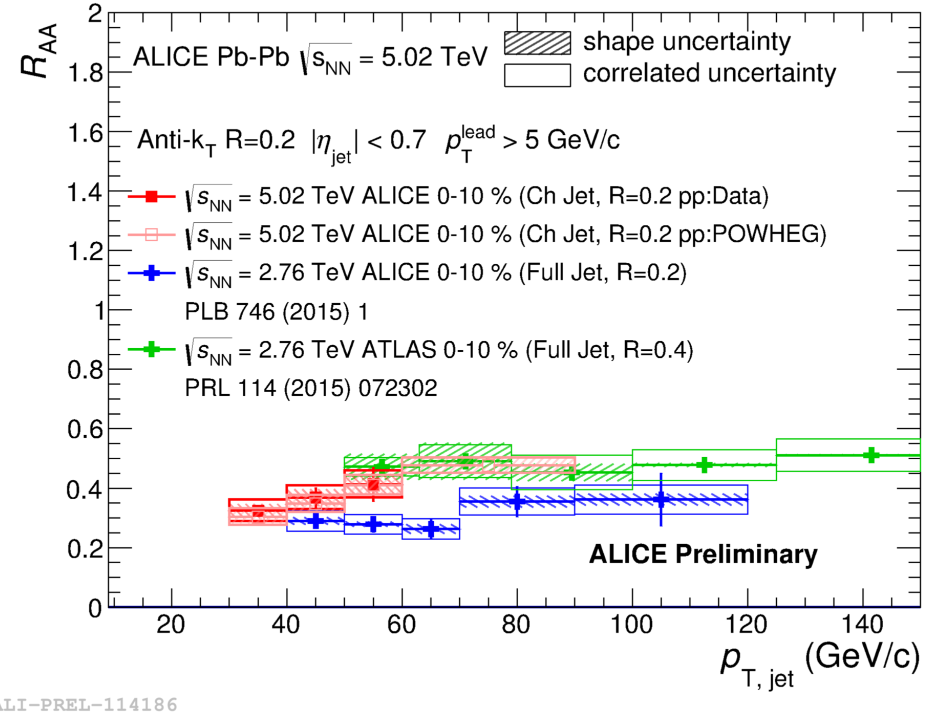

Jets are "extended" objects
→ provide complementary information to single particle observables
→Address spatial distribution and kinetic properties of radiated energy

Jet suppression → Out-of-cone radiation

Is the jet internal structure modified?

- Kinetic properties
- Spatial distribution of jet constituents
- Particle specie composition

Many studies performed/ongoing

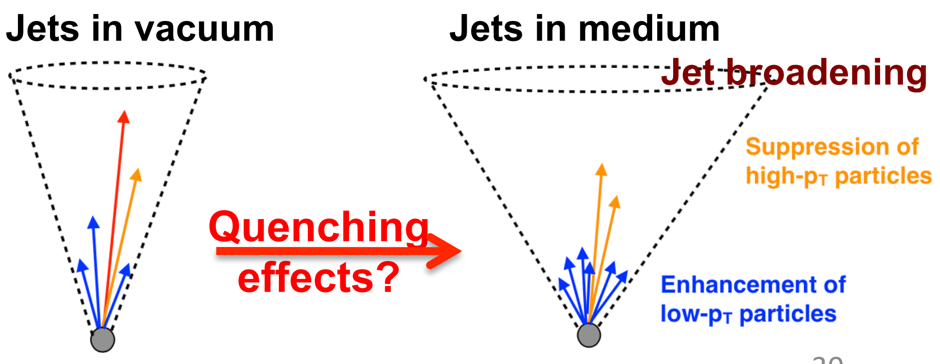

Open charm and beauty

ALICE, JHEP 1511 (2015) 205
CMS, EPJ C 77 (2017) 252

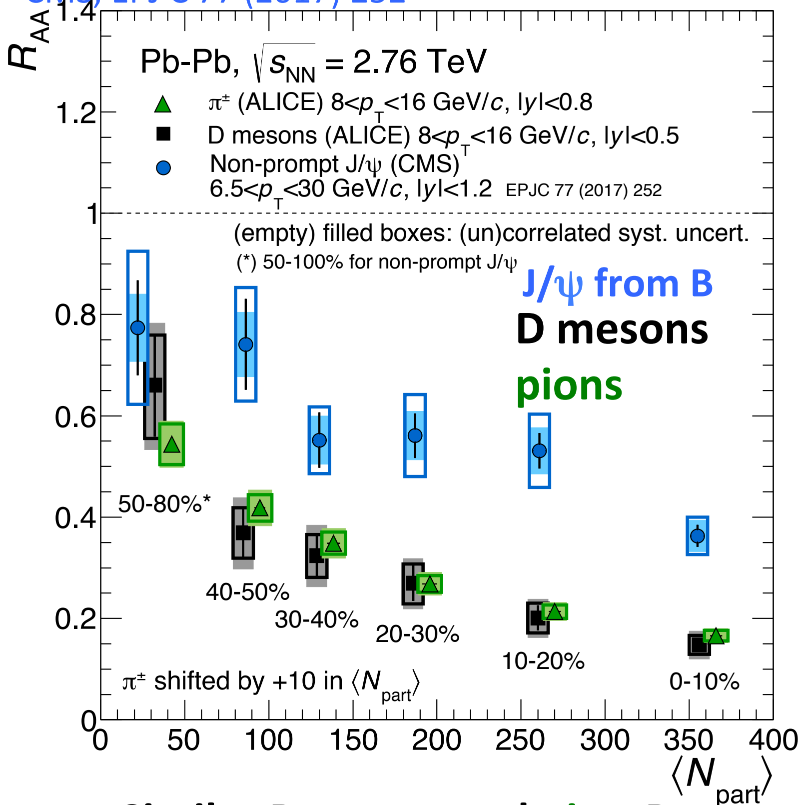

Similar D meson and pion R_{AA}
Expected from small charm-quark mass + differences between charm and gluon/LF spectra slope and fragmentation

R_{AA} (J/ψ from B) > **R_{AA}(D)** in central collisions

⇩

Indication of R_{AA} (B) > R_{AA}(D)

The different suppression and the centrality dependence as expected from **models with quark-mass dependent energy loss ($\Delta E_g > \Delta E_{lq} \geq \Delta E_c > \Delta E_b$)**

Expected from dead cone effect:

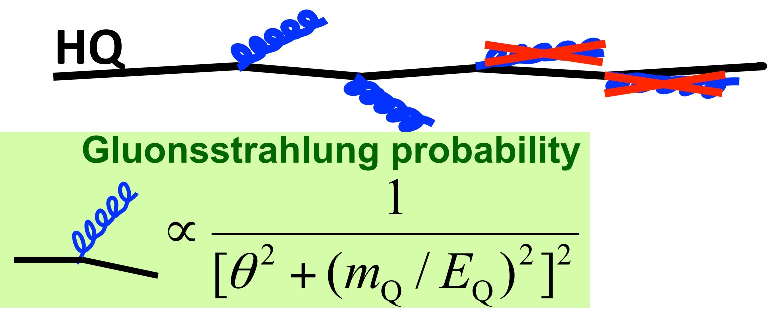

$$\propto \frac{1}{[\theta^2 + (m_Q / E_Q)^2]^2}$$

Dokshitzer, Khoze, Troyan, JPG 17 (1991) 1602.
Dokshitzer and Kharzeev, PLB 519 (2001) 199.

Open charm and beauty

Today on arxiv: arXiv:1707.01005

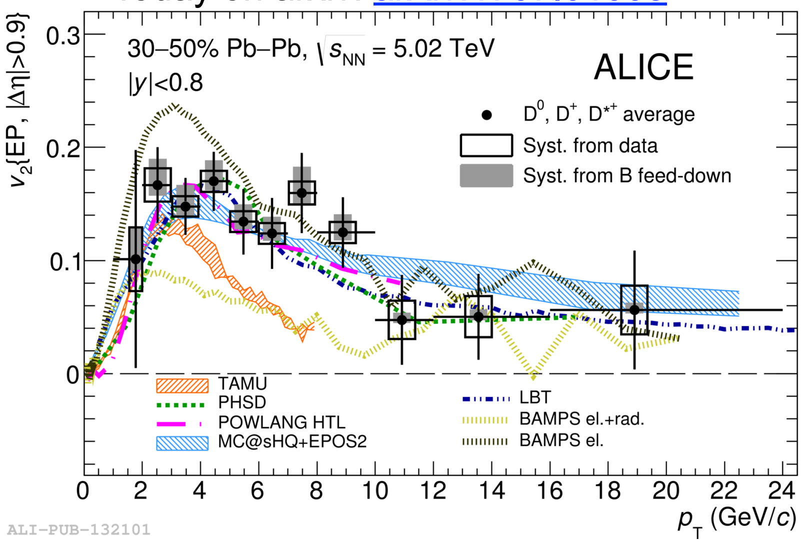

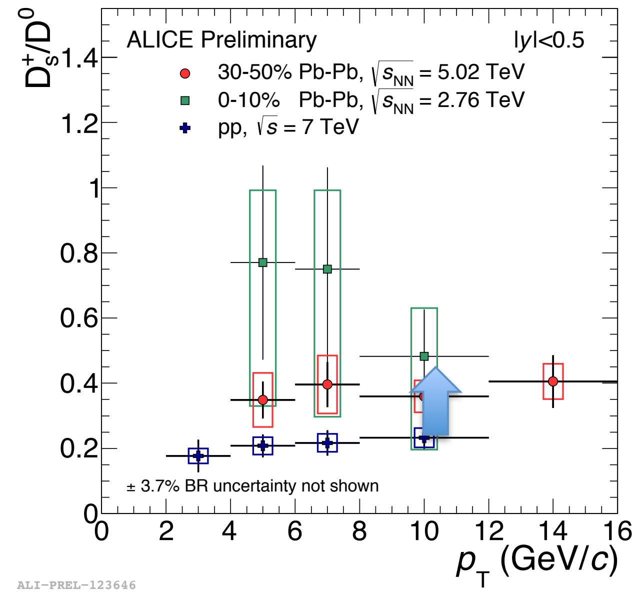

Charm flows →important constraints to models

D_s vs. non strange D: modification of particle species abundances?

→hadronisation via coalescence?

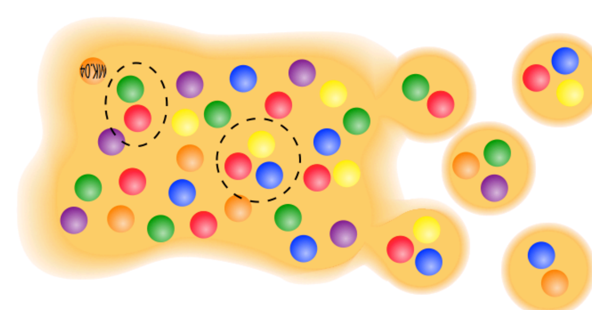

→ Charm participates to system collective motion

→ Possible thermalisation? Need more precision at low p_T

Prospects for the future

ALICE data-taking in Run-2

System	Year	$\sqrt{s_{NN}}$ (TeV)	L_{int}
pp	2015-2016	13	~14 pb^{-1}
pp	2015 (~4 days)	5.02	~100 nb^{-1}
p-Pb	2016	5.02	~3 nb^{-1}
p-Pb	2016	8.16	~20 nb^{-1}
Pb-p	2016	8.16	~20 nb^{-1}
Pb-Pb	2015	5.02	~0.4 nb^{-1}

- Goals for 2017-18:
  - Pb-Pb: reach 1/nb target
  - pp 13 TeV: reach 40/pb target
  - High statistics pp 5 TeV sample

ALICE after Run-2

new ITS

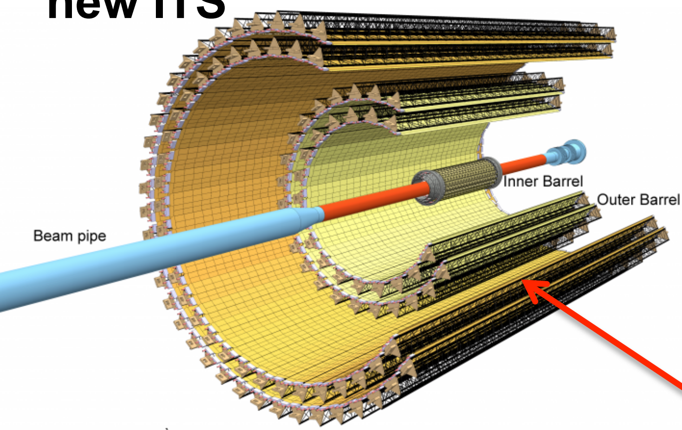

Pixel muon forward tracker

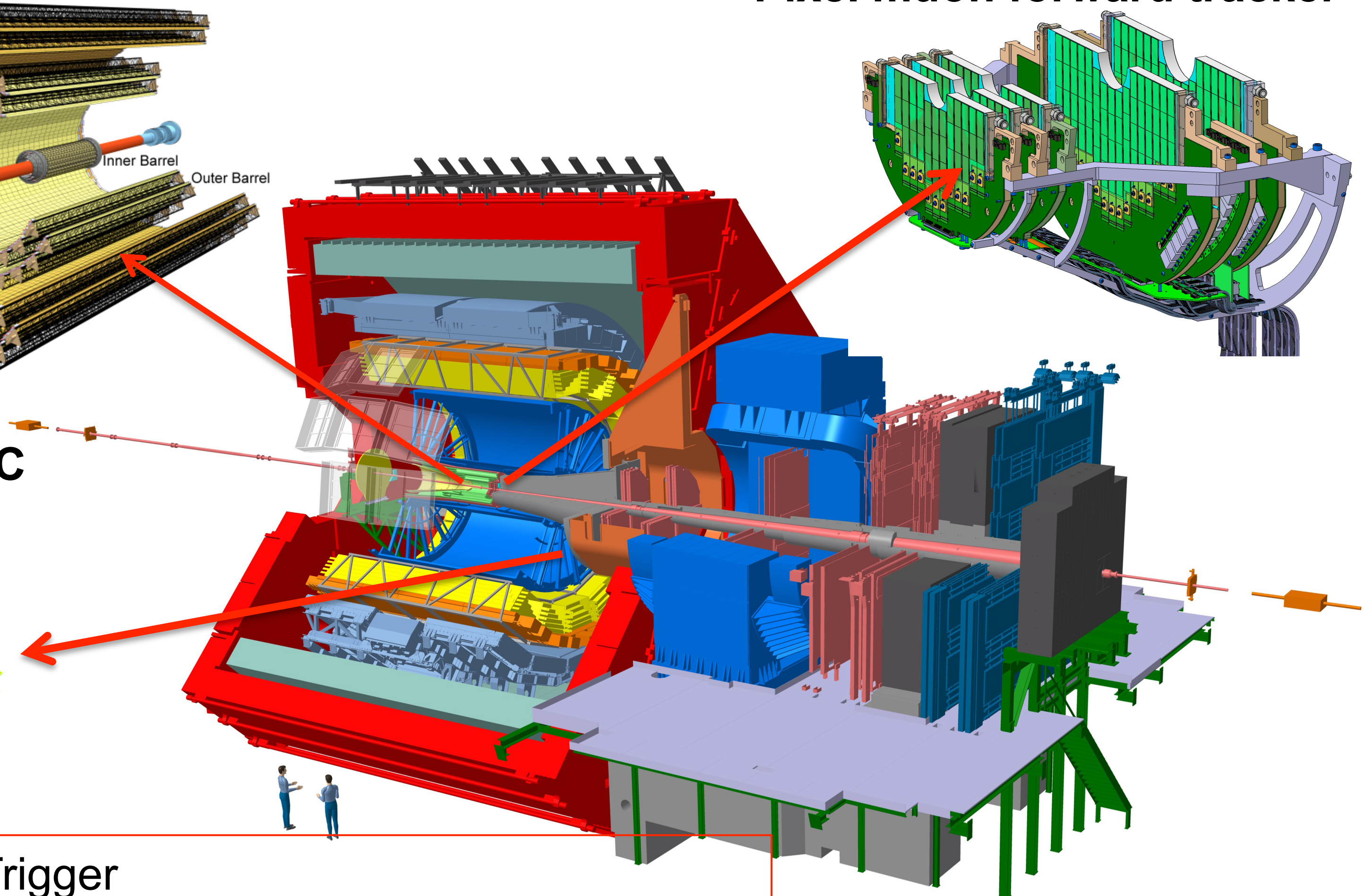

GEM-based TPC chambers

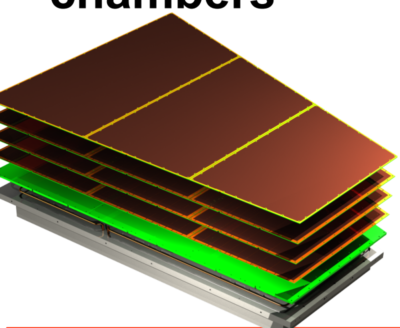

Fast Interaction Trigger
New Online-Offline system
Readout upgrade of other detectors
Goal: collect 10 nb^{-1} of min. bias Pb-Pb collisions
x100 gain w.r.t. run 1+2 for min. bias

All projects moving into production phase this year

Performance examples for HF signals

Access to charm and beauty down to very low p_T

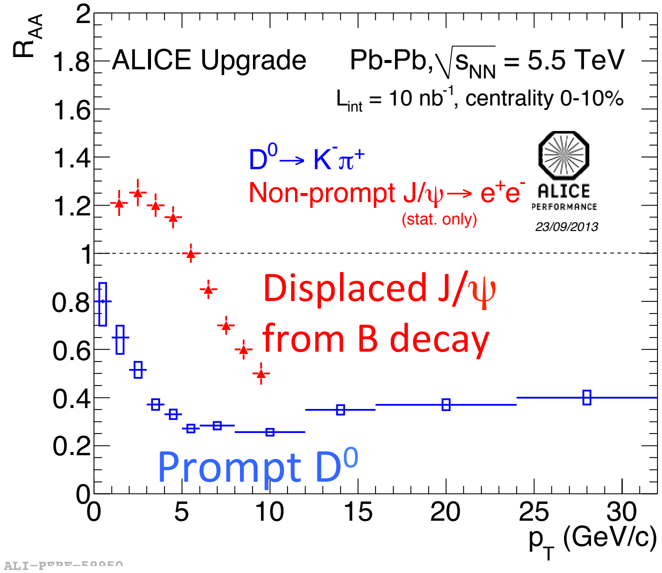

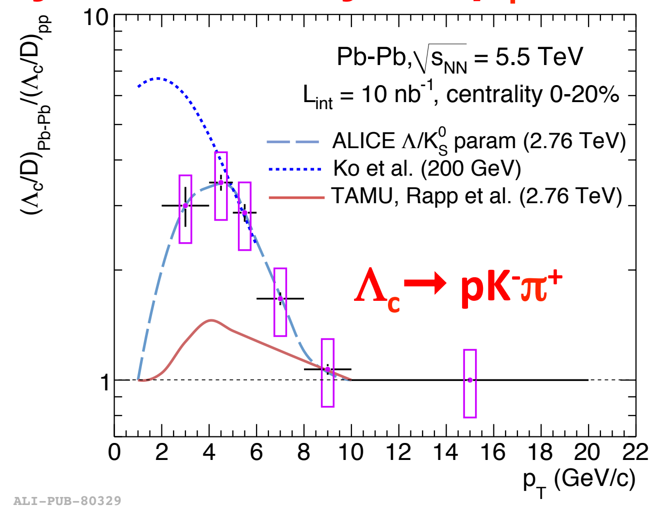

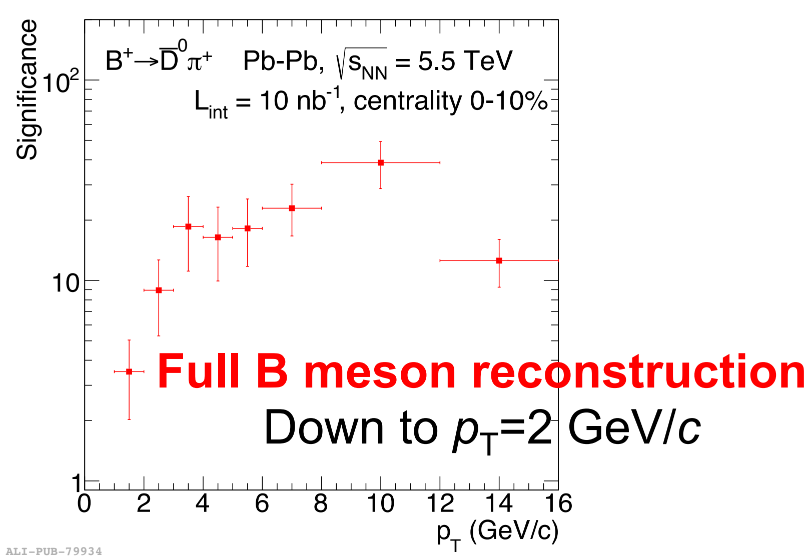

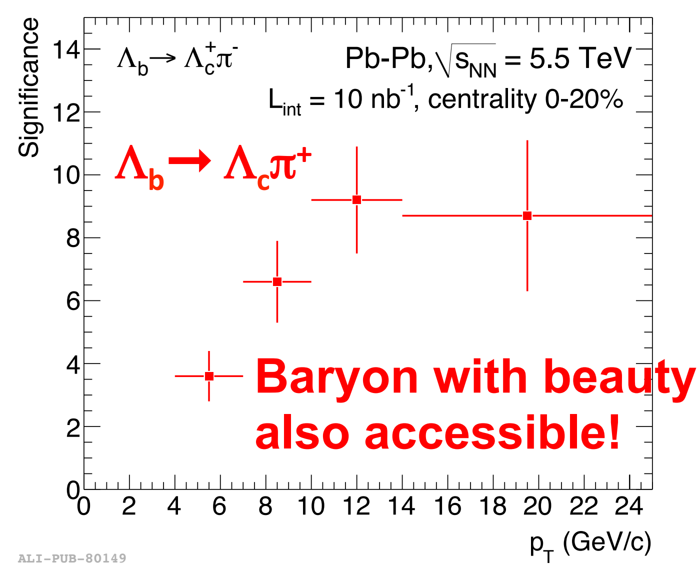

QGP in small systems?

The future has already started!!

The multi collision-system experimental approach: the initial design

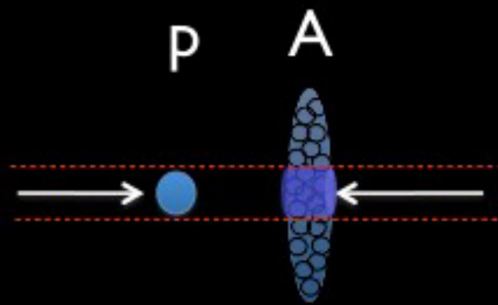

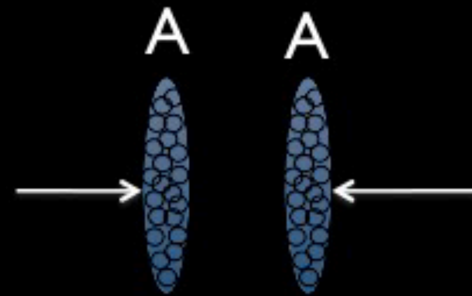

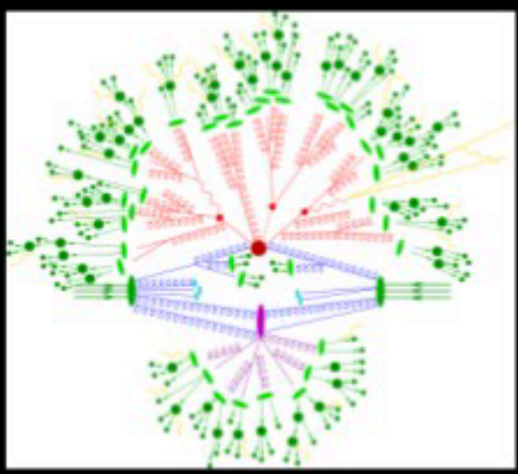

Local structure of QCD vacuum

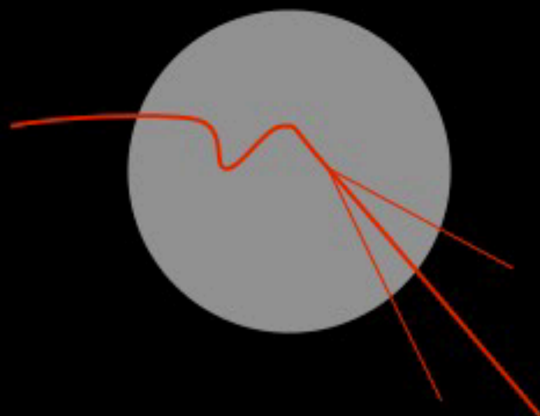

Local QCD
+
initial state/cold nuclear matter

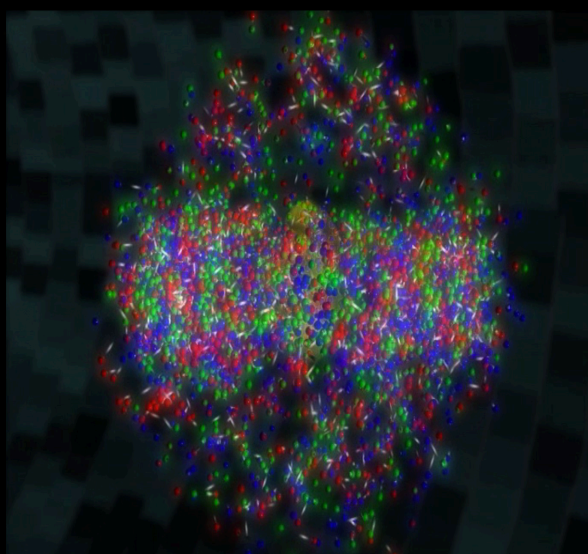

Local QCD
+
initial state/cold nuclear matter
+
Quark-Gluon Plasma

Copied by. C. Loizides who adapted it from G. Roland

Long range correlations and flow in p-Pb

ALICE, PLB 719 (2013) 29

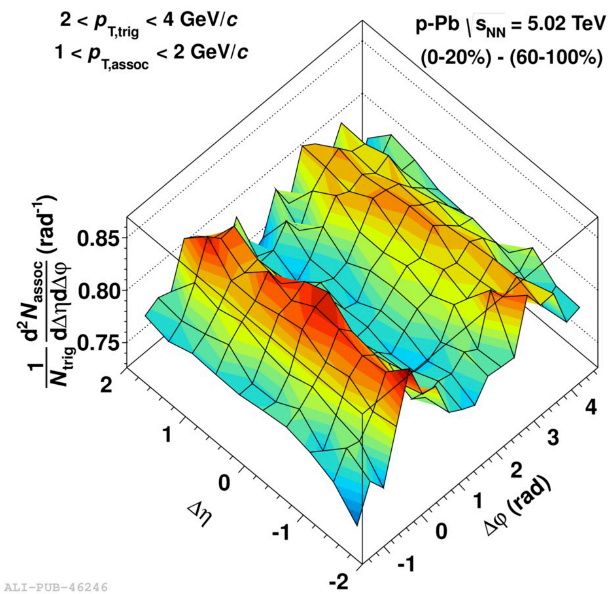

ALICE, PLB 726 (2013) 164

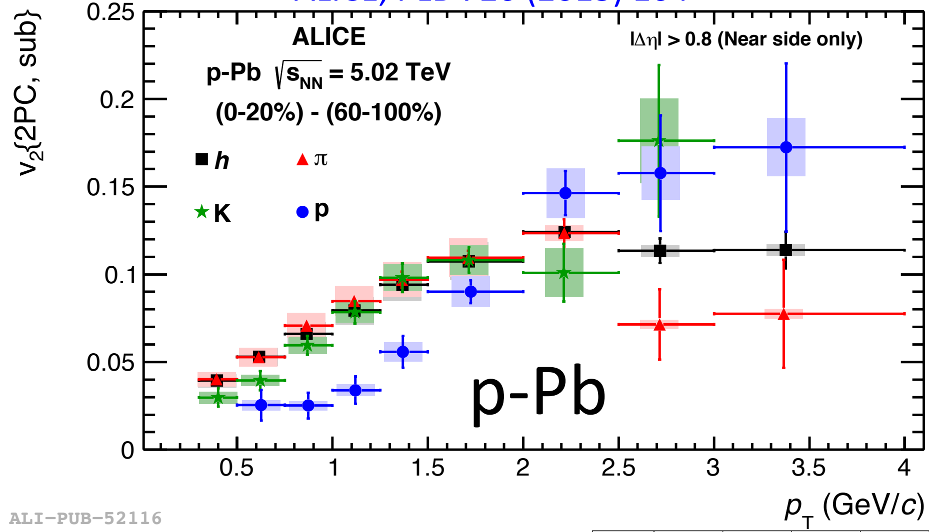

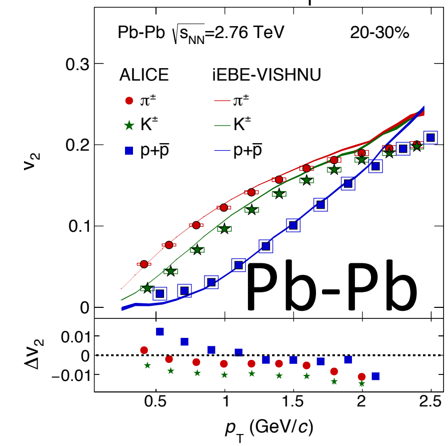

arxiv:1606.06057

Large v_2 (elliptic flow) values!

Mass ordering and "crossing" similar to Pb-Pb, where data are reproduced by hydrodynimical models

Strangeness enhancement

PLB449 (1999) 401

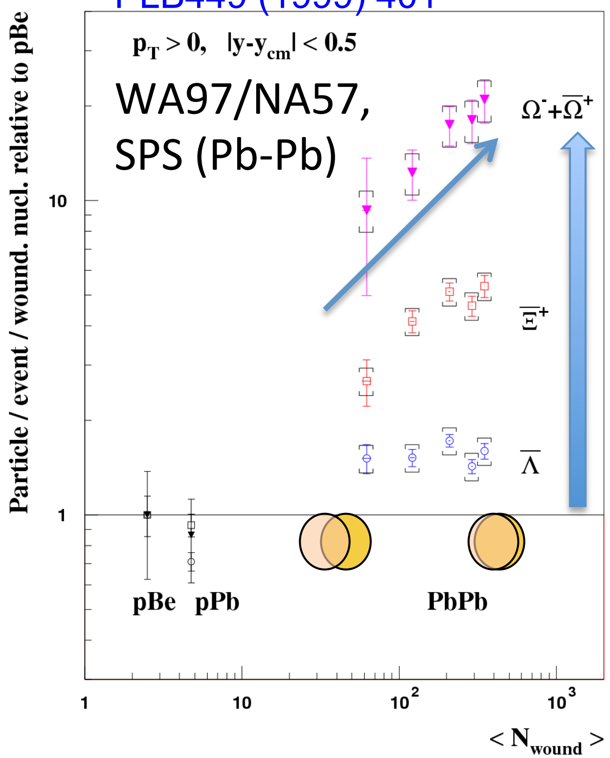

- Increase of strange particle yield with collision centrality
- Stronger effect for particles with larger strangeness content
- Historical QGP "smoking gun" (Rafelski, Müller, PRL48(1982)1066), associated with partial chiral symmetry restoration (see backup) and removal of canonical suppression

Strangene

PLB449 (1999) 401

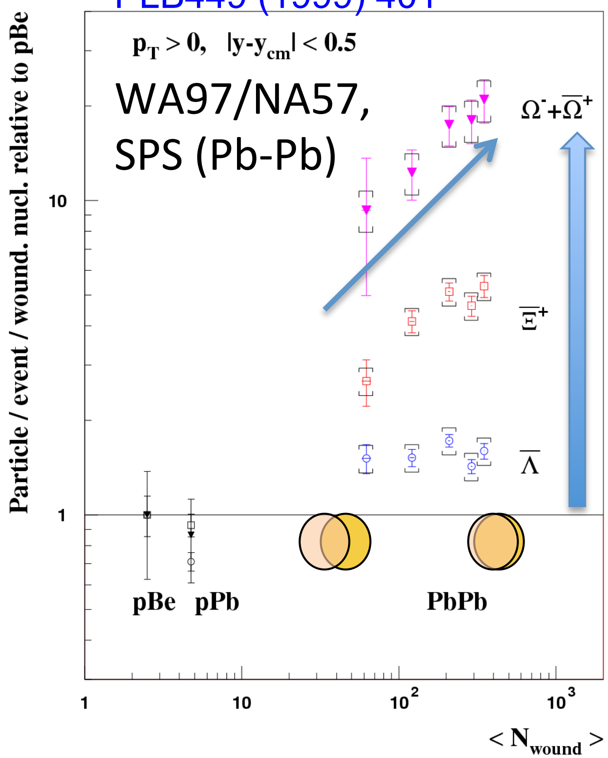

- Increase of strange particle yield v
- Stronger effect for particles with la
- Historical QGP "smoking gun" (Raf
chiral symmetry restoration (see b

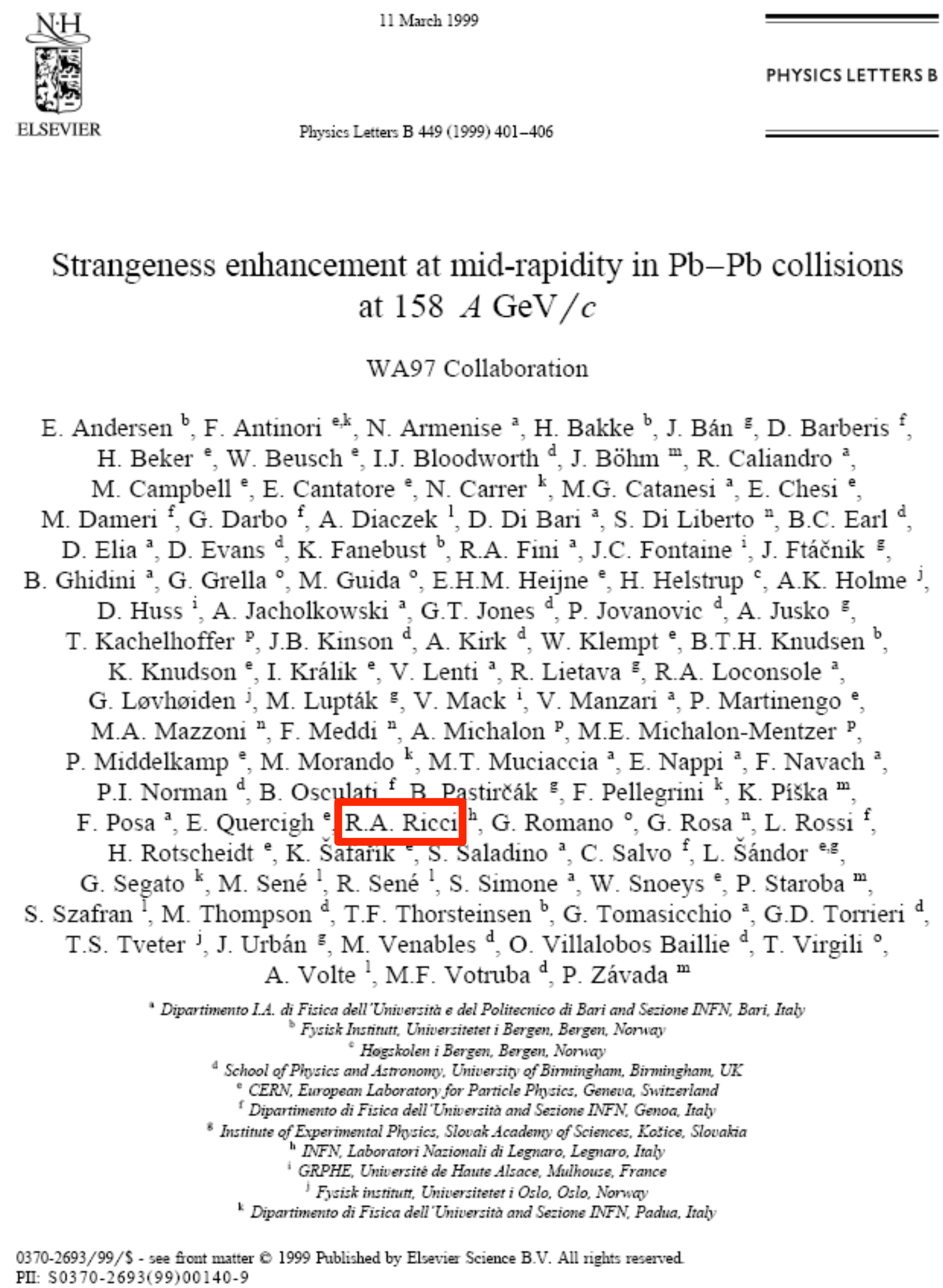

ELSEVIER

11 March 1999

PHYSICS LETTERS B

Physics Letters B 449 (1999) 401–406

Strangeness enhancement at mid-rapidity in Pb–Pb collisions at 158 A GeV/c

WA97 Collaboration

E. Andersen [b], F. Antinori [e,k], N. Armenise [a], H. Bakke [b], J. Bán [g], D. Barberis [f], H. Beker [e], W. Beusch [e], I.J. Bloodworth [d], J. Böhm [m], R. Caliandro [a], M. Campbell [e], E. Cantatore [e], N. Carrer [k], M.G. Catanesi [a], E. Chesi [e], M. Dameri [f], G. Darbo [f], A. Diaczek [l], D. Di Bari [a], S. Di Liberto [n], B.C. Earl [d], D. Elia [a], D. Evans [d], K. Fanebust [b], R.A. Fini [a], J.C. Fontaine [i], J. Ftáčnik [g], B. Ghidini [a], G. Grella [o], M. Guida [o], E.H.M. Heijne [e], H. Helstrup [c], A.K. Holme [j], D. Huss [i], A. Jacholkowski [a], G.T. Jones [d], P. Jovanovic [d], A. Jusko [g], T. Kachelhoffer [p], J.B. Kinson [d], A. Kirk [d], W. Klempt [e], B.T.H. Knudsen [b], K. Knudson [e], I. Králik [e], V. Lenti [a], R. Lietava [g], R.A. Loconsole [a], G. Løvhøiden [j], M. Lupták [g], V. Mack [i], V. Manzari [a], P. Martinengo [e], M.A. Mazzoni [n], F. Meddi [n], A. Michalon [p], M.E. Michalon-Mentzer [p], P. Middelkamp [e], M. Morando [k], M.T. Muciaccia [a], E. Nappi [a], F. Navach [a], P.I. Norman [d], B. Osculati [f], B. Pastirčák [g], F. Pellegrini [k], K. Píška [m], F. Posa [a], E. Quercigh [e], R.A. Ricci [h], G. Romano [o], G. Rosa [n], L. Rossi [f], H. Rotscheidt [e], K. Šafařík [e], S. Saladino [a], C. Salvo [f], L. Šándor [e,g], G. Segato [k], M. Sené [l], R. Sené [l], S. Simone [a], W. Snoeys [e], P. Staroba [m], S. Szafran [l], M. Thompson [d], T.F. Thorsteinsen [b], G. Tomasicchio [a], G.D. Torrieri [d], T.S. Tveter [j], J. Urbán [g], M. Venables [d], O. Villalobos Baillie [d], T. Virgili [o], A. Volte [l], M.F. Votruba [d], P. Závada [m]

[a] Dipartimento I.A. di Fisica dell'Università e del Politecnico di Bari and Sezione INFN, Bari, Italy
[b] Fysisk Institutt, Universitetet i Bergen, Bergen, Norway
[c] Høgskolen i Bergen, Bergen, Norway
[d] School of Physics and Astronomy, University of Birmingham, Birmingham, UK
[e] CERN, European Laboratory for Particle Physics, Geneva, Switzerland
[f] Dipartimento di Fisica dell'Università and Sezione INFN, Genoa, Italy
[g] Institute of Experimental Physics, Slovak Academy of Sciences, Košice, Slovakia
[h] INFN, Laboratori Nazionali di Legnaro, Legnaro, Italy
[i] GRPHE, Université de Haute Alsace, Mulhouse, France
[j] Fysisk institutt, Universitetet i Oslo, Oslo, Norway
[k] Dipartimento di Fisica dell'Università and Sezione INFN, Padua, Italy

PII: S0370-2693(99)00140-9

Strangeness enhancement

PLB449 (1999) 401

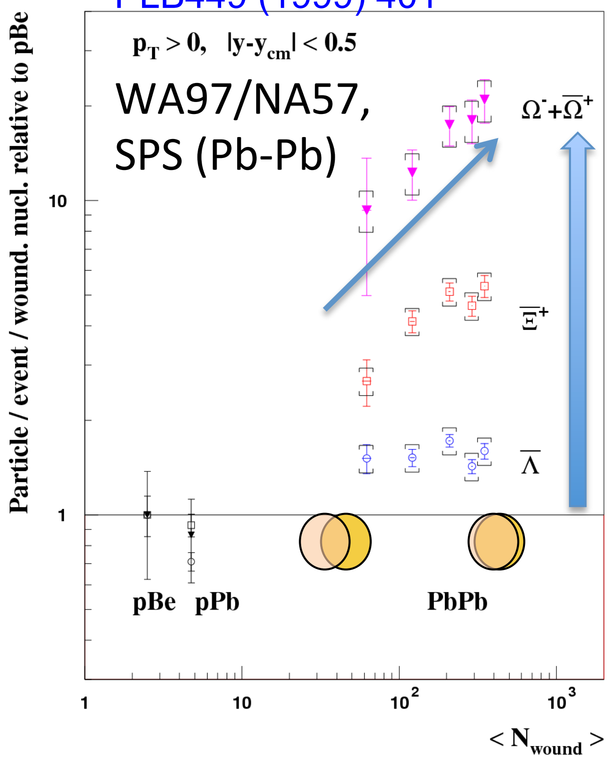

Nature Physics (2017) doi:10.1038/nphys4111

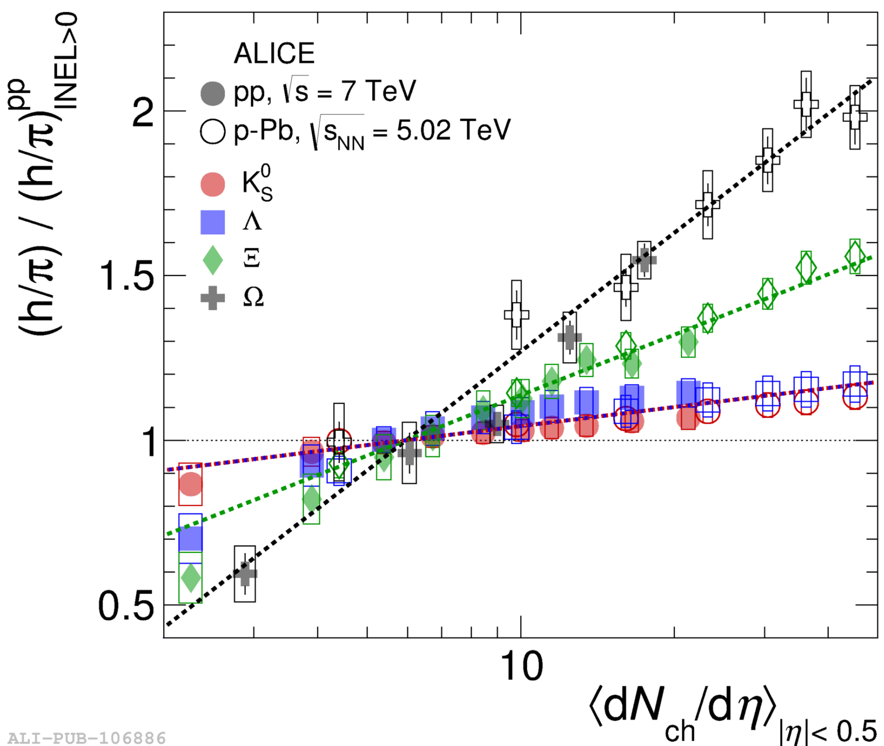

- Increase of strange particle yield with collision centrality
- Stronger effect for particles with larger strangeness content
- Historical QGP "smoking gun" (Rafelski, Müller, PRL48(1982)1066), associated with partial chiral symmetry restoration (see backup) and removal of canonical suppression

Now observed also in pp collisions at high multiplicity

→ New research direction

Summary

… only a snapshot of the main results presented

After 30 years of studies QGP formation in heavy-ion collisions quite established

The experimental goal is now to measure precisely its properties and achieve a comprehensive microscopic description of the medium

- Event-by-event studies and fluctuations
- Push precision for particle chemistry (baryon/mesons, resonances,…)
- Hard-probes: still much room for improving precision and for more differential measurements → still a lot to learn!

Recent years: indication of collective QGP-like effects in small collision systems with particle multiplicity a possible “collant”/common scale

→ Really QGP in pp/p-A collisions?

→ Possibility to study onset of these phenomena?

→ New research direction

A lot of work for ongoing and future/upgraded experiments!

SPARES

System size: HBT interferometry

Hanbury-Brown and Twiss

"Bose-Einstein" enhancement in the momentum correlation of identical bosons emitted close in phase ⟶ Probe "homogeneity emission region" and decoupling time

source emitting particles

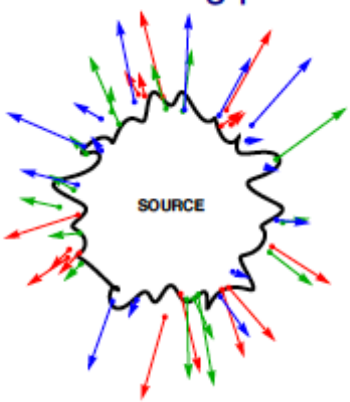

two identical pions, $\pi^+\pi^+$, $\pi^-\pi^-$

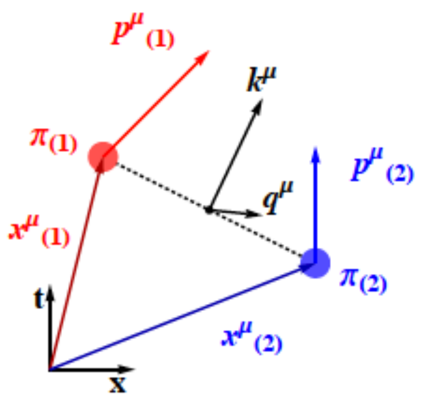

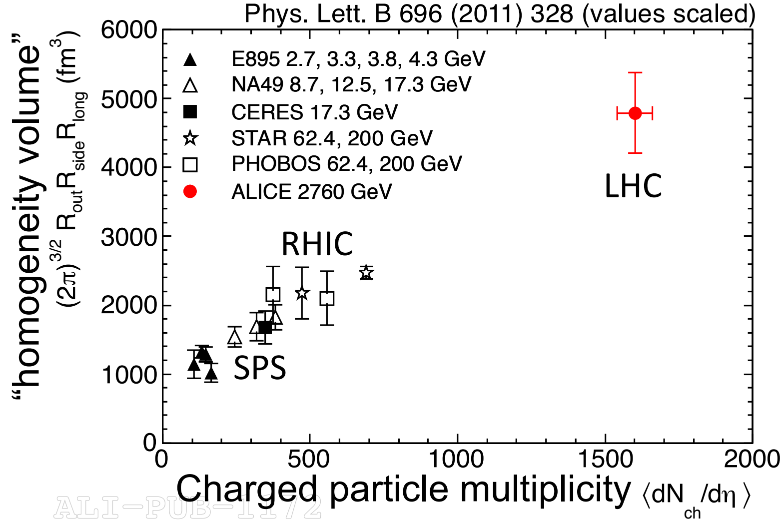

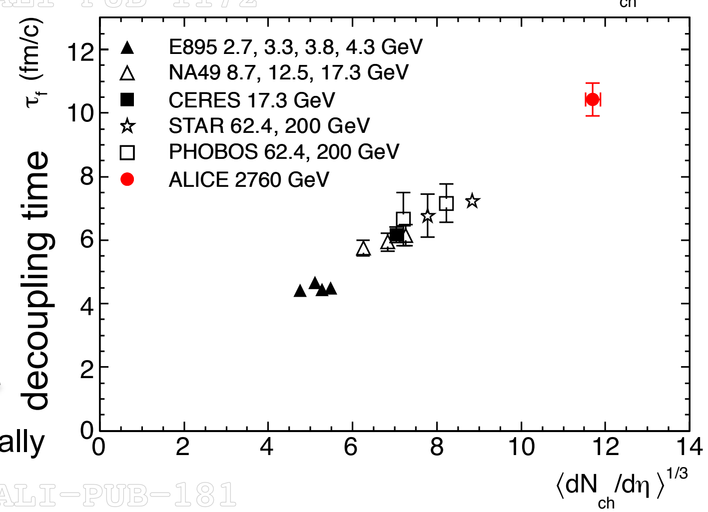

From R_{long}, assuming longitudinally expanding emission source

$R_{out} \sim R_{side} \sim 6$ fm

$R_{long} \sim 8$ fm

As expected, larger-size and longer living system produced at the LHC

Energy density

- Particle multiplicity at mid-rapidity → transverse energy density

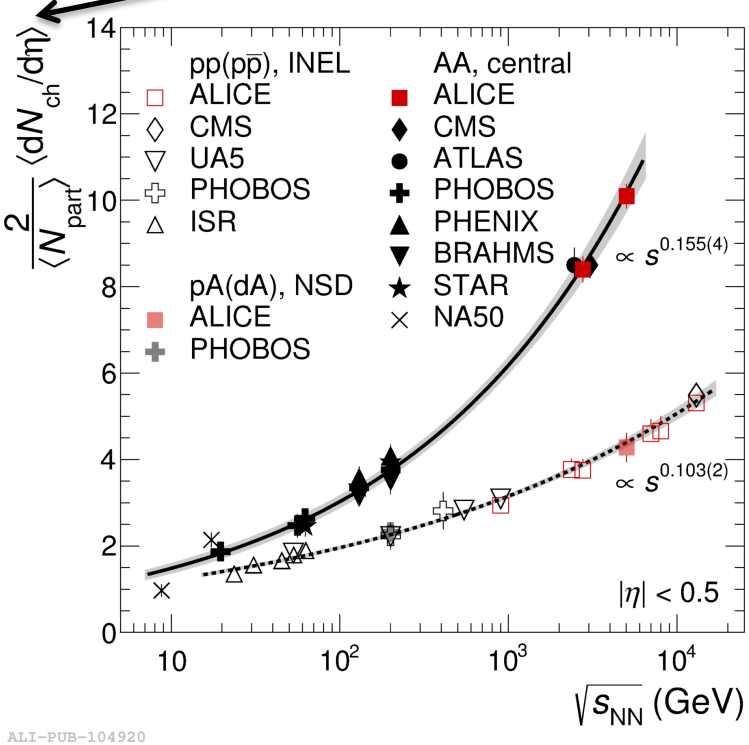

Phys. Rev. Lett. 116 (2016) 222302

Bjorken formula:

$$\varepsilon = \frac{E}{V} = \frac{1}{Sc\tau_0} \frac{dE_T}{dy}\bigg|_{y=0}$$

S = transverse dimension of nucleus

τ_0 = "formation time" ~1 fm/c

	SPS	RHIC	LHC
$\frac{dE_T}{dy}\Big\|_{y=o}$ (GeV) *	400	800	2000
ε (GeV/fm^3) *	2.5	5	12

*Indicative numbers

More than enough for deconfinement!

ε_c ~ 0.6 GeV/fm^3

Thermal model and chemical freeze-out temperature

Chemical freeze-out temperature estimated from **relative particle abundances**
Model assuming statistical hadronization: particle abundances determined by their mass and quantum numbers (spin) at by system properties (T_{ch},u_B,..)

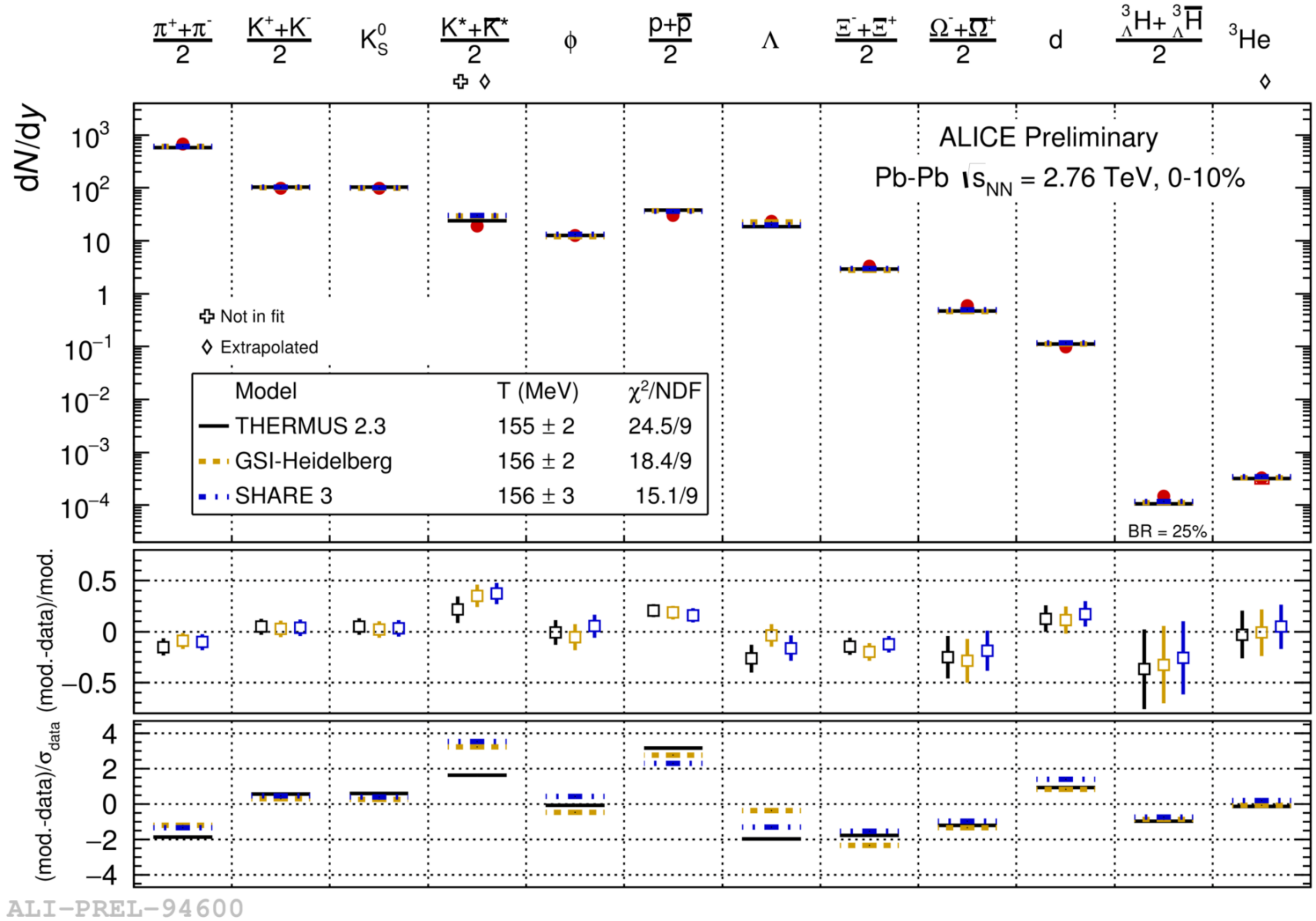

Hadron yields described assuming chemical equilibrium and T_{ch}~156 MeV → close to lattice QCD expectation for T_{crit}

Some tension for protons and K*

Kinetic freeze-out temperature

Phys. Rev. C 88, 044910 (2013)

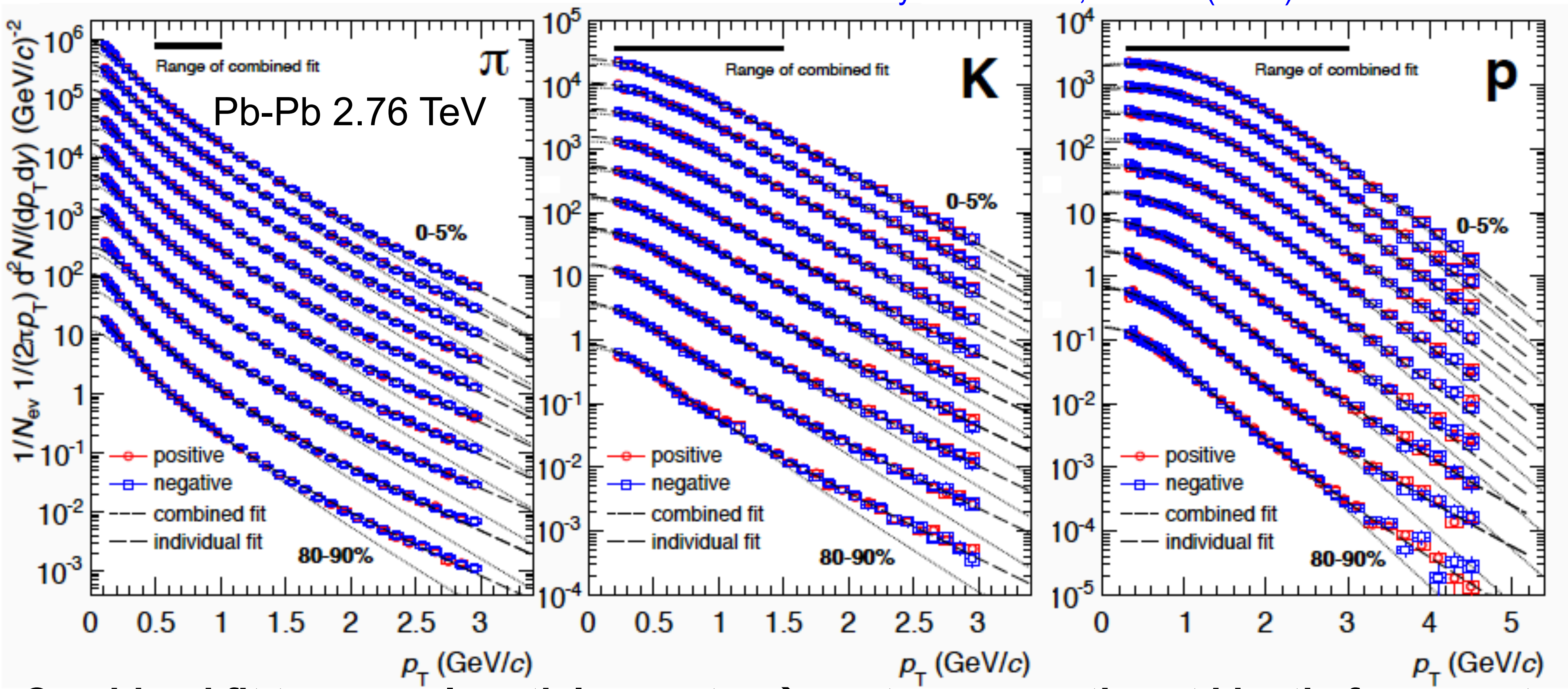

Combined fit to several particle spectra → system properties at kinetic freeze-out

"Blast-wave" model: thermalized volume elements expanding in a common velocity field (→ convolution of thermal velocity with expansion velocity)

- Goodness of the global fit → hydro-dynamical description holds

Kinetic freeze-out temperature

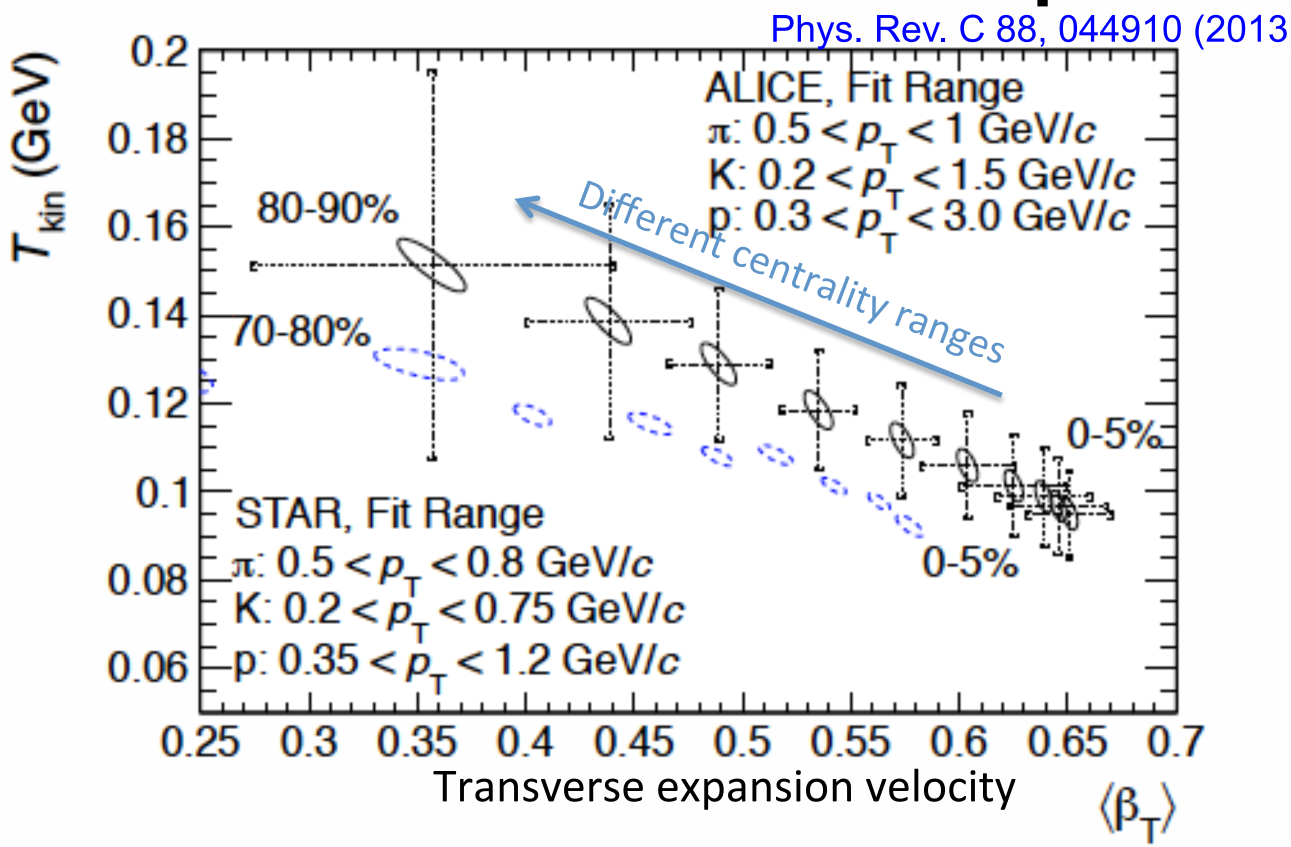

Combined fit to several particle spectra → system properties at kinetic freeze-out
"Blast-wave" model: thermalized volume elements expanding in a common velocity field (→ convolution of thermal velocity with expansion velocity)

- Goodness of the global fit → hydro-dynamical description holds
- In central collisions at LHC: $\boldsymbol{T_{kin}}$ **~ 90 MeV, transverse expansion velocity ~0.65 *c***

Elliptic flow at 5 TeV

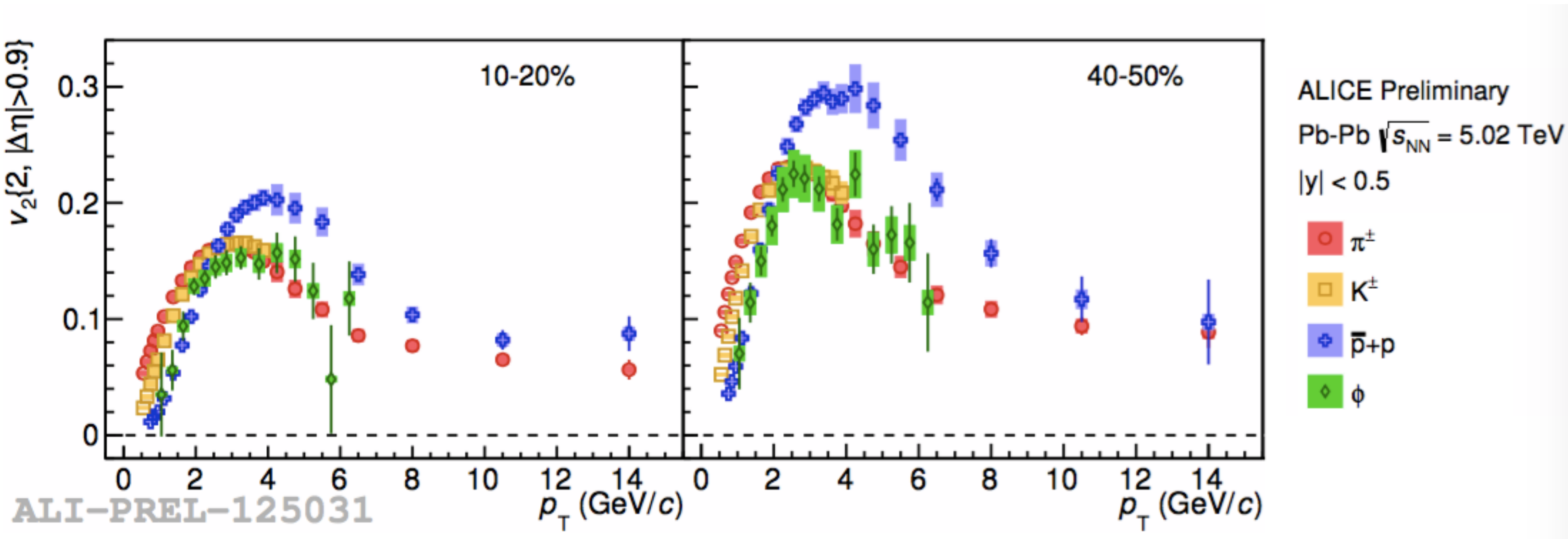

ϕ flow vs. p_T:

- Mass ordering at low p_T
- Baryon vs. meson grouping at higher p_T (2-6 GeV/c)

Quark-level flow + recombination?

Temperature from Photon spectrum

- Photons in heavy-ion collisions
  - Photons from QCD hard scattering: power law spectrum – dominant at high p_T
  - Thermal photons, emitted by the hot system (analogy with black body radiation): exponential spectrum – dominant at low p_T
    - From inverse slope:

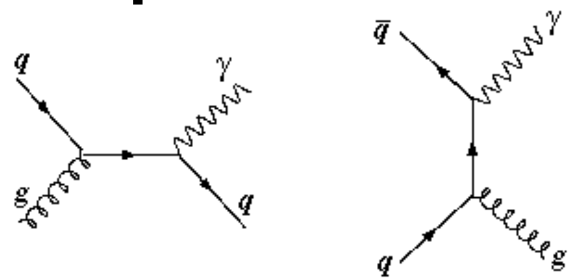

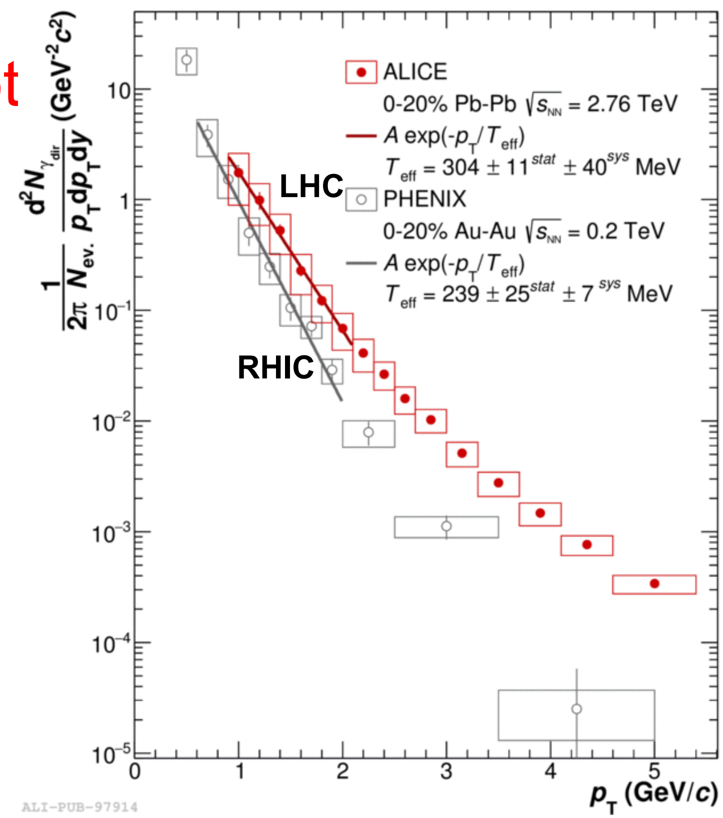

$T_{eff}{}^{*}$ **= 304 ± 41 MeV**
~ 2 T_c **(**T_c**~160 MeV)**
~ 1.25 x T_{eff}**(RHIC)**

* "Average" over whole medium evolution

ALICE, Phys.Lett. B754 (2016) 235

J/ψ elliptic flow

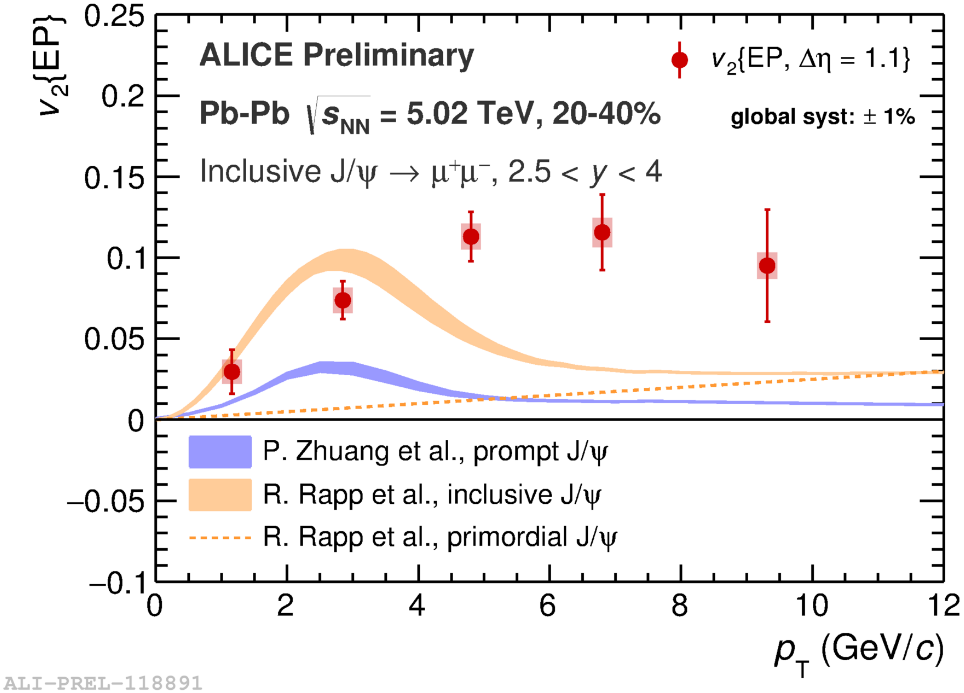

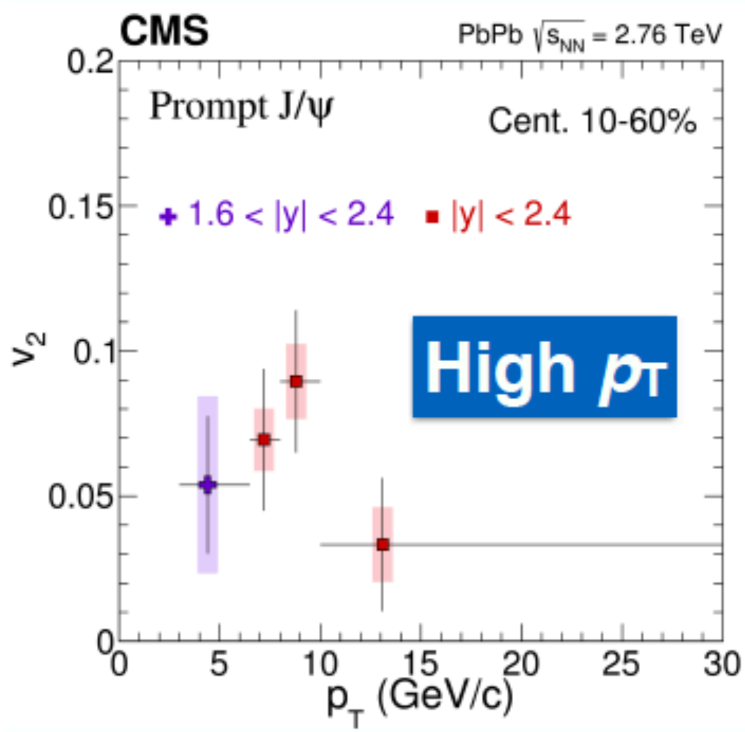

EPJC 77 (2017) 252

Positive J/ψ elliptic flow
Expected for J/ψ from recombination
Remains high at high p_T → not expected from models

QGP tomography with heavy quarks

- Early production in hard-scattering processes with high Q^2
- Production cross sections calculable with pQCD
- Strongly interacting with the medium
- Hard fragmentation ➜ measured meson properties closer to parton ones

at all p_T for charm and beauty (large masses >> Λ_{QCD})

⇨ **"Calibrated probes" of the medium**

Study parton interaction with the medium

- **energy loss via radiative** ("gluon Bremsstrahlung")

  collisional processes

  - path length and medium density
  - **color charge** (Casimir factor)
  - **quark mass** (e.g. from dead-cone effect)

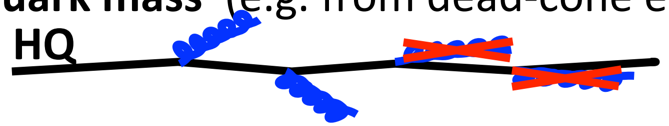

Gluonsstrahlung probability

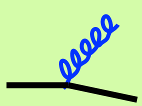

$$\propto \frac{1}{[\theta^2 + (m_Q / E_Q)^2]^2}$$

Dokshitzer, Khoze, Troyan, JPG 17 (1991) 1602.
Dokshitzer and Kharzeev, PLB 519 (2001) 199.

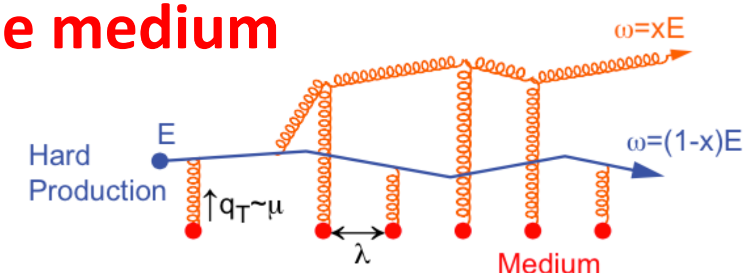

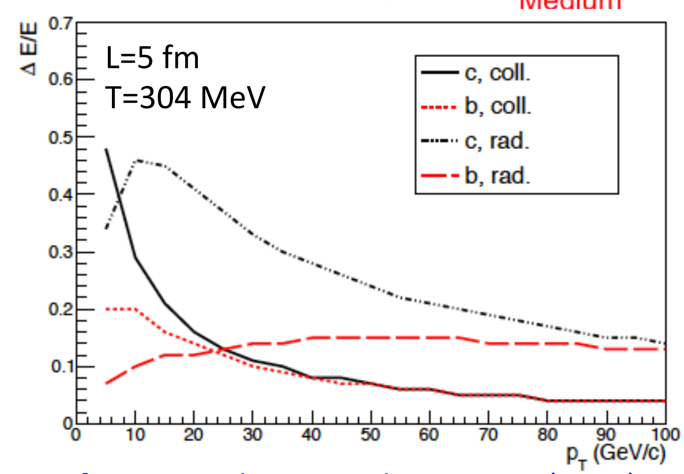

Figure from A. Andronic *et al.*, EPJC C76 (2016)
M. Djordjevic, Phys. Rev. C80 064909 (2009), Phys. Rev. C74 064907 (2006).

QGP tomography with heavy quarks

- Early production in hard-scattering processes with high Q^2
- Production cross sections calculable with pQCD
- Strongly interacting with the medium
- Hard fragmentation ➜ measured meson properties closer to parton ones

at all p_T for charm and beauty (large masses >> Λ_{QCD})

⇨ **"Calibrated probes" of the medium**

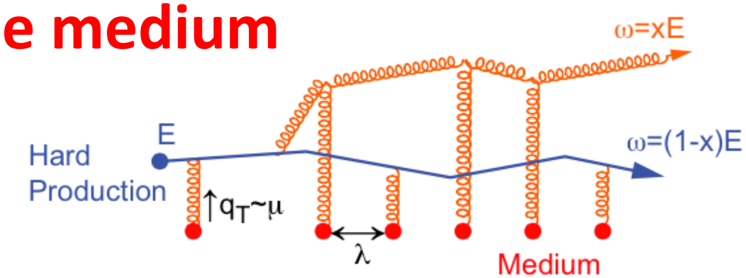

Study parton interaction with the medium

- **energy loss via radiative** ("gluon Bremsstrahlung")
  collisional processes
  - path length and medium density
  - **color charge** (Casimir factor)
  - **quark mass** (e.g. from dead-cone effect)

$$\Delta E_g > \Delta E_{u,d,s} > \Delta E_c > \Delta E_b$$

- medium **modification to HF hadron formation**
  - hadronization via quark coalescence

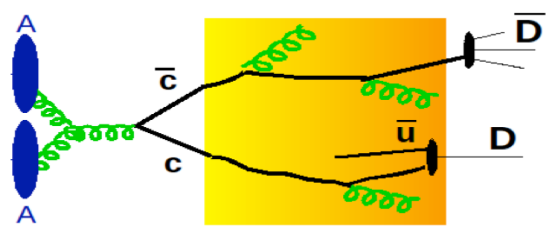

- participation in collective motion ➜ azimuthal anisotropy of produced particle

Open charm and beauty

ALICE, JHEP 1511 (2015) 205
CMS, EPJ C 77 (2017) 252

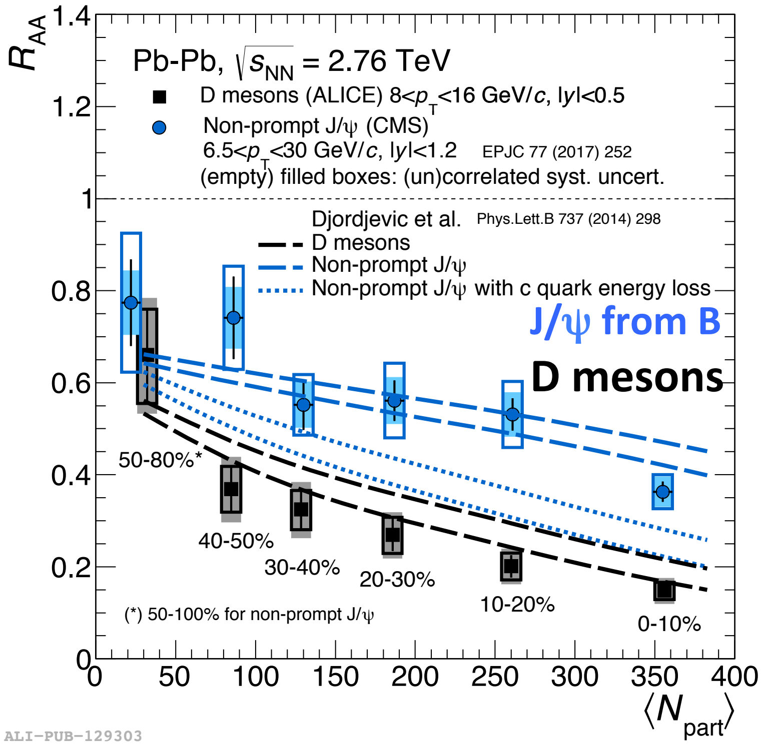

Similar D meson and pion R_{AA}
Expected from small charm-quark mass + differences between charm and gluon/LF spectra slope and fragmentation

R_{AA} (J/ψ from B) > **R_{AA}(D)** in central collisions

Indication of R_{AA} (B) > R_{AA}(D)

The different suppression and the centrality dependence as expected from **models with quark-mass dependent energy loss ($\Delta E_g > \Delta E_{lq} \geq \Delta E_c > \Delta E_b$)**

Expected from dead cone effect:

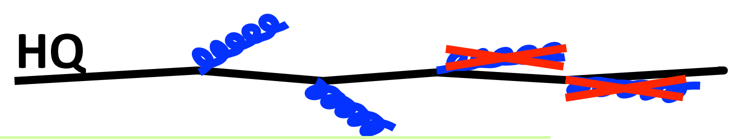

Gluonsstrahlung probability

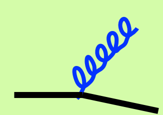

$$\propto \frac{1}{[\theta^2 + (m_Q / E_Q)^2]^2}$$

Dokshitzer, Khoze, Troyan, JPG 17 (1991) 1602.
Dokshitzer and Kharzeev, PLB 519 (2001) 199.

Open charm and beauty

Today on arxiv: arXiv:1707.01005

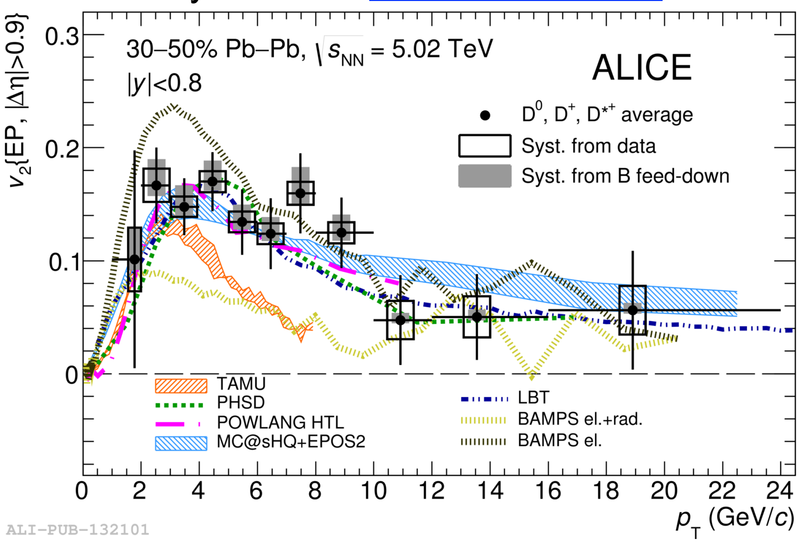

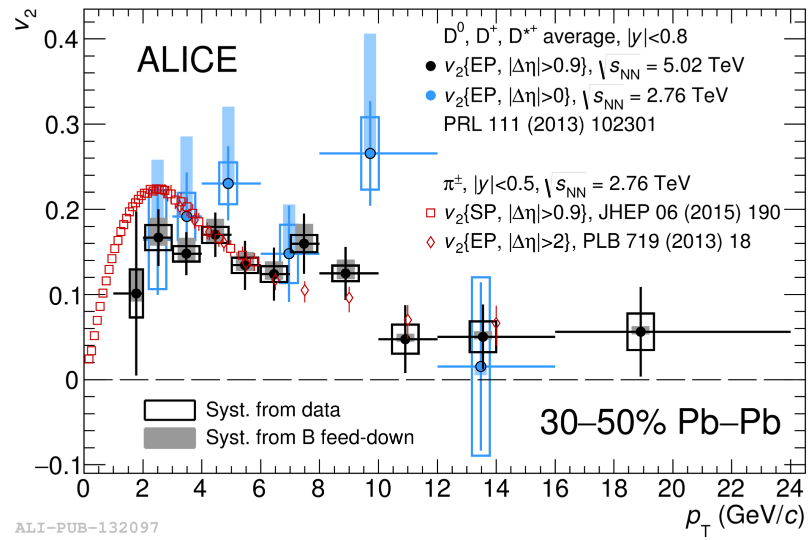

Charm flows →important constraints to models

D_s vs. non strange D: modification of particle species abundances?

→hadronisation via coalescence?

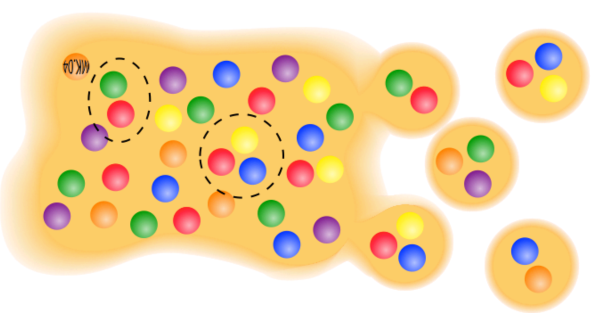

→ Charm participates to system collective motion

→ Possible thermalisation? Need more precision at low p_T

QGP tomography with high-energy partons

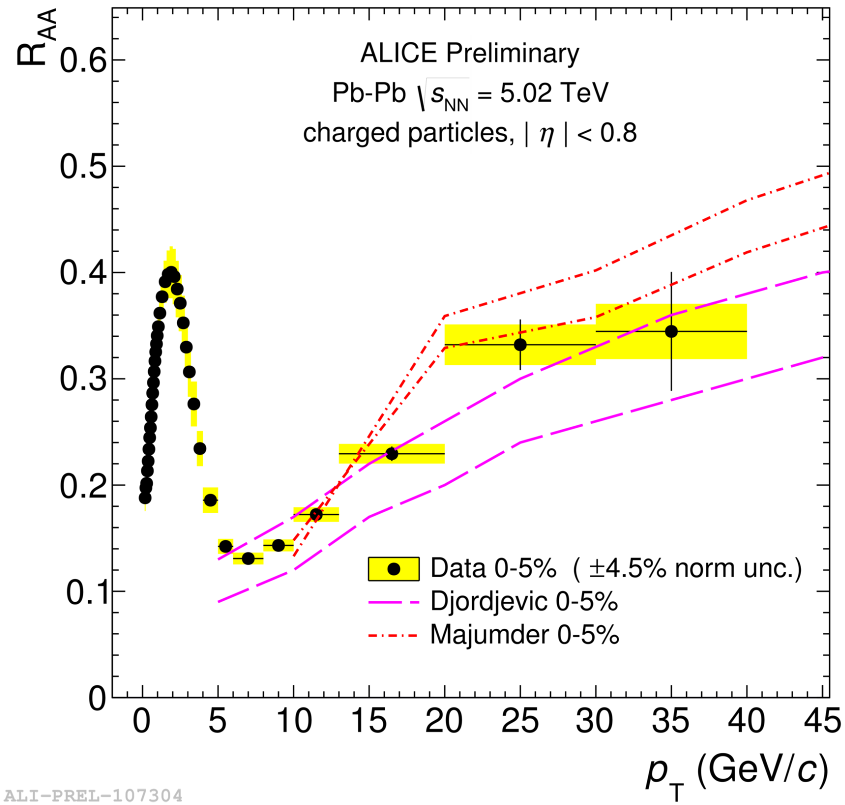

Very similar result at 5 TeV (run-2)

Strong suppression of intermediate/ high p_T particles in central Pb-Pb collisions

Absent in p-Pb collisions (no QGP expected)

→ final-state effect

→ Evidence of in-medium partonic energy loss

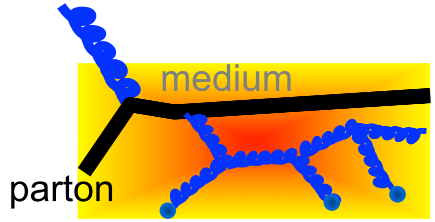

QGP tomography with high-energy partons

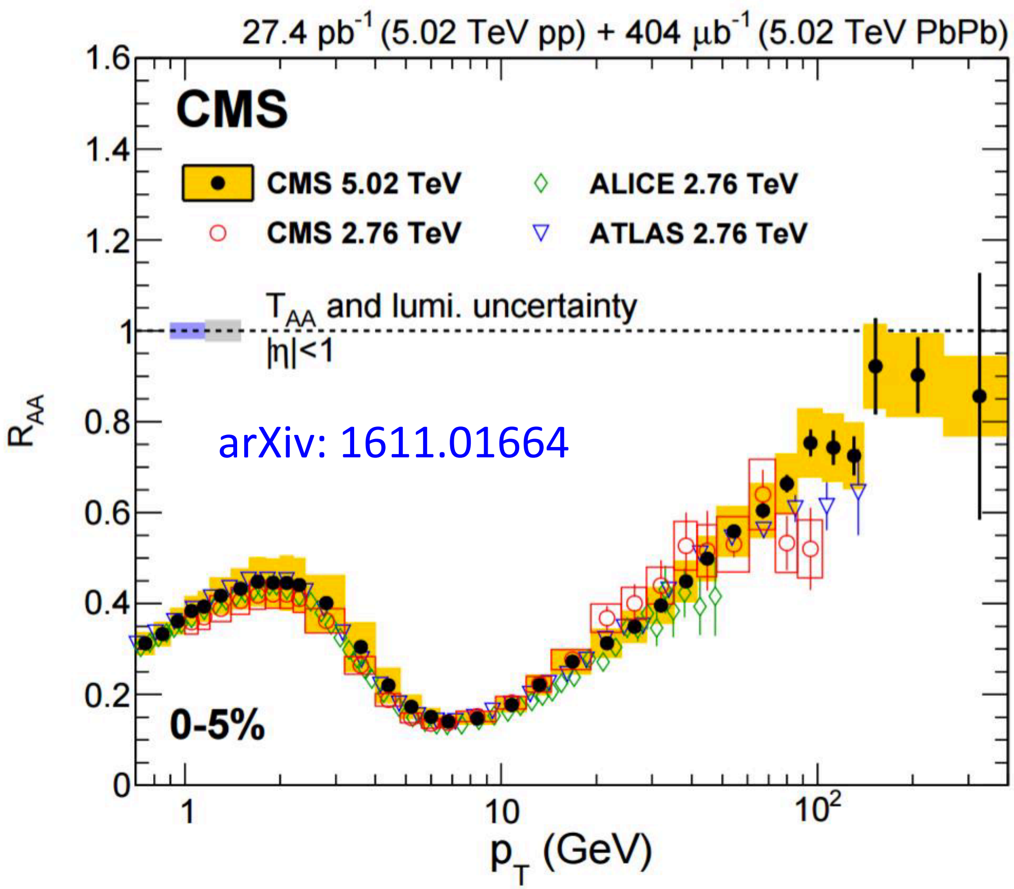

Suppression up to very high p_T

Strong suppression of intermediate/ high p_T particles in central Pb-Pb collisions

Absent in p-Pb collisions (no QGP expected)

→ final-state effect

→ Evidence of in-medium partonic energy loss

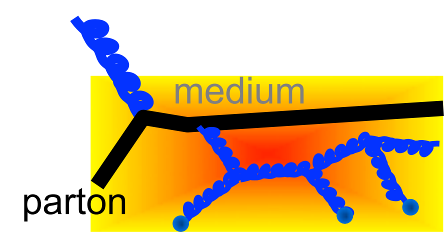

Started to extract information from data

From analysis of inclusive charged particle spectra at RHIC and LHC and considering many models

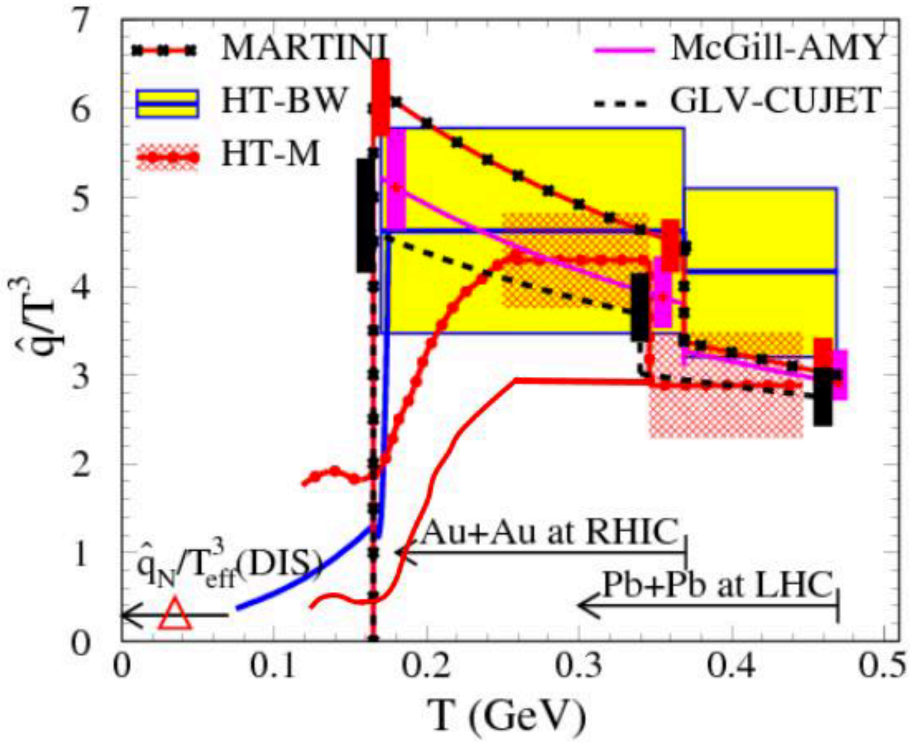

Only a starting point!

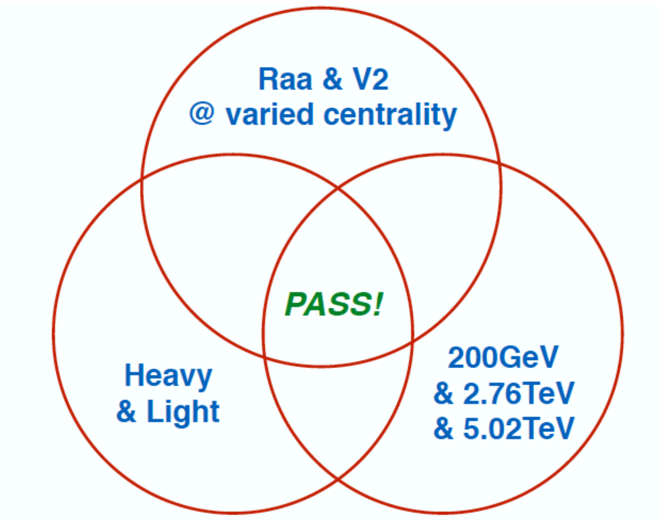

from J. Liao, QM2017

Nucl.Phys. A931 (2014) 404-409

$$\hat{q} = 1.2 \pm 0.3 \text{ GeV}^2/\text{fm (central Au-Au } \sqrt{s_{NN}} = 200 \text{ GeV)}$$

$$\hat{q} = 1.9 \pm 0.7 \text{ GeV}^2/\text{fm (central Pb-Pb } \sqrt{s_{NN}} = 2.76 \text{ TeV)}$$

Jet quenching

Jets are “extended” objects → provide complementary information to single particle observables

- Address spatial distribution and kinetic properties of radiated energy
  - **Out-of-cone radiation → jet suppression**

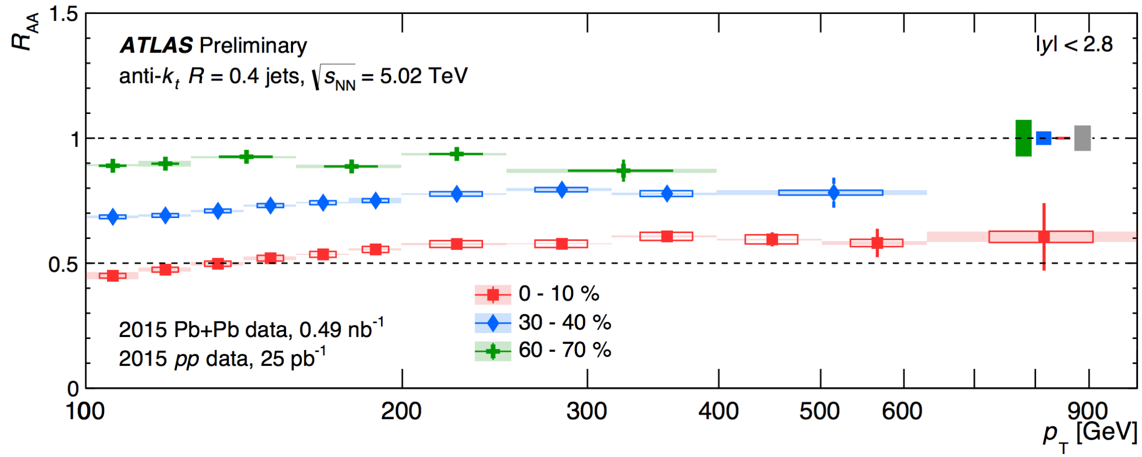

Jet suppression up to ~1 TeV!

Is the jet internal structure modified?

- Kinetic properties
- Spatial distribution of jet constituents
- Particle specie composition

Many studies performed

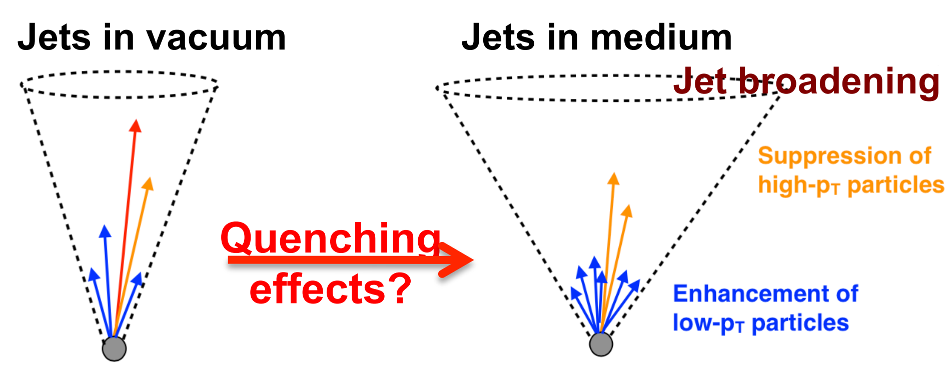

Jet-structure modifications

- First measurement of jet mass in Pb-Pb (and in p-Pb):

$$M = \sqrt{p^2 - p_T^2 - p_z^2}.$$

$$p_z = \sum_{i=1}^{n} p_{T_i} \sinh \eta_i, \quad p = \sum_{i=1}^{n} p_{T_i} \cosh \eta_i$$

- Large M: soft constituents far from jet axis
- Small M: few hard constituents close to axis
- $\langle M_{\text{quark jet}} \rangle < \langle M_{\text{gluon jet}} \rangle$

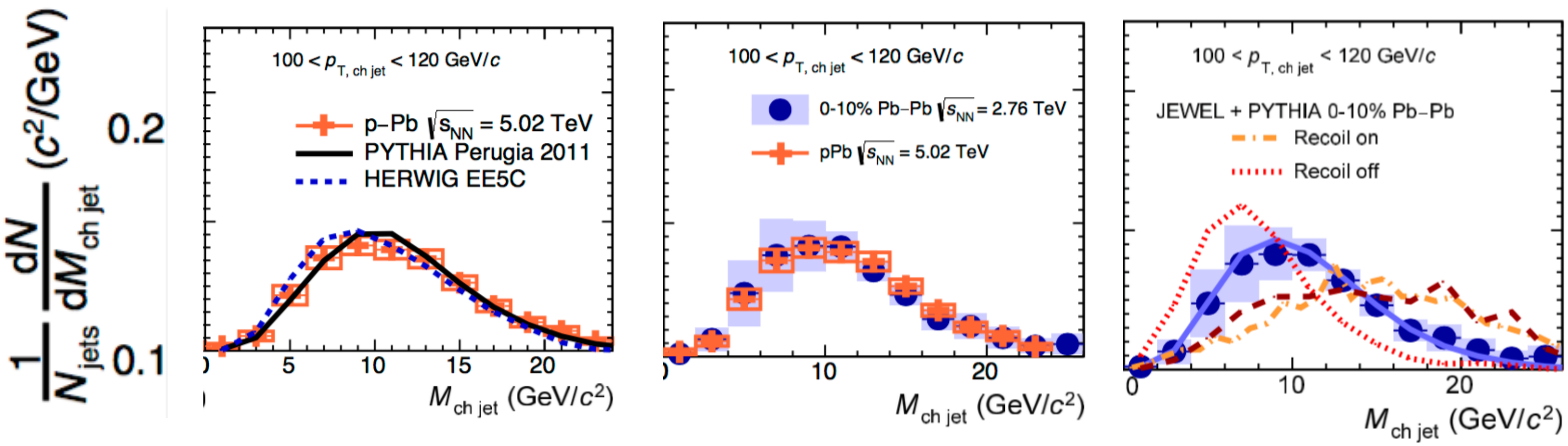

p-Pb baseline described by PYTHIA and HERWIG

No significant modification of jet structure in central Pb-Pb wrt p-Pb

Pb-Pb better described by PYTHIA than by generators with gluon radiation in a QGP

Bottomonium suppression

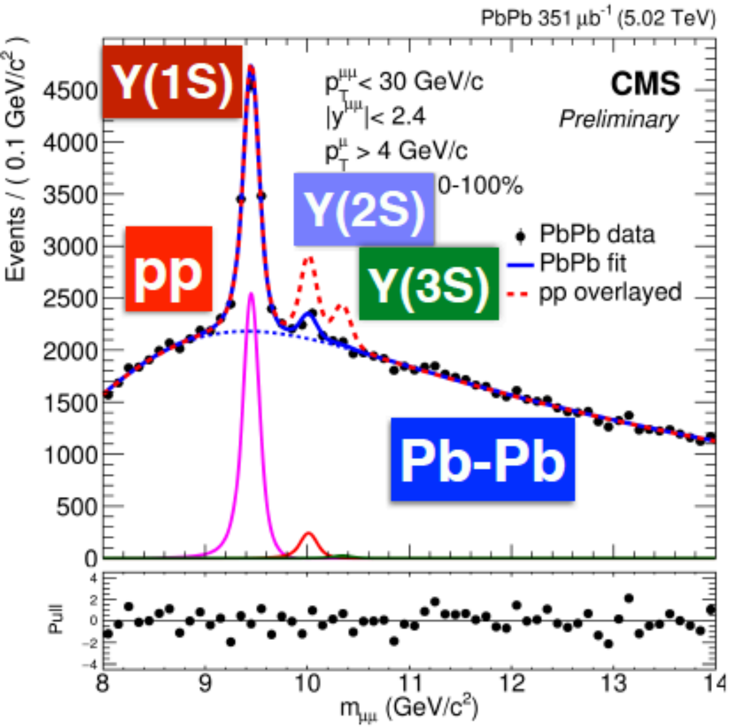

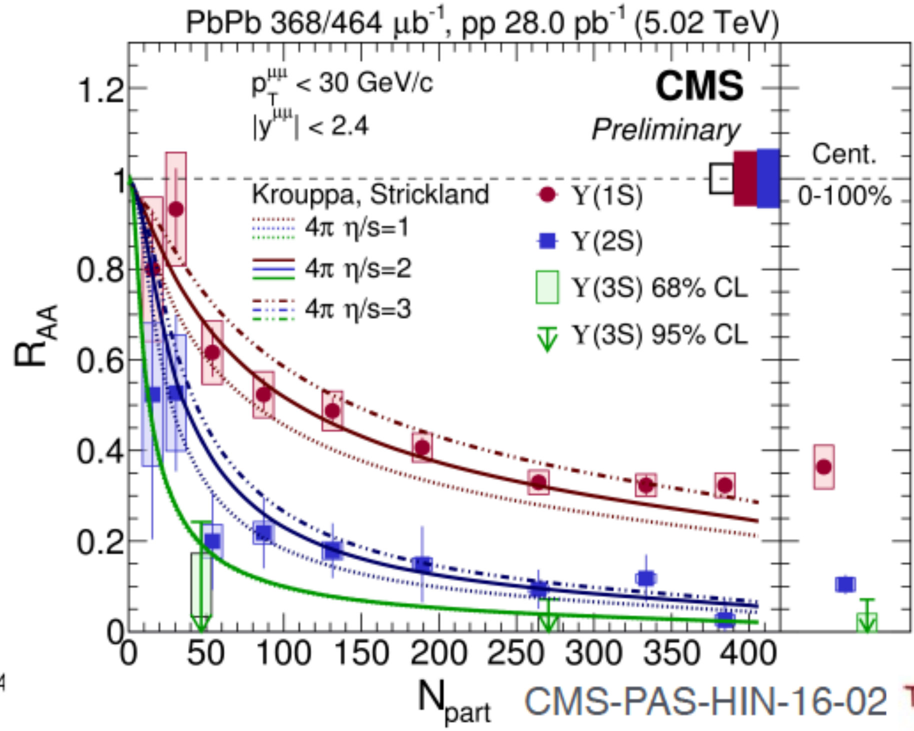

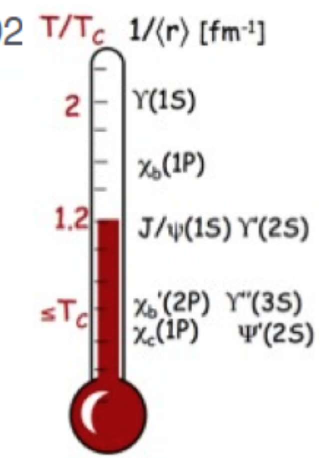

- Y(1s) ($E_{binding}$~1100 MeV), Y(2s) and Y(3s) (Eb~200 MeV) have different sensitivity to the medium
- Strong suppression of Y(2s,3s) with respect to Y(1s) increasing with centrality

→Trend expected from "sequential suppression"

Few introductory concepts: centrality, R_{AA}

Nuclear modification factor (R_{AA}): compare particle production in Pb-Pb with that in pp scaled by a "geometrical" factor (from Glauber model) to account for the larger number of nucleon-nucleon collisions

$$R_{AA}(p_T) = \frac{dN_{AA}/dp_T}{\langle N_{coll} \rangle \times dN_{pp}/dp_T}$$

Pb-Pb

pp

Binary nucleon-nucleon collisions, encodes collision geometry

If R_{AA}=1 → no nuclear effects

If R_{AA}≠1 → nuclear effects

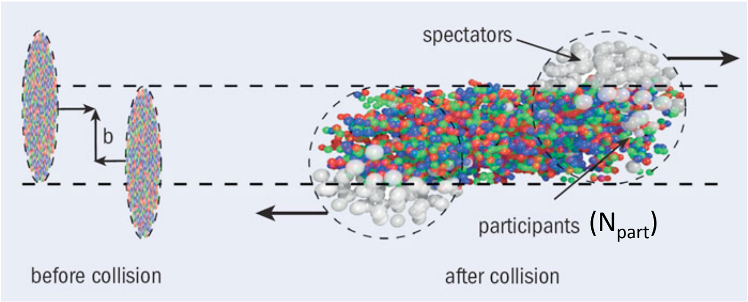

$\langle N_{part} \rangle$,$\langle N_{coll} \rangle$ from "geometrical" Glauber model

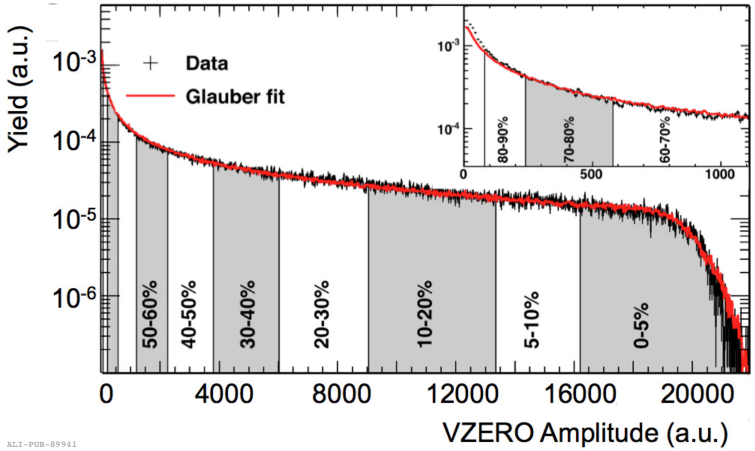

~ particle multiplicity/deposited energy

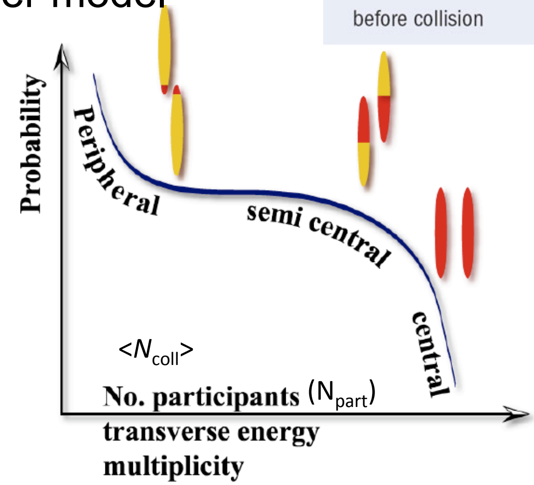

Note: N_{coll} scaling expected to hold only for hard (rare) processes

Geometry of heavy ion collisions

How can we be sure that we have the collision geometry under control?

Smaller/simpler collision systems (QGP not formed / not big impact on hard-probes production)

Probes not sensitive to medium formation
→ electroweak signals (γ,W, Z bosons)

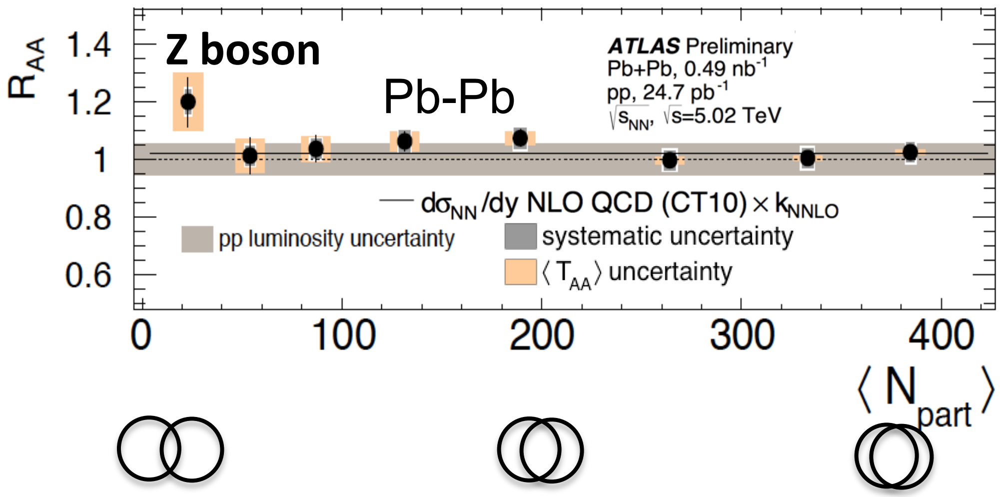

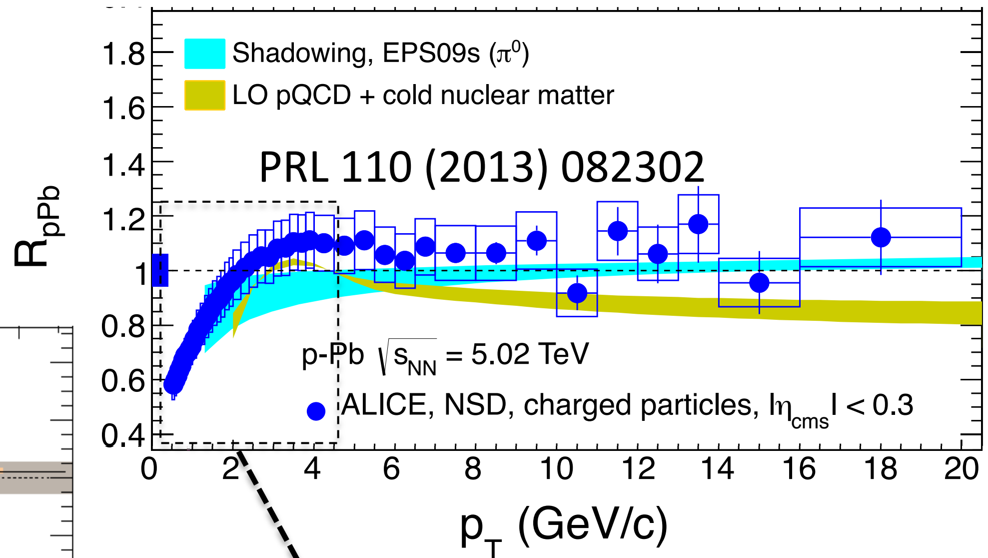

Caveats: breaking of N_{coll} scaling (soft processes) + initial state/ cold-nuclear matter effects at low p_T

CONF-2017-010

Signals reconstructed with central barrel

“V0” (K^0_s,Λ^0) and “Cascades” (Ξ,Ω)

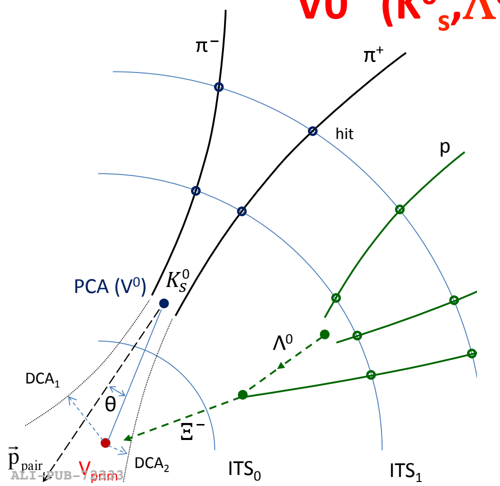

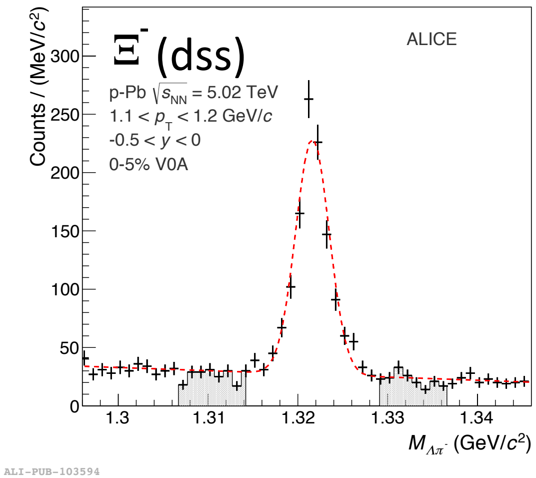

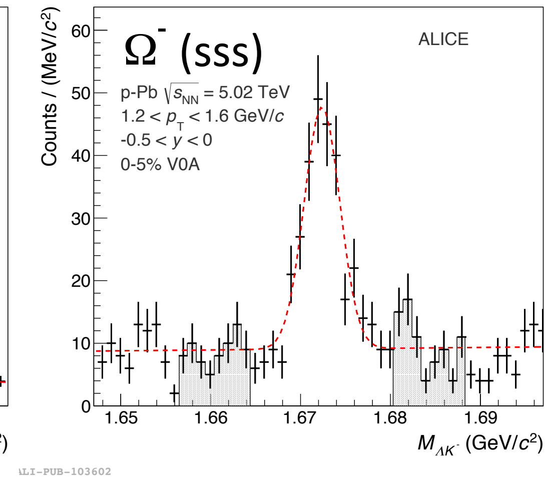

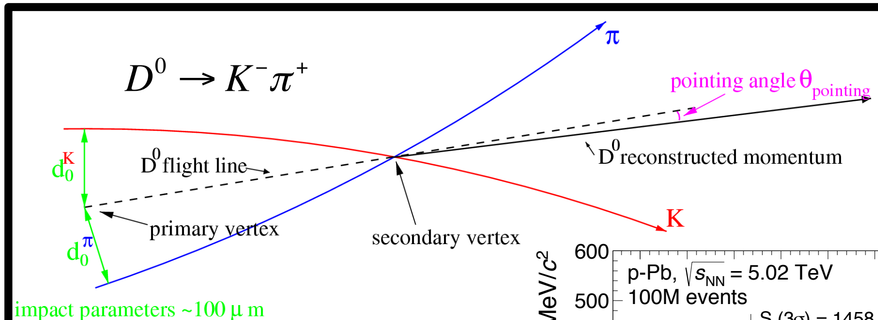

D mesons (e.g. $D^0(c\bar{u})$)

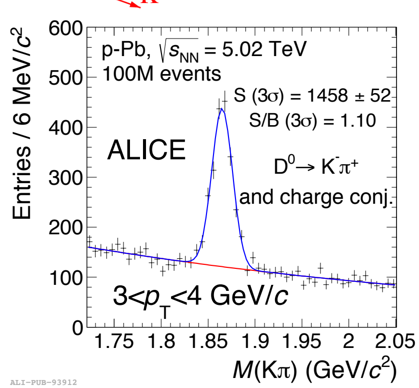

J/ψ ($c\bar{c}$) → e^+e^-

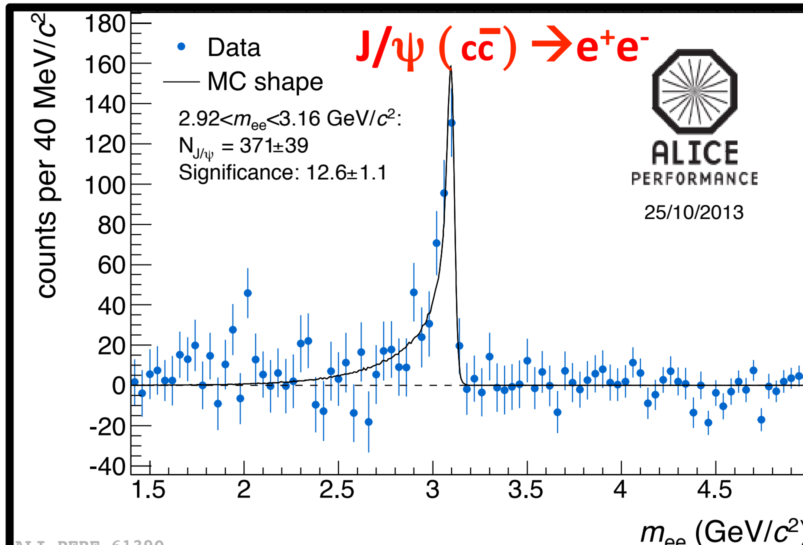

+ spectra of identified particles

Lattice QCD: Phase Transition

Lattice QCD is neither a calculation not a simulation: “realization” of QCD over a discretized space. It allows to compute thermodynamical properties of a system even in a non-perturbative regime of QCD

$$\frac{\varepsilon}{T^4} \; vs. \; T \longrightarrow$$ Proportional to number of degrees of freedom (ndof) (S. Boltzmann’s law)

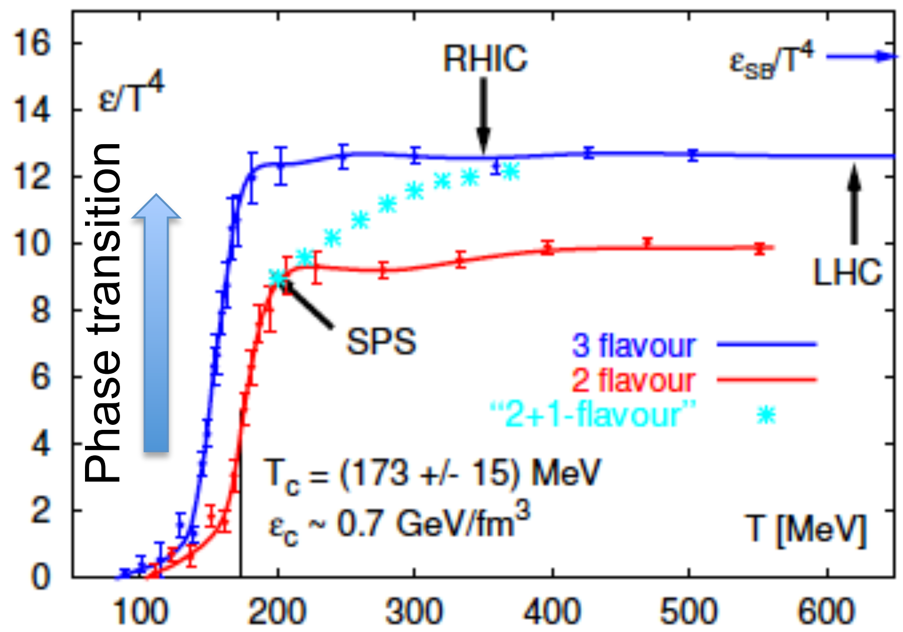

- Zero baryon density, 2(u, d) or 3 (u, d, s) quark flavours
- **ε changes rapidly around T_c**
- **→ signal change in number of degrees of freedom**

- Most recent calculations:

  T_c ~ 155 MeV :

  → ε_c ~ 0.6 GeV/fm^3

F. Karsch. Lattice QCD at High Temperature and Density. Lecture Notes of Physics, vol. 583, 2002. arXiv:hep-lat/0106019.

Strangeness enhancement

Most of light particle mass (and thus of matter) is due to spontaneous breaking of chiral symmetry of QCD

In the QGP chiral symmetry is expected to be partially restored (more details in backup)
[Raf. Rep. elski: Phys88 (1982) 331]
[Rafelski-Müller: Phys. Rev. Lett. 48 (1982) 1066]

Quarks reacquire the “bare” mass values they have in the QCD Lagrangian

m(u,d): ~ 350 MeV → a few MeV
m(s): ~ 500 MeV → ~ 150 MeV

The symmetry is exact only for massless particles, therefore its restoration is only partial.

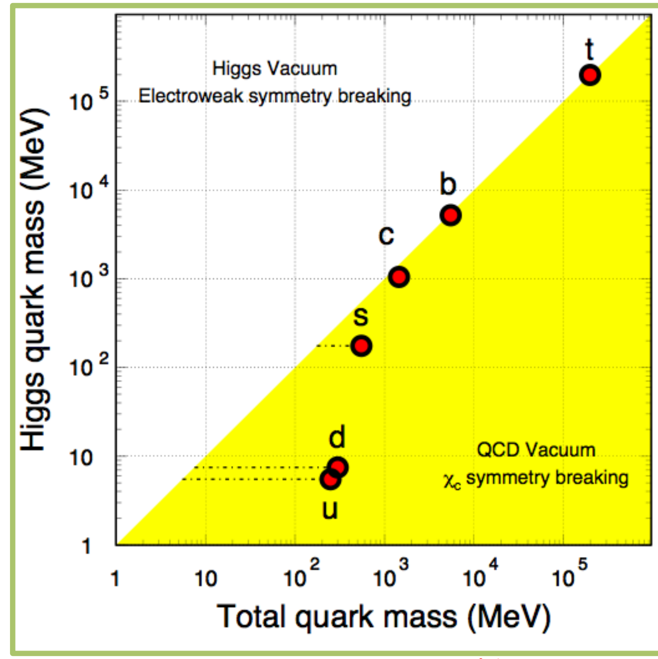

Consequence:
→abundant strange quark pair production
→easier to form multi-strange hadrons

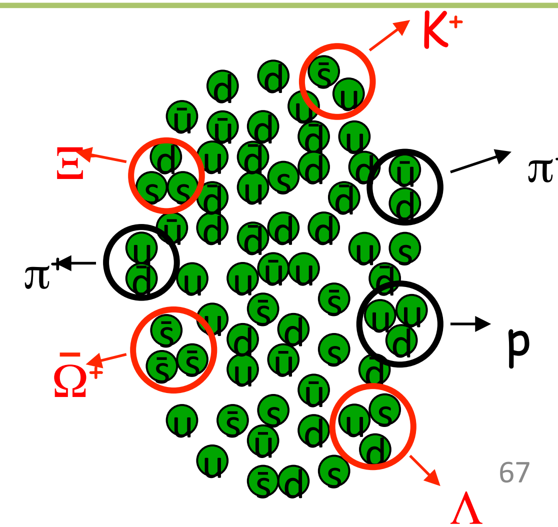

QCD Lagrangian and spontaneous breaking of chiral symmetry

$$\mathcal{L}_{\rm QCD} = \bar{\psi}_i \left(i(\gamma^\mu D_\mu)_{ij} - m\,\delta_{ij}\right) \psi_j - \frac{1}{4} G^a_{\mu\nu} G^{\mu\nu}_a$$

with m = "bare" mass

In the limit of vanishing quark masses, the QCD Lagrangian becomes symmetric under transformations under the group $SU(N_f)_L \times SU(N_f)_R$: **chiral symmetry.**

However, chiral symmetry is spontaneously broken by the non-zero expectation value of the chiral condensate in vacuum, $\langle \psi\bar{\psi} \rangle \neq 0$, i.e. the QCD vacuum (at T=0) breaks the chiral symmetry. This mechanisms generates a **"dynamical" mass for quarks**, which is responsible for **most of the matter mass.**
This symmetry is approximately valid for u,d,(s) quarks (lightest).

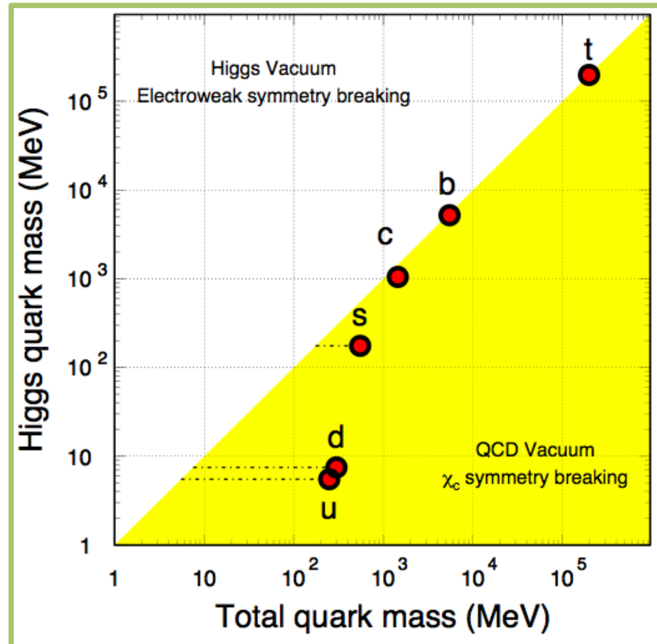

X.Zhu et al., PLB 647 (2007) 366

Restoration of bare quark masses in the QGP (T>0)

Deconfinement is expected to be accompanied by a "Partial Restoration of Chiral Symmetry", due to the vanishing of the $\langle \psi\bar{\psi} \rangle$ expectation value. Quarks reacquire the "bare" mass values they have in the QCD Lagrangian

- m(u,d): ~ 350 MeV $\rightarrow$ a few MeV
- m(s): ~ 500 MeV $\rightarrow$ ~ 150 MeV

Since the symmetry is exact only for massless particles, therefore its restoration here is only partial.

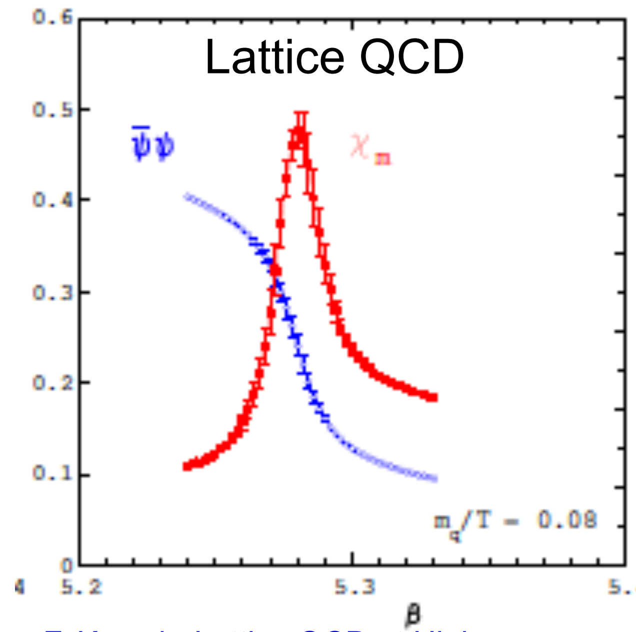

F. Karsch. Lattice QCD at High Temperature and Density. Lecture Notes of Physics, vol. 583, 2002. arXiv:hep-lat/0106019

Consequence:
it's easier to produce strange quarks!

Strangeness enhancement searched for as a proof of chiral symmetry restoration (- - > deconfinement, with some caveats)

Constraining further viscosity: example with a model

J. E. Bernhard et al. Phys. Rev. C 94, 024907 (2016)

9 parameters: 3 initial state, 4 for QGP response, 2 model parameters

Particle yields, <p_T>, flow coefficients used to calibrate the model parameters to reproduce data

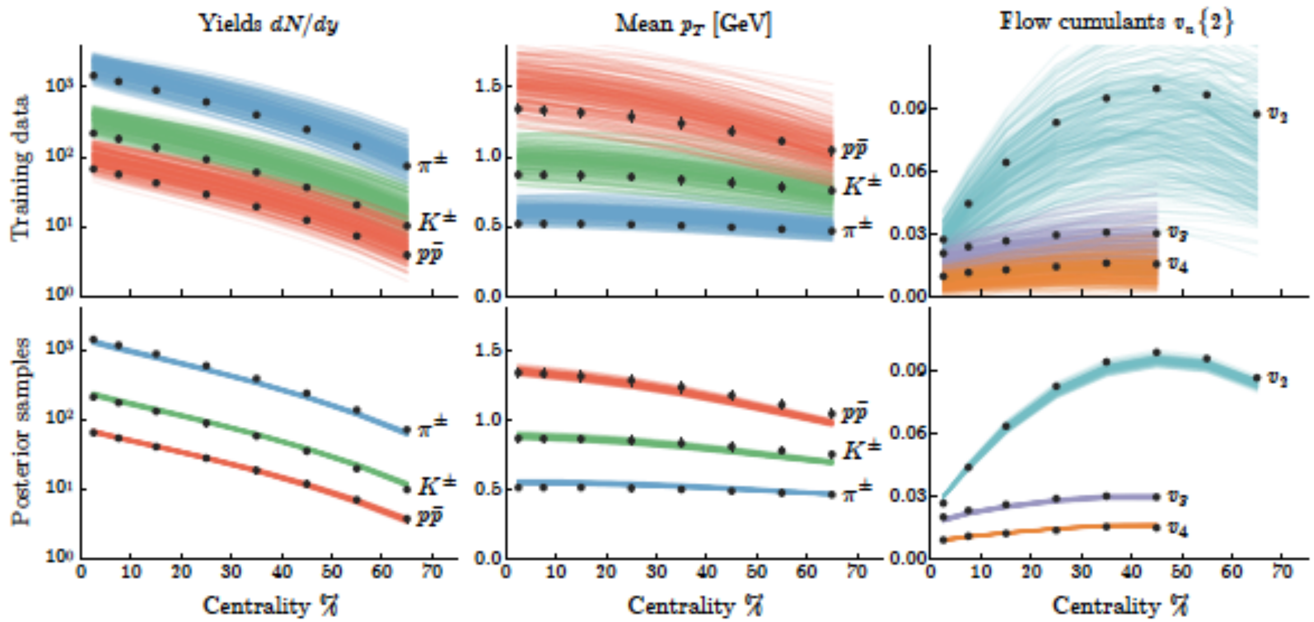

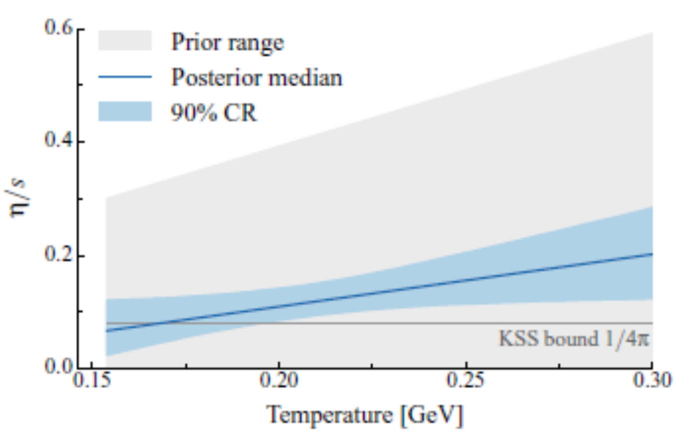

Bayes method used to extract probability distribution for the true values of the parameters

Main results: viscosity vs. temperature

QGP viscosity very low (lower than any atomic matter)

The ALICE detector: “small-angle” detectors

Event selection (min bias) + centrality determination

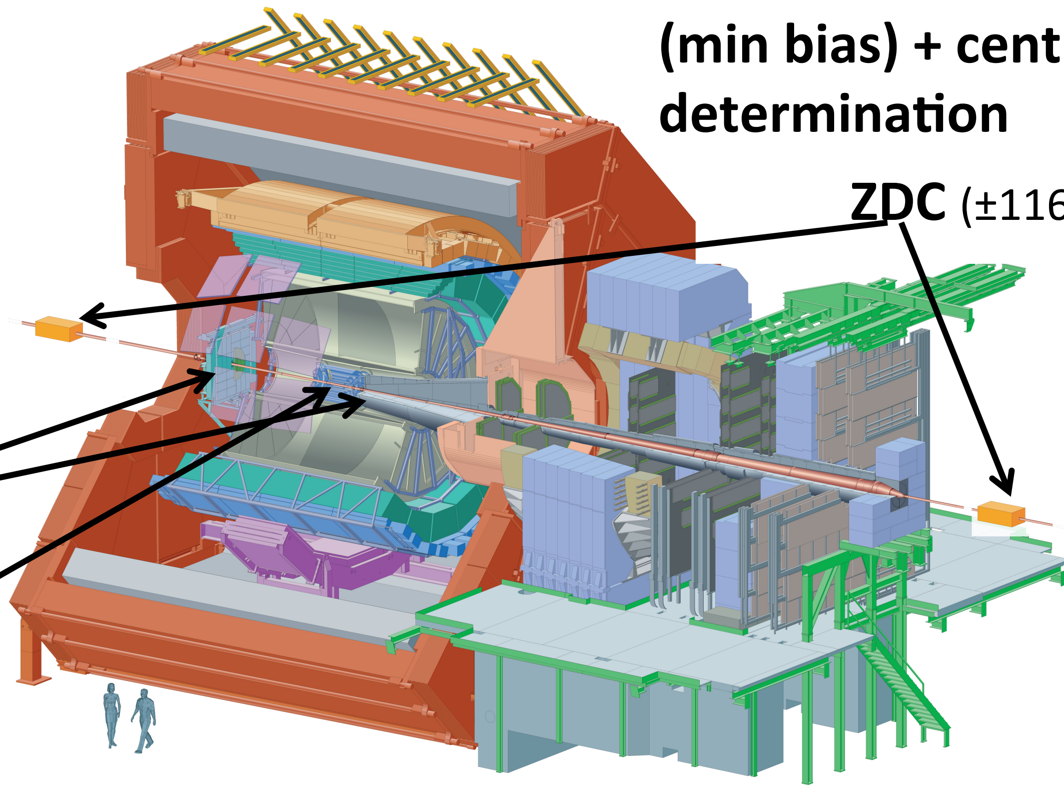

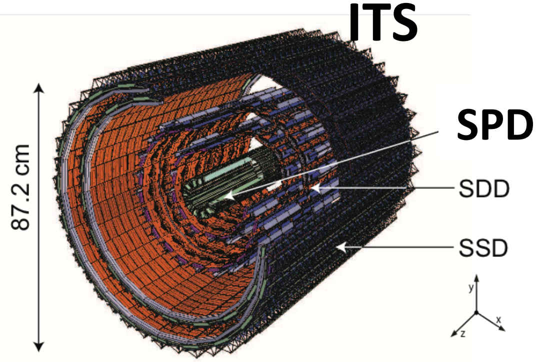

The ALICE detector: central barrel

|η|<0.9
B=0.5 T

Track reconstruction

Transverse momentum (p_T) resolution: 0.8% (2%) at 1 (10) GeV/c

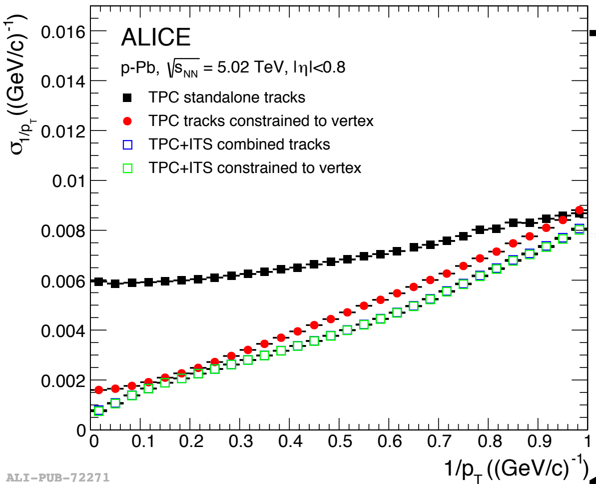

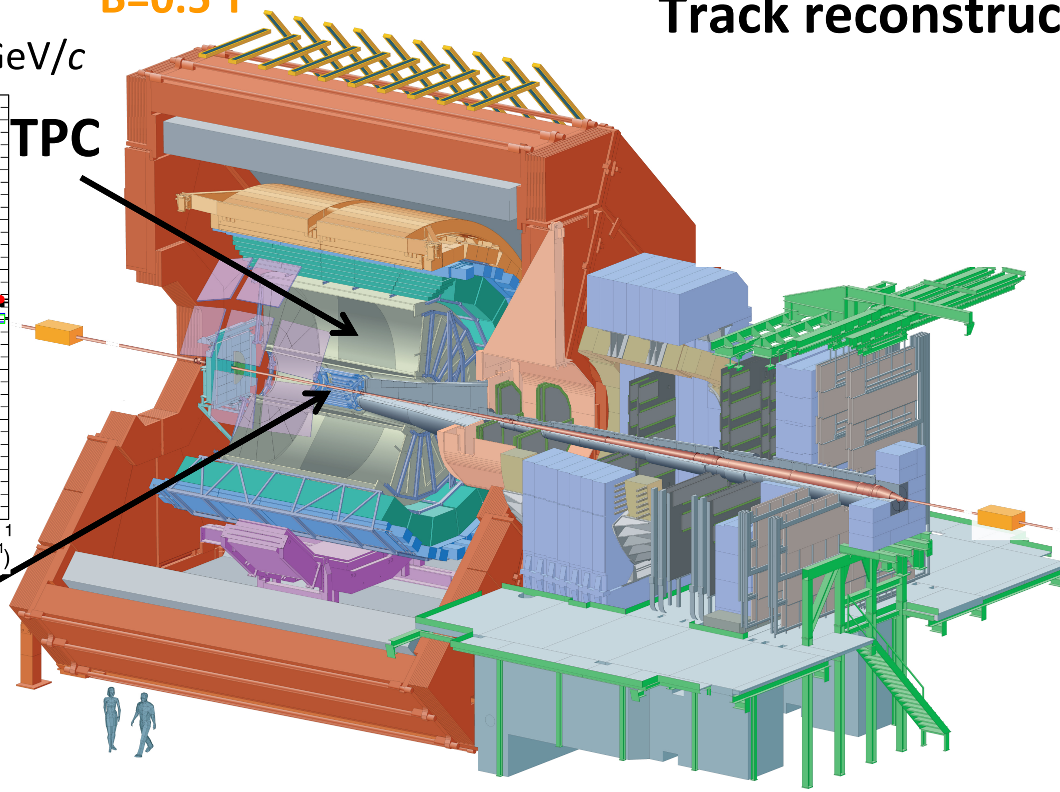

ITS

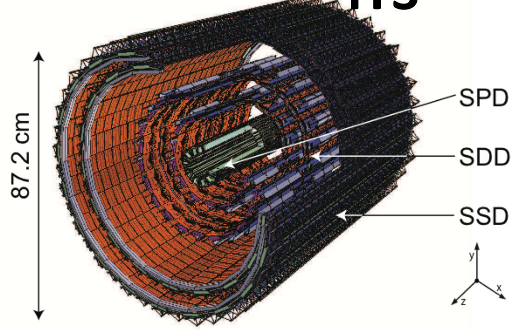

The ALICE detector: forward muon spectrometer

MUON SPECTROMETER
$-4<\eta<-2.5$ ($2° < \theta < 9°$)

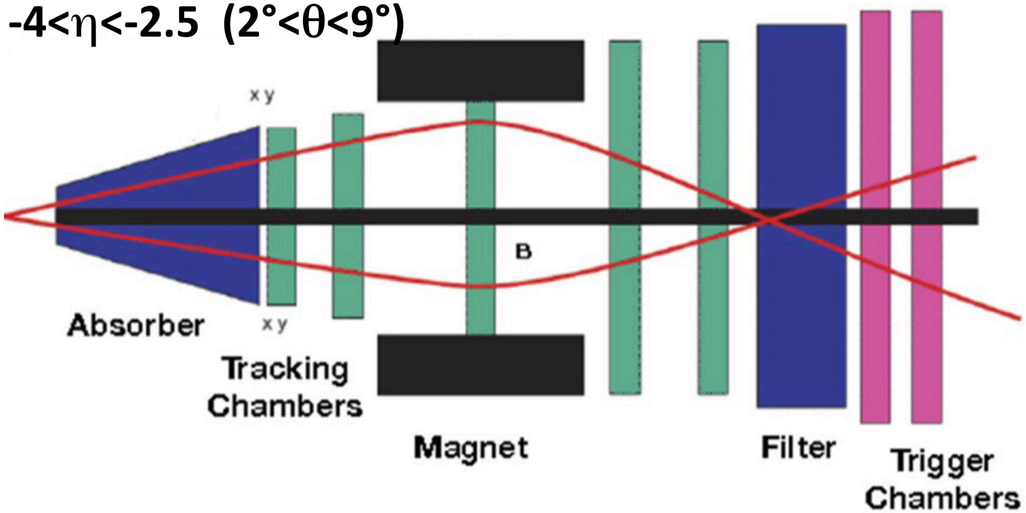

Quarkonia

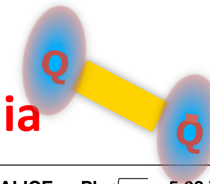

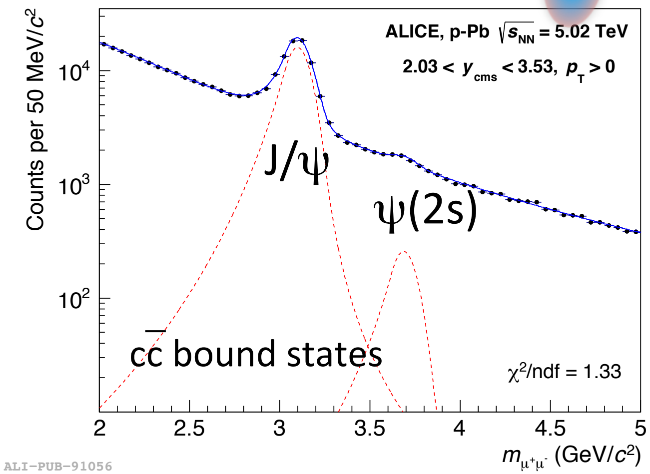

Muons from semi-leptonic heavy-flavour hadron decays

D,B, Λ_c,..→ μ X

(after subtraction of muons from non-HF sources)

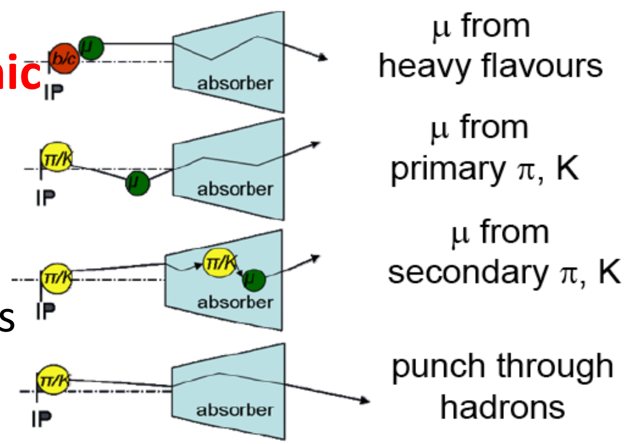

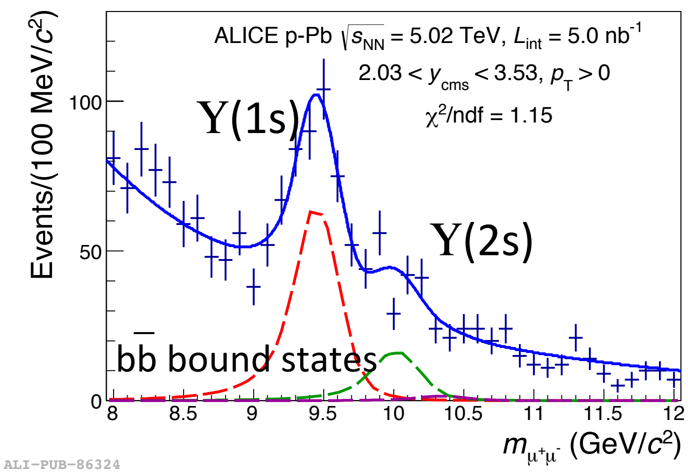

High Luminosity (HL)-LHC era

RUN2 $\sqrt{s_{NN}}$ =5.02 TeV

$\sqrt{s_{NN}}$ =5.5 TeV

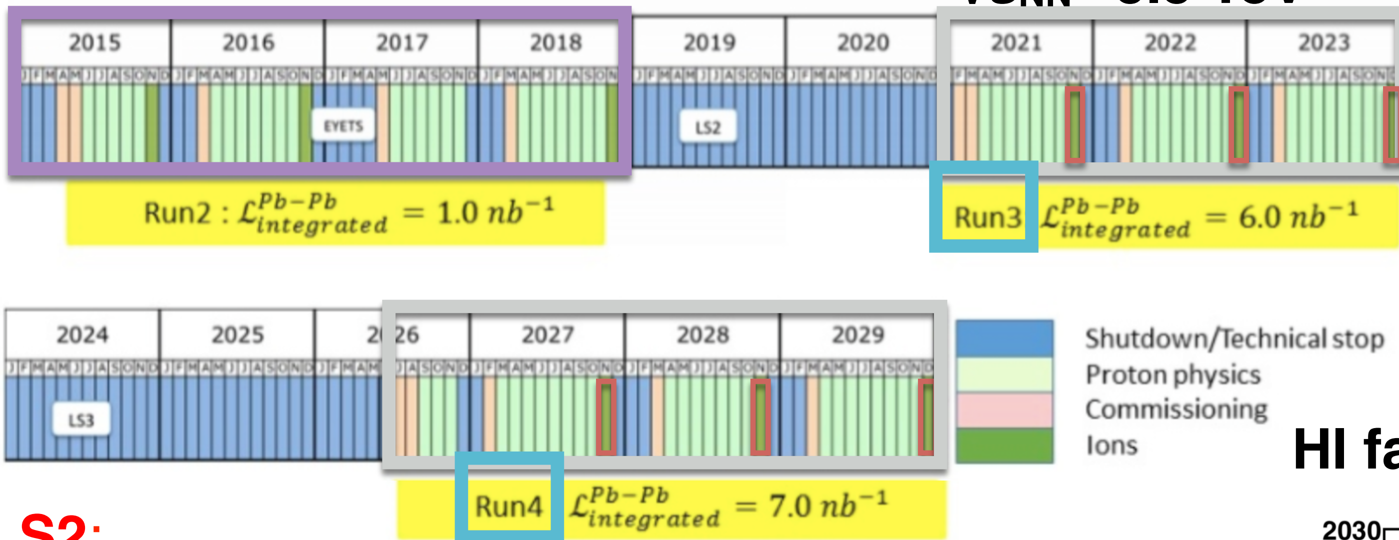

LS2:

- LHC **injector upgrades**: interaction rate **up to 50kHz** (now <10 kHz)

→x10 more statistics w.r.t. the current available data

- Experiments upgrade LS2 and LS3

Run 3+4: "HL-HI-LHC"

- All the four LHC experiments will participate to HI program
  - request: 1 month of Pb-Pb collisions/year > 10/nb
    - corresponds to x100 more statistics for min. bias for ALICE

- Possible interest by experiment for lighter ion run (Ar or Xe)

HI facilities up to 2030

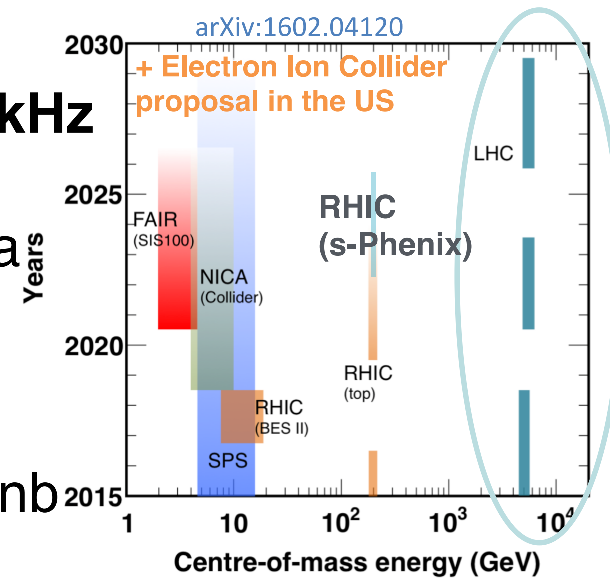

ALICE upgrade: New ITS

Design requirements:

1. **Improve impact parameter resolution by a factor ~3 (5) in rφ (z)**
   - ➜ Reduce pixel size (currently 50 μm x 425 μm)
     - monolithic (MAPS) with size ~ 28 μm x 28 μm
   - ➜ Go closer to interaction point:
     - ➜ new smaller beam pipe: 2.9 cm ➜ 1.9 cm
     - ➜ first layer with smaller radius (2.3 cm, currently 3.9 cm)
   - ➜ Reduce material thickness: 50 μm silicon, X/X_0 from current ~1.13% to ~0.3(0.8)% per layer

2. **High standalone tracking performance** (efficiency, spatial and momentum resolutions)
   - ➜ Increase granularity
   - ➜ Add 1 layer (from 6 to 7)

3. **Faster (x50) readout**: Pb-Pb interactions up to 100 kHz

4. **Maintenance:** allow for removal/ insertion of faulty detector components during annual winter shutdown

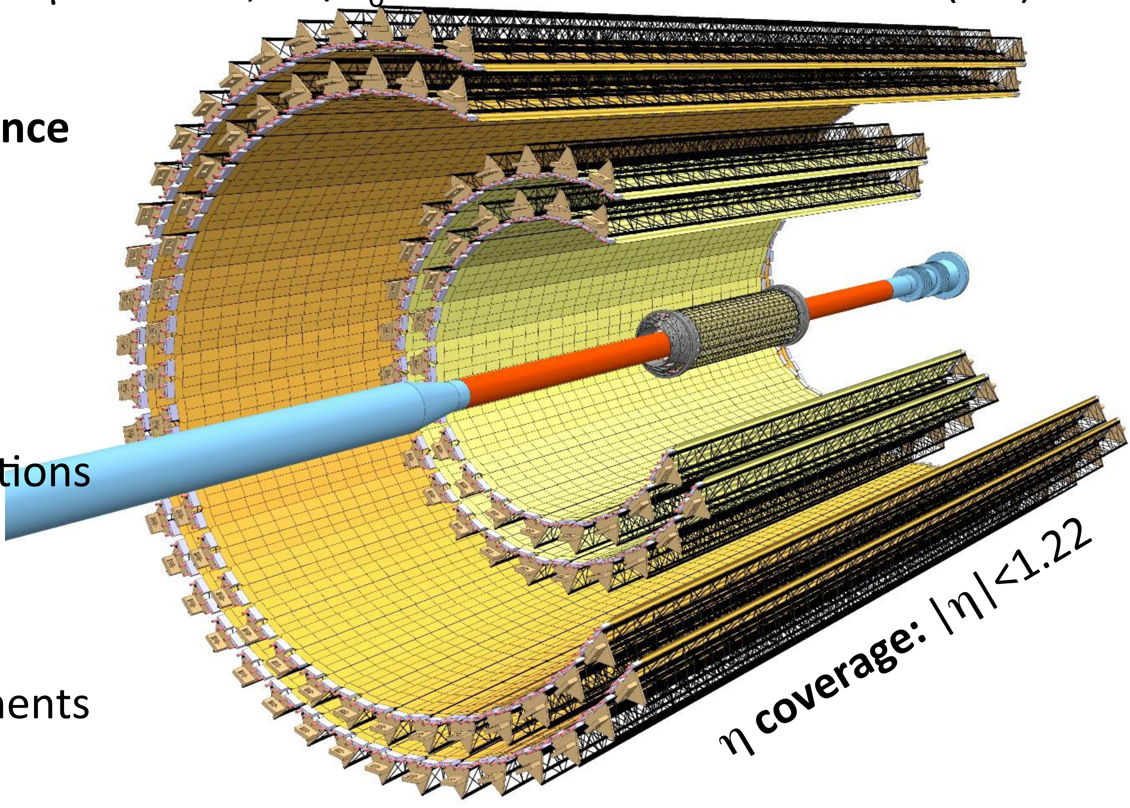

New ITS: performance

Studies done with simulations with realistic and complete detector geometry and material budget description.

Track reconstruction efficiency

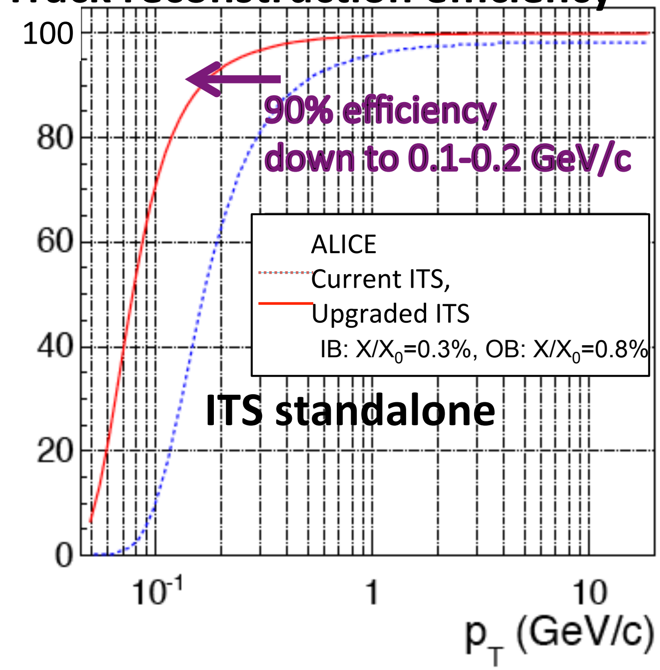

Track spatial resolution at the primary vertex

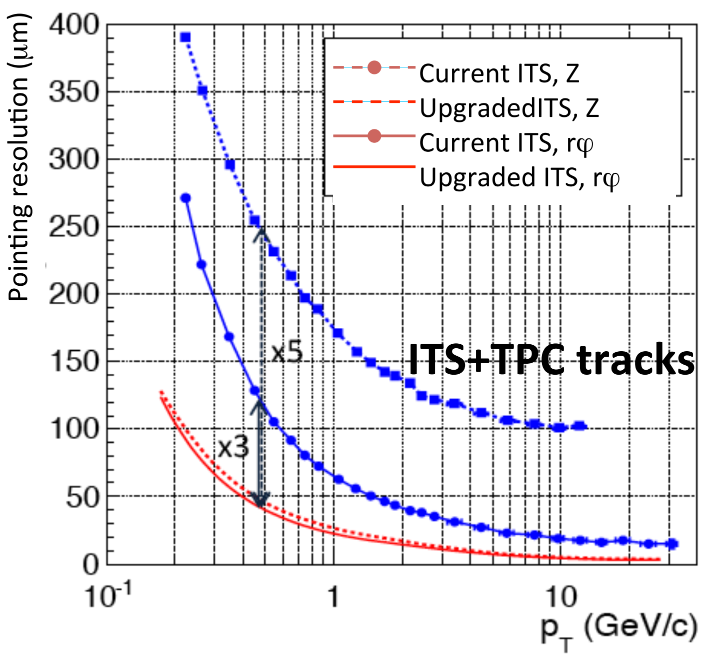

Find more in ALICE ITS TDR:

CERN-LHCC-2013-024 ; ALICE-TDR-017

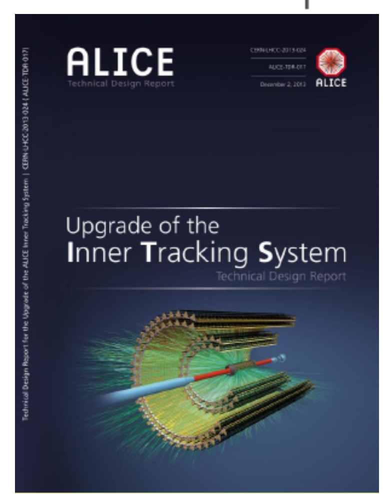

Muon Forward Tracker

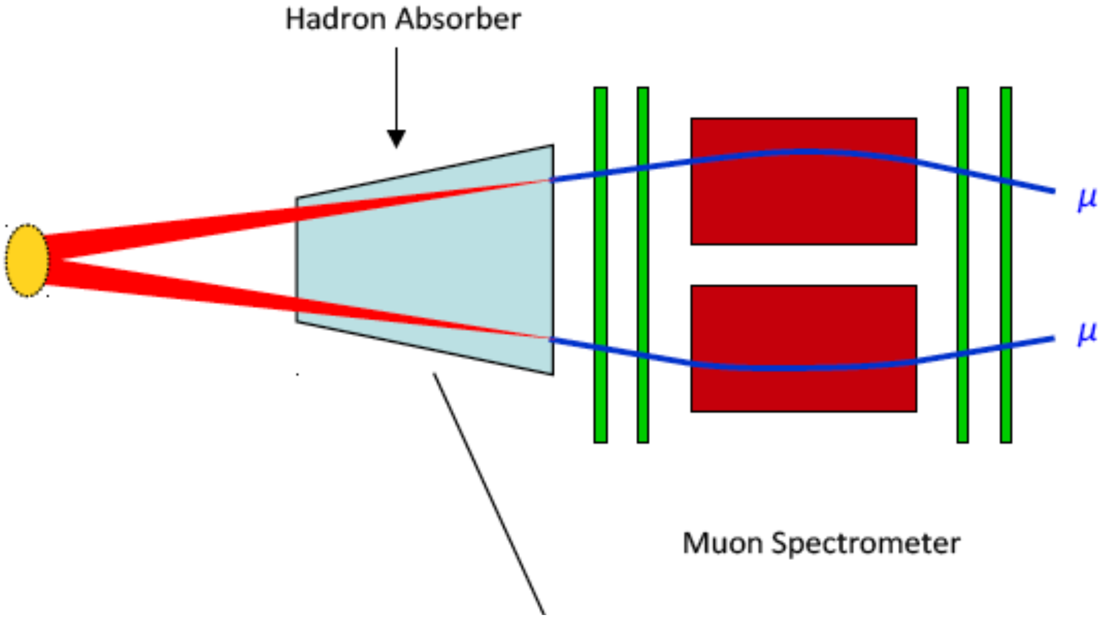

Complementing muon spectrometer at forward rapidity

Extrapolating back to the vertex region degrades the information on the kinematics and trajectory

➔ Cannot separate prompt and displaced muons

Muon Forward Tracker

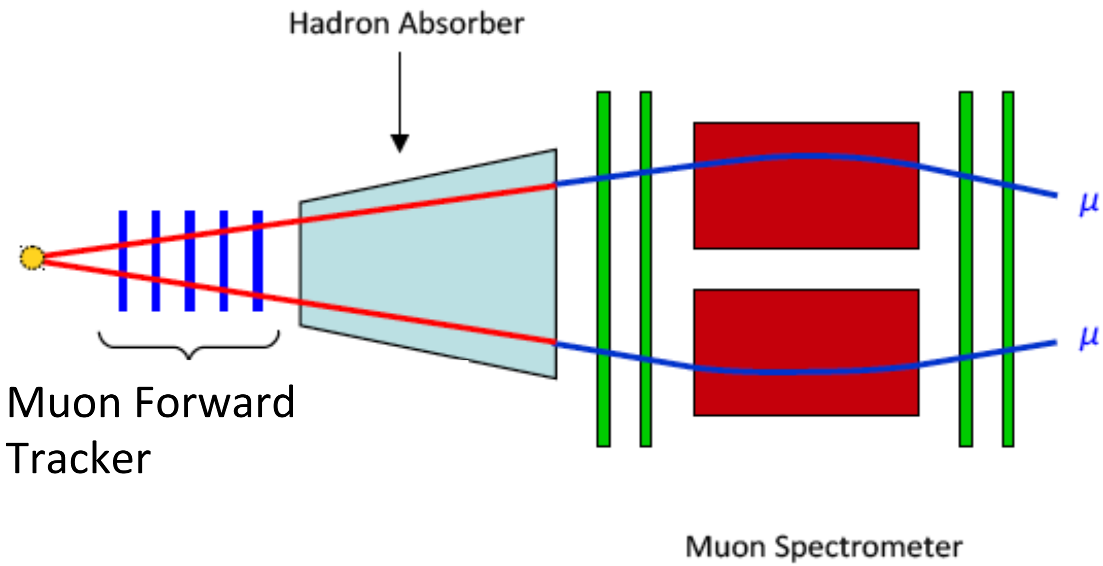

Complementing muon spectrometer at forward rapidity

Muon tracks are extrapolated and matched to the MFT clusters before the absorber

High pointing accuracy

Separation of charm and beauty signals (single μ, J/ψ)

Muon Forward Tracker

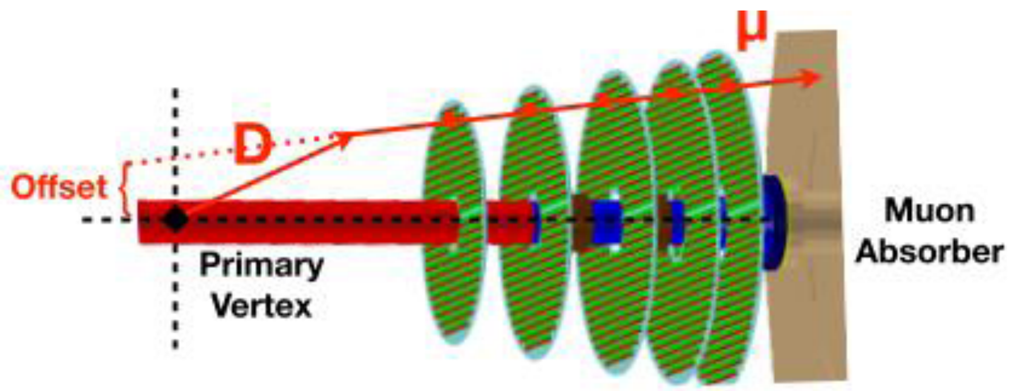

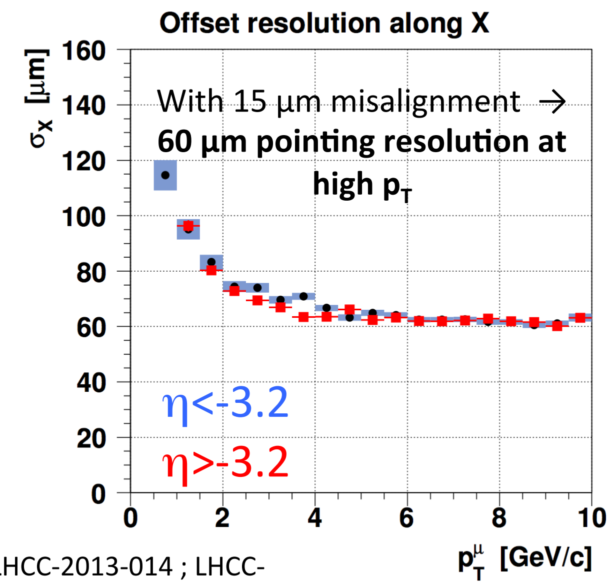

CERN-LHCC-2013-014 ; LHCC-I-022-ADD-1

5-6 planes of CMOS silicon pixel sensors
(same technology as ITS):

- $50 < z < 80$ cm
- $R_{min} \approx 2.5$ cm (beam pipe constraint)
- $11 < R_{max} < 16$ cm
- Area ≈ 2700 cm^2
- $X/X_0 = 0.4\%$ per plane
- Current pixel size scenario: ~28 x 28 μm^2

ALICE at high rate: TPC Upgrade

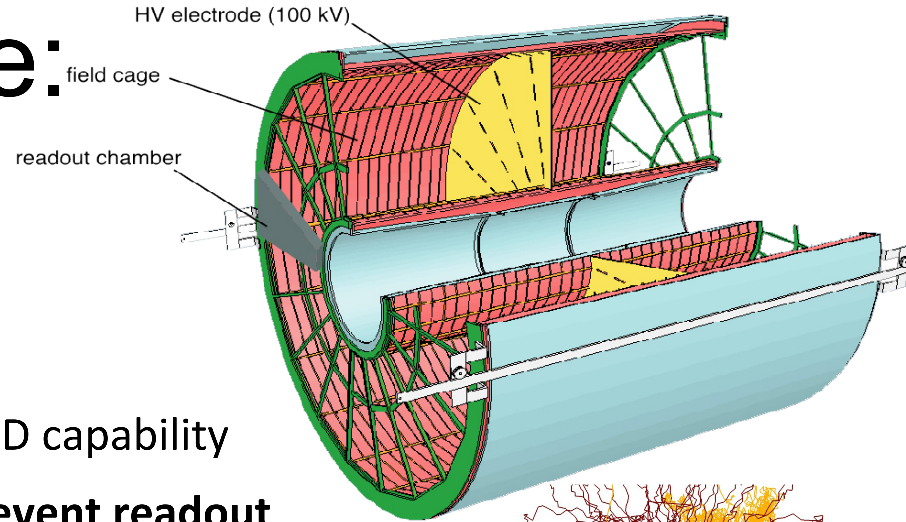

Goals

- Operate TPC at 50 kHz
- Preserving current momentum resolution and PID capability

Current TPC readout based on MWPC limits the event readout rate to 3.5 kHz

➜ Upgrade TPC strategy

- **New readout chambers:** MWPC replaced with micropattern gaseous detectors, including **GEM (Gas Electron Multiplier)**
  - No gating, small ion backflow
- Redesign TPC front-end and readout electronic systems to allow for continuous readout
- Significant online data reduction to comply with the limited bandwidth
  - Online cluster finding and cluster-track association

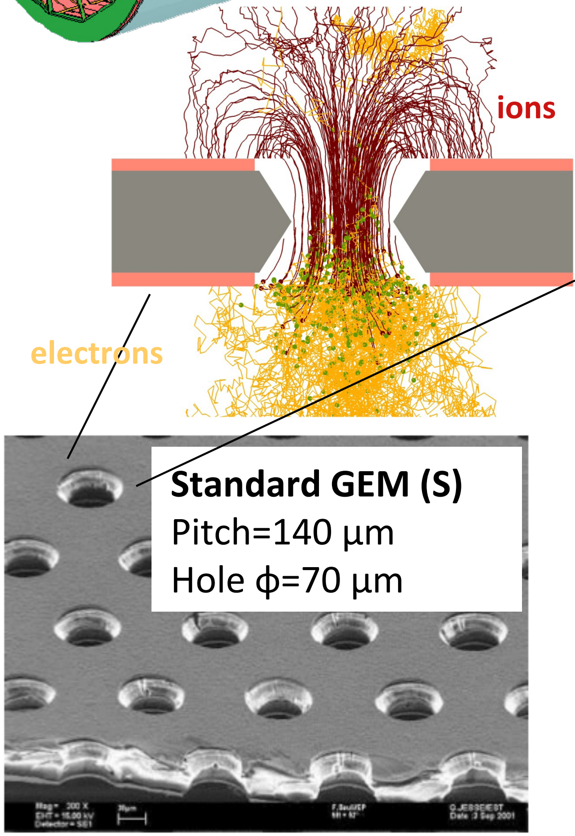

Di-electron production

One of the most fundamental measurements, sensitive to:

- chiral-symmetry restoration by modification of ρ-meson spectral function
- partonic equation of state studying space–time evolution with invariant-mass and p_T distributions of dileptons
- photon thermal emission extrapolating to zero dilepton mass

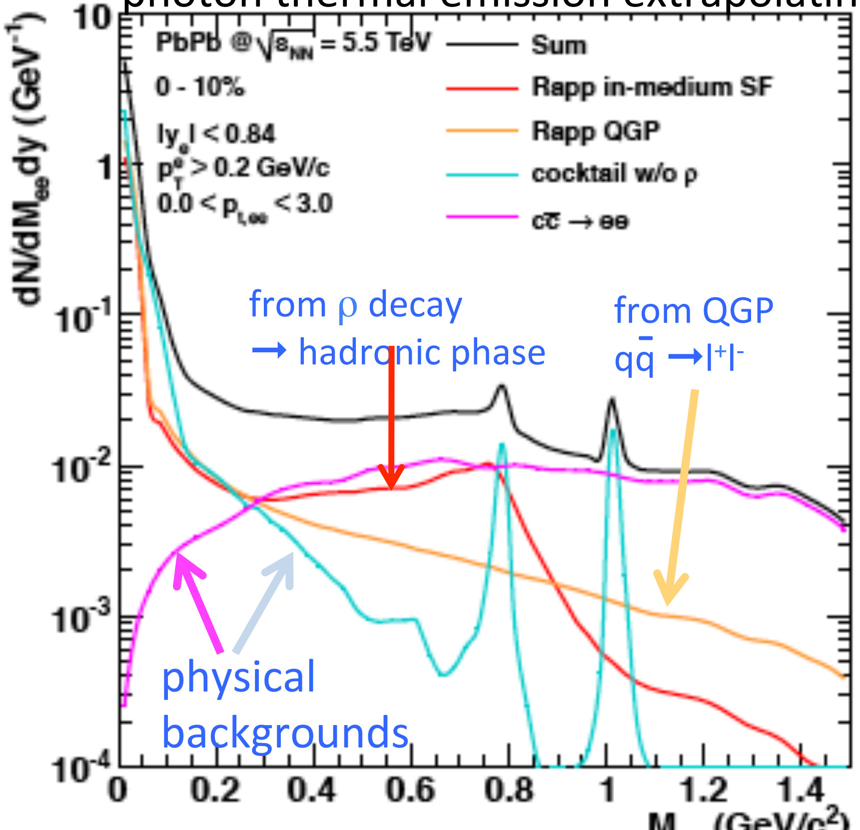

CERN-LHCC-2012-005, LHCC-G-159, 2012.

Target measurements:

- di-electron yield vs. mass and p_T (require background subtraction)
- di-electron elliptic flow

New ITS

- Reduced combinatorial background (reduce impact of γ-conversions)
- Charm rejection

Di-electron production

Excess after background subtraction

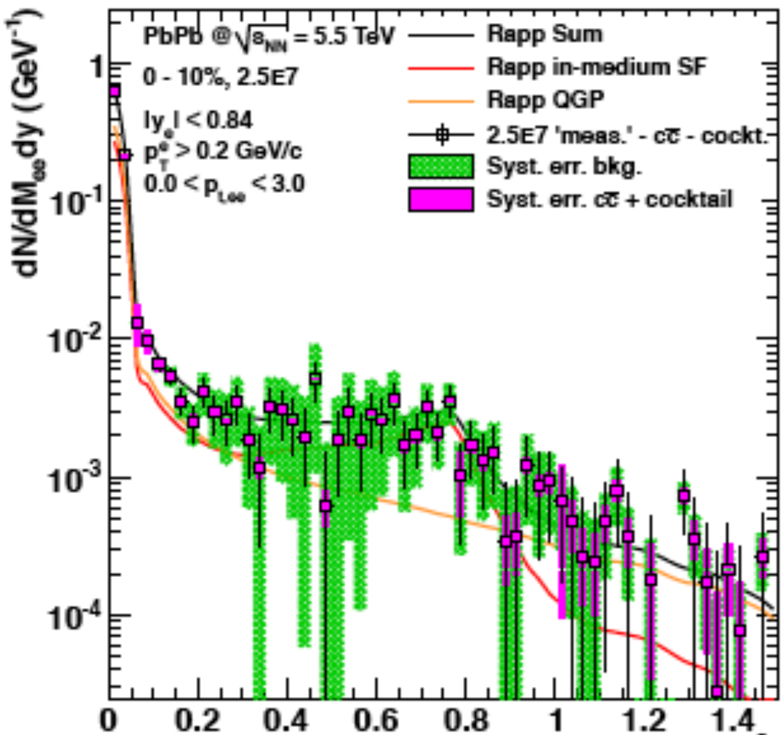

CERN-LHCC-2012-005, LHCC-G-159, 2012.

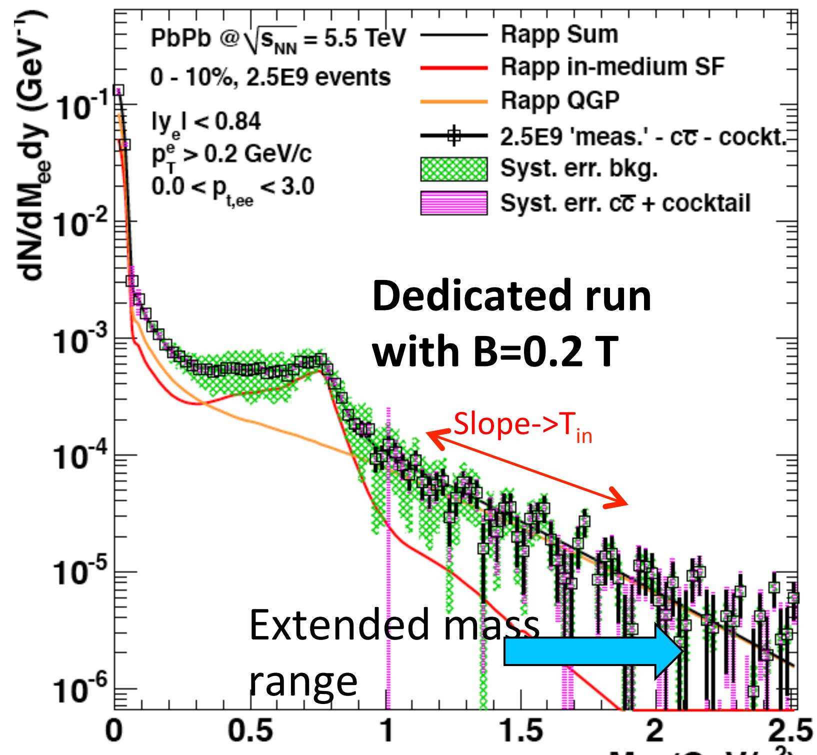

CERN-LHCC-2013-024 ; ALICE-TDR-017

current ITS and event rate:
large statistical and systematic uncertainties

new ITS and high-rate:
precise measurement

Allows for an estimation of the **temperature at various phases of system expansion** with 10-20% precision (stat.+syst.)